

# **GREEN COATINGS/PROCESSING USING LIQUID AND SUPERCRITICAL CO<sub>2</sub> WITH NON-FLUOROUS CO<sub>2</sub>-PHILES**

*Thesis submitted to the  
University of Calicut in partial fulfilment of  
the requirements for the award of the degree of*

**DOCTOR OF PHILOSOPHY IN CHEMISTRY**  
*under the Faculty of Sciences*

by

**ANU ANTONY**

Under the guidance of  
**Dr. P. Raveendran**



**DEPARTMENT OF CHEMISTRY  
UNIVERSITY OF CALICUT  
KERALA-673 635  
SEPTEMBER 2019**

*“We stand now where two roads diverge. But unlike the roads in Robert Frost's familiar poem, they are not equally fair. The road we have long been travelling is deceptively easy, a smooth superhighway on which we progress with great speed, but at its end lies disaster. The other fork of the road — the one less travelled by — offers our last, our only chance to reach a destination that assures the preservation of the earth.”*

— **Rachel Carson** in *Silent Spring*

## **CERTIFICATE**

Certified that the thesis entitled “**GREEN COATINGS/ PROCESSING USING LIQUID AND SUPERCRITICAL CO<sub>2</sub> WITH NON-FLUOROUS CO<sub>2</sub>-PHILES**” is an authentic record of the research work carried out by **Ms. Anu Antony** under my guidance for the award of the degree of **Doctor of Philosophy** in Chemistry under the Faculty of Sciences, University of Calicut, Kerala, and that the same has not been submitted elsewhere for any degree or diploma.

Calicut University  
17.12.2019

**Dr. P. Raveendran**  
(Supervising Teacher)

## **CERTIFICATE**

Certified that the thesis entitled **“GREEN COATINGS/ PROCESSING USING LIQUID AND SUPERCRITICAL CO<sub>2</sub> WITH NON-FLUOROUS CO<sub>2</sub>-PHILES”** is an authentic record of the research work carried out by **Ms. Anu Antony** under my guidance for the award of the degree of **Doctor of Philosophy** in Chemistry under the Faculty of Sciences, University of Calicut, Kerala, and that the same has not been submitted elsewhere for any degree or diploma. I also hereby certify that the corrections/suggestions from the adjudicators have been incorporated in the revised thesis.

Calicut University  
17.12.2019



**Dr. P. Raveendran**  
(Supervising Teacher)

## **DECLARATION**

It is hereby declared that the thesis entitled **“GREEN COATINGS/PROCESSING USING LIQUID AND SUPERCRITICAL CO<sub>2</sub> WITH NON-FLUOROUS CO<sub>2</sub>-PHILES”** submitted herewith is an authentic record of the research work carried out by me under the supervision of Prof. Dr. P. Raveendran, Department of Chemistry, University of Calicut, in partial fulfilment of the requirements for the award of the degree of Doctor of Philosophy in Chemistry under the Faculty of Sciences, University of Calicut, Kerala. The contents of this thesis have not been submitted to any other institute or University for the award of any degree or diploma.

Calicut University  
17.12.2019

Anu Antony

## ACKNOWLEDGEMENTS

*The work presented in this thesis would not have been possible without the support and guidance of many people who were always with me.*

*At the outset, I would like to acknowledge my indebtedness and sincere gratitude to my supervisor, Prof. Dr. P. Raveendran, Department of Chemistry, University of Calicut for his whole-hearted and infallible guidance, support and encouragement throughout my doctoral research endeavour. I was very fortunate to work under his guidance and without his persistent guidance and support, this dissertation would not have been possible.*

*I would like to thank our Head of the Department, Dr. Yahya. A. I. and all other faculty members of the department for their constant support and their encouragement. My sincere thanks are also due to the non-teaching staff of our department. A special mention for Sri. K. Satheesan for his dedication and sincerity as the Technical Officer of our department.*

*Special thanks to my colleague Ms. Jyothi. P. R. for her support and valuable suggestions throughout my work. I also thank the other members of our research group, Dr. Bindu U., Anju Ajayan, Vineeth M., Sumitha Chandran, Roy K. B. Ajila, Anila and Athira, for their constant support.*

*I gratefully acknowledge the love and support given by all the research scholars of the Department of Chemistry.*

*Dr. Anju. M needs a special mention for her constant support, suggestions and encouragement. I would also like to express my*

*sincere thanks to Bintu Thomas, Anju Paulson, Safna Hussain and Anju of Department of Physics, University of Calicut.*

*I gratefully acknowledge the financial assistance received from UGC and KSCSTE. I acknowledge the support from NIT Calicut, SAIF Mahatma Gandhi University and CSIF University of Calicut for providing me facilities for instrumental analysis.*

*Special thanks are due to my husband for his constant support, understanding and encouragement during my research period.*

*The persons with the greatest indirect contribution to this work are my parents. I place this thesis before my parents. Words cannot express how grateful I am to my father and mother, for all of the sacrifices and struggles that they have made on my behalf. Their prayer for me was what sustained me thus far. I thank them for supporting me for everything. I would also like to thank my brother for his unconditional support and encouragement.*

*I would like to express my thanks to my beloved son Mathew Paul, for being such a good boy, always cheering me up.*

*Finally, I thank almighty for giving me strength and patience to work through all these years for the successful completion of my work. Even during the difficult times of my life, he never let me down instead constantly infused the belief that sooner good times will bless me. I thank him for always showing me the right path and for enlightening my soul with love and compassion for the other human beings.*

Anu Antony

# CONTENTS

	Page No.
<b>Chapter 1 INTRODUCTION</b>	<b>1-28</b>
<b>1.1 Green chemistry</b>	2
<b>1.2 Alternative solvents</b>	7
1.2.1 Water	8
1.2.2 Ionic liquids	9
1.2.3 Fluorous Solvents	10
1.2.4 Supercritical fluids (SCFs)	10
1.2.4.1 Supercritical water	12
<b>1.3 Liquid and supercritical carbon dioxide (scCO<sub>2</sub>)</b>	13
1.3.1 Solvent attributes of CO <sub>2</sub>	14
1.3.2. Solvation of fluorocarbons in CO <sub>2</sub>	15
1.3.3 Polar attributes of scCO <sub>2</sub>	17
1.3.4 Design of non-fluorous CO <sub>2</sub> -philes	20
<b>1.4 Applications of liquid and scCO<sub>2</sub>- A brief summary</b>	21
<b>1.5 Present work</b>	26
<b>Chapter 2 MATERIALS AND METHODS</b>	<b>29-45</b>
<b>2.1 Introduction</b>	29
<b>2.2 Materials</b>	29
<b>2.3 Experimental</b>	33
2.3.1 Supercritical CO <sub>2</sub> Facility	33
2.3.2 Experimental procedure for various applications	35
2.3.2.1 Sizing of yarns using liquid/scCO <sub>2</sub>	35
2.3.2.2 Desizing of sized yarns in scCO <sub>2</sub>	36
2.3.2.3 Sizing of yarns using Ethyl Acetate and Acetone	36
2.3.2.4 Sizing of paper using liquid/scCO <sub>2</sub>	36
2.3.2.5 Impregnation/coating of wood	37
2.3.2.6 Preparation of composites of Urea in scCO <sub>2</sub>	37



2.3.2.7 Preparation of composites of urea in Ethyl Acetate	38
2.3.2.8 Preparation of composites of Urea with combination of coating materials in scCO <sub>2</sub>	38
2.3.2.9 Preparation of Atenolol-exci-pient composites in scCO <sub>2</sub>	38
2.3.2.10 Preparation of Atenolol-exci-pient composites in Ethyl Acetate	39
<b>2.4 Characterization techniques</b>	<b>39</b>
2.4.1 Field Emission Scanning Electron Microscopy (FE-SEM)	40
2.4.2 Stereo Microscope	40
2.4.3 Universal Testing Machine	40
2.4.4 Fourier Transform Infrared (FTIR) Spectroscopy	41
2.4.5 Fourier Transform Raman (FT-Raman) Spectroscopy	41
2.4.5 UV-Visible Spectroscopy (UV-VIS)	42
2.4.6 Atomic Force Microscopy (AFM)	43
2.4.7 Contact angle measurements	43
2.4.8 X-Ray Diffraction (XRD)	44
2.4.9 Thermogravimetry (TG)	44
2.4.10 Cobb <sub>60</sub> * measurement	45
<b>Chapter 3 SIZING AND DESIZING OF COTTON AND POLYESTER YARNS</b>	<b>47-64</b>
<b>3.1 Introduction</b>	<b>47</b>
<b>3.2 Results and Discussion</b>	<b>51</b>
<b>3.3 Summary and Conclusions</b>	<b>63</b>
<b>Chapter 4 SIZING OF PAPER</b>	<b>65-82</b>
<b>4.1 Introduction</b>	<b>65</b>
<b>4.2 Results and Discussion</b>	<b>67</b>
4.2.1 FT-IR-ATR studies	67
4.2.2 FT- Raman studies	69
4.2.4 SEM studies	71
4.2.5 AFM studies	73

4.2.6 Hydrophobicity studies	76
4.2.7 Mechanical properties	80
<b>4.3 Summary and Conclusions</b>	<b>81</b>
<b>Chapter 5 IMPREGNATION/COATING OF WOOD</b>	<b>83-92</b>
<b>5.1 Introduction</b>	<b>83</b>
<b>5.2 Results and Discussion</b>	<b>86</b>
<b>5.3 Summary and Conclusions</b>	<b>92</b>
<b>Chapter 6 COMPOSITES OF UREA WITH CONTROLLED RELEASE PROFILES</b>	<b>93-119</b>
<b>6.1 Introduction</b>	<b>93</b>
6.1.1 Controlled and Slow Release Fertilizers	93
6.1.2 Classification of CRFs	94
6.1.3 Advantages and disadvantages of CRFs	95
6.1.4 Controlled release urea fertilizers	96
<b>6.2 Results and Discussion</b>	<b>100</b>
6.2.1 XRD studies	101
6.2.2 Raman spectroscopic studies	102
6.2.3 Optical microscopic studies	106
6.2.4 SEM Studies	106
6.2.5 Urea release studies	108
6.2.6 Effect of concentration of Urea	111
6.2.7 Combinatorial approach for tailoring the UR release	113
6.2.7.1 XRD studies	114
6.2.7.2 SEM studies	115
6.2.7.3 Urea release kinetics	117
<b>6.3 Summary and Conclusions</b>	<b>118</b>
<b>Chapter 7 PREPARATION OF DRUG-EXCIPIENT COMPOSITES FOR CONTROLLED DRUG RELEASE: THE CASE OF ATENOLOL</b>	<b>121-151</b>
<b>7.1 Introduction</b>	<b>121</b>
7.1.1 Components of medication	121
7.1.2 Amorphous Solid Dispersions	122
7.1.2.1 Importance of amorphous state in pharmaceutical systems	123

7.1.3 Different methods for the preparation of solid dispersions	124
7.1.3.1 Melting method	124
7.1.3.2 Solvent method	126
7.1.4 Supercritical fluid methods	127
7.1.4.1 SCF used as solvent	128
7.1.4.2 SCF used as antisolvent	128
7.1.5 Applications of SCF technologies	131
<b>7.2 Results and Discussion</b>	<b>133</b>
7.2.1 XRD studies	133
7.2.2 Raman spectroscopic studies	137
7.2.3 SEM studies	141
7.2.4 Drug release studies	143
7.2.5 Effect of concentration of drug	147
<b>7.3 Summary and Conclusions</b>	<b>150</b>
<b>Chapter 8 CONCLUSIONS AND OUTLOOK</b>	<b>153-157</b>
<b>REFERENCES</b>	<b>159-191</b>
<b>PUBLICATIONS</b>	
<b>PRESENTATIONS</b>	

## LIST OF TABLE

<i>Table No.</i>	<i>Title</i>	<i>Page No.</i>
1.1.	Critical parameters of some of the generally used SCFs.	12
2.1	List of chemicals used and their purity.	30
3.1	Mechanical properties of bare and sized yarns.	56
3.2	Mass determination studies of bare, sized and desized yarns.	59
3.3	Mechanical properties of CY and PY sized with SOA in conventional solvents (EA and AC).	62
4.1	Topographic parameters obtained by AFM.	75
4.2	Variation in the contact angles for different frames depending on time for RP, SOA, AGLU and PEG-coated papers.	78
4.3	Cobb <sub>60</sub> * values for RP, SOA, AGLU, and PEG-coated papers.	79
4.4	Mechanical properties of RP, SOA, AGLU and PEG-coated papers.	81

## LIST OF FIGURES

<i>Figure No.</i>	<i>Title</i>	<i>Page No.</i>
1.1.	Phase diagram of CO <sub>2</sub> . <sup>28</sup>	13
1.2	Illustration of bond dipoles and atomic charges on atoms of (I) H <sub>2</sub> O and (II) CO <sub>2</sub> . <sup>33</sup>	18
1.3	Schematic of LA-LB interactions between the carbonyl oxygen atom and carbon atom of CO <sub>2</sub> molecule, and also cooperative C-H···O hydrogen bonding between oxygen atom of CO <sub>2</sub> and the C <sub>n</sub> H bond. <sup>33</sup>	19
2.1	Structure of the CO <sub>2</sub> -philes used (I) SOA, (II) AGLU, and (III) PEG.	31
2.2	Structures of (I) Urea and (II) Atenolol.	33
2.3	Schematic diagram (I) and photographic image (II) of the scCO <sub>2</sub> facility.	34
3.1	Pictorial representation for the sizing and desizing of yarn	50
3.2	Optical microscopic images of (a) bare CY b) CY-SOA c) CY-AGLU and d) CY-PEG	52
3.3	Optical microscopic images of a) bare PY b) PY-SOA c) PY-AGLU and d) PY-PEG.	53
3.4	FE-SEM images of a) bare CY b) CY-SOA c) CY-AGLU and d) CY-PEG.	54
3.5	FE-SEM images of (a) bare PY (b) PY-SOA (c) PY-AGLU and (d) PY-PEG.	55
3.6	FE-SEM images of the desized yarns	60
3.7	Sizing using conventional solvents: (a) & (b) Optical microscopic images of CY-SOA-EA and CY-SOA-AC; (c) & (d) FE-SEM images of CY-SOA-EA and CY-SOA-AC.	61
3.8	Sizing using conventional solvents: (a) & (b) Optical microscopic images of PY-SOA-EA and PY-SOA-AC; (c) & (d) FE-SEM images of PY-SOA-EA and PY-SOA-AC.	62

4.1	FT-IR-ATR spectra of a) size compound, b) RP, and c) SP for (I) SOA, (II) AGLU, and (III) PEG.	68
4.2	FT-Raman spectra of a) size compound, b) RP, and c) SP for (I) SOA, (II) AGLU, and (III) PEG.	70
4.3	SEM images of (a) RP, (b) SOA-coated paper, (c) AGLU-coated paper and (d) PEG-coated paper.	72
4.4	AFM images of (a) and (b) RP; (c) and (d) SOA-coated paper; (e) and (f) AGLU-coated paper; and (g) and (h) PEG-coated paper.	74
4.5	Photographs of drop impact on (a) and (b) RP; (c) and (d) SOA-coated paper; (e) and (f) AGLU-coated paper and, (g) and (h) PEG-coated paper at 0 <sup>th</sup> and 72 <sup>nd</sup> frame.	75
5.1	FE-SEM images of a) untreated wood b) treated wood, and optical microscopic images of c) untreated wood d) treated wood.	86
5.2	The FT-IR-ATR spectra of a) SOA, b) untreated wood, and c) treated wood.	88
5.3	FT-Raman spectra of a) SOA, b) untreated wood, and c) treated wood.	89
5.4	X-ray diffractograms of untreated and treated wood samples.	90
5.5	TGA and DTA curves of untreated and SOA-treated wood samples.	91
6.1	XRD pattern for UR, AGLU, SOA, and the different composites prepared using EA and CO <sub>2</sub> : (I) (a) UR (b) AGLU (c) AGLU-UR-EA, and (d) AGLU-UR-CO <sub>2</sub> ; (II) (a) UR (b) SOA (c) SOA-UR-EA, and (d) SOA-UR-CO <sub>2</sub> .	101
6.2	FT-Raman spectra of AGLU and AGLU-UR-CO <sub>2</sub> in different regions: (I) 1720-1770 cm <sup>-1</sup> and (II) 2900-3050 cm <sup>-1</sup> .	103
6.3	FT-Raman spectra of SOA and SOA- UR-CO <sub>2</sub> in different regions: (I) 1720-1780 cm <sup>-1</sup> and (II) 2900-3000 cm <sup>-1</sup> .	104
6.4	FT-Raman spectra of UR and SOA-UR-CO <sub>2</sub> : 990 to 1030 cm <sup>-1</sup> vibrational frequency region.	105
6.5	Optical microscopic images of (a) AGLU-UR-CO <sub>2</sub>	106

---

	and (b) SOA-UR-CO <sub>2</sub> .	
6.6	FE-SEM images of a) UR, b) AGLU, c) AGLU-UR-EA, d) AGLU-UR-CO <sub>2</sub> , e) SOA, f) SOA-UR-EA, and g) SOA-UR-CO <sub>2</sub> .	107
6.7	The release kinetics of UR from AGLU-UR composites prepared in EA and CO <sub>2</sub> .	109
6.8	The release kinetics of UR from SOA-UR composites prepared in EA and CO <sub>2</sub> .	110
6.9	Release kinetics of UR from AGLU matrix with different UR-AGLU ratios.	112
6.10	Release kinetics of UR from SOA matrix with different UR-SOA weight ratios.	112
6.11	XRD patterns for the different composites of UR with varying compositions of AGLU and SOA (a) 100% SOA (b) SOA:AGLU 80:20 (c) SOA:AGLU 60:40 (d) SOA:AGLU 50:50 (e) SOA:AGLU 40:60 (f) SOA: AGLU 20:80 (g) AGLU 100 %.	114
6.12	SEM images of the composites of UR with various combinations of AGLU and SOA. (a) 100% AGLU (b) AGLU:SOA 80:20 (c) AGLU:SOA 60:40 (d) AGLU:SOA 50:50 (e) AGLU:SOA 40:60 (f) AGLU:SOA 20:80 (g) 100% SOA.	116
6.13	Release kinetics of UR from composites prepared using varying amounts of AGLU and SOA.	118
7.1	XRD pattern for AT, AGLU, and the different composites prepared using EA and CO <sub>2</sub> : (a) AT (b) AGLU, (c) AGLU-AT-EA, and (d) AGLU-AT-CO <sub>2</sub> .	134
7.2	XRD pattern for AT, SOA, and the different composites prepared using EA and CO <sub>2</sub> : (a) AT (b) SOA, (c) SOA-AT-EA, and (d) SOA-AT-CO <sub>2</sub> .	135
7.3	XRD patterns for AT, PEG, and the different composites prepared using EA and CO <sub>2</sub> : (a) AT (b) PEG, (c) PEG-AT-EA, and (d) PEG-AT-CO <sub>2</sub> .	136
7.4	FT-Raman spectra of AGLU and AGLU composites at two different regions: (I) 1700-1800 cm <sup>-1</sup> and (II) 2900-3050 cm <sup>-1</sup> .	137
7.5	FT-Raman spectra of SOA and SOA composites at two different regions: (I) 1700-1800 cm <sup>-1</sup> and (II)	138

---

---

	2900-3000 $\text{cm}^{-1}$ .	
7.6	FT-Raman spectra of AT and SOA-AT-CO <sub>2</sub> : 1550 to 1650 $\text{cm}^{-1}$ vibrational frequency region.	139
7.7	FT-Raman spectra of PEG and PEG composites at three different regions.	140
7.8	FT-Raman spectra of AT and PEG-AT-CO <sub>2</sub> in the 1550-1650 $\text{cm}^{-1}$ region.	141
7.9	FE-SEM images of a) AT, b) AGLU, c) AGLU-AT-EA, d) AGLU-AT-CO <sub>2</sub> , e) SOA, f) SOA-AT-EA, g) SOA-AT-CO <sub>2</sub> , h) PEG, i) PEG-AT-EA, and j) PEG-AT-CO <sub>2</sub> , respectively.	142
7.10	Drug release profile of AT from AGLU-AT-EA and AGLU-AT-CO <sub>2</sub> .	144
7.11	Drug release profile of AT from SOA-AT-EA and SOA-AT-CO <sub>2</sub> .	145
7.12	Drug release profile of AT from PEG-AT-EA and PEG-AT-CO <sub>2</sub> .	146
7.13	Drug release kinetics of AT from AGLU matrix with different AT/AGLU ratios.	148
7.14	Drug release kinetics of AT from SOA matrix with different AT/SOA ratios.	149
7.15	Drug release kinetics of AT from PEG matrix with different AT/PEG ratios.	149

---



## LIST OF ABBREVIATIONS

Supercritical	:	sc
Supercritical Fluid	:	SCF
Volatile Organic Compound	:	VOC
Sucrose octaacetate	:	SOA
$\alpha$ -D-Glucose pentaacetate	:	AGLU
Poly(ethylene glycol)	:	PEG
Acetone	:	AC
Ethyl Acetate	:	EA
Urea	:	UR
Atenolol	:	AT

## **PREFACE**

Utilization of liquid and supercritical (sc) CO<sub>2</sub> as an environmentally benign alternative solvent platform has been one of the major themes of green chemistry. Over the years, many novel and innovative industrial strategies using this solvent system have emerged by virtue of the inherent capabilities of this solvent system such as ease of solvent removal and tunability of solvent parameters. In addition to being abundant and inexpensive, this solvent system has many environmentally friendly attributes such as non-toxicity, non-flammability and importantly, easily attainable critical temperature and pressure, making this as an environmentally acceptable and economically viable solvent alternative for the chemical industry. In spite of its limitations in terms of understanding its full solvent capabilities, it has made inroads into several important areas such as fluoropolymer synthesis, dry cleaning, chemical separations and processing, pharmaceutical and textiles industry, microelectronic cleaning, extraction of natural products and synthetic organic chemistry. One of the major challenges in the area was the identification of non-fluorous and inexpensive CO<sub>2</sub>-philes for enabling such applications. It was identified that one can develop CO<sub>2</sub>-philes based on site-specific solute-solvent interactions such as Lewis Acid-Lewis Base interactions and was shown that simple functionalizations such as acetylation of carbohydrates can be employed for the design of inexpensive, non-fluorous CO<sub>2</sub>-philes.

In this work we have employed three non-fluorous CO<sub>2</sub>-philes, viz.,  $\alpha$ -D-Glucose pentaacetate (AGLU), Sucrose octaacetate (SOA) and Poly(ethylene glycol) (PEG; MW 1500). The first two belongs to the class of sugar acetates and the last one belongs to the class of oxygenated polymers. The integration of these CO<sub>2</sub>-philes with liquid/scCO<sub>2</sub>, for developing newer applications in the field of textiles, paper, wood, agricultural and pharmaceutical industries were investigated. Also, liquid/scCO<sub>2</sub> is compared with conventional solvents such as Acetone or Ethyl Acetate for the various applications studied.

The thesis is divided into eight chapters. Chapter 1 provides a detailed introduction to evolution and principles of green chemistry, alternative solvents, supercritical fluids, solvent attributes of scCO<sub>2</sub> and finally the specific objectives of the present work.

The specifications of various materials used, detailed description of supercritical CO<sub>2</sub> facility, methodologies adopted, and characterization techniques have been presented in Chapter 2.

Chapter 3 presents the results of our investigation on the sizing and desizing of cotton and polyester yarns using CO<sub>2</sub>-philes as the size material and liquid/scCO<sub>2</sub> as alternative solvent. Sizing of yarns were also carried out in Acetone and Ethyl Acetate medium and compared.

Chapter 4 presents the sizing of paper using CO<sub>2</sub>-philes as the size material and liquid/scCO<sub>2</sub> as the alternative solvent.

Chapter 5 deals with the study of the impregnation of wood using SOA in scCO<sub>2</sub> medium.

Chapter 6 discusses the preparation of composites of urea with CO<sub>2</sub>-philes using scCO<sub>2</sub> as the solvent for the sustained release of urea. The results obtained are compared with the release kinetics obtained for composites prepared using Ethyl Acetate medium.

Chapter 7 presents the application of scCO<sub>2</sub> as the solvent for the preparation of drug-excipient composites for the sustained release of Atenolol. The results were compared with composites prepared using Ethyl Acetate medium.

Finally, the major conclusions of the work and the future outlook for extending these applications to an industrial level are presented in Chapter 8.

## CHAPTER 1

# INTRODUCTION

---

Chemical industry has been an integral part of man's development in terms of the advancements it made in the diverse areas of human well-being from the development of fertilizers and pesticides for agriculture to new materials for housing and better pharmaceuticals. The quality of human life has significantly improved during the past century. Chemistry had played a significant role in warfare. Chemists were also engaged to aid the military for developing more powerful chemicals and newer technologies. In the post-war scenario, many of these were transformed into benign use with significant commercial potential. The case of DDT (1,1,1-trichloro-2,2-di(4-chlorophenyl)ethane), is a well-documented example.<sup>1</sup> Being a highly potent insecticide, it was used during the war to prevent the spread of typhoid, malaria and some other diseases spread by insects and could save millions of lives during the war. In the post-war days, DDT continued its journey worldwide as an easily available insecticide without anyone foreseeing its hazardous consequences to human health and environment. The public awareness of the hazards and the bioaccumulation of pesticides gathered momentum with significant efforts from Rachel Carson, the American conservationist and journalist. It was her book *The Silent Spring* in 1962 that gathered worldwide attention on how certain chemicals and pesticides affect the biosphere and marked the beginning of a green revolution in chemistry. The author also highlighted the unintended hazards of pesticides on our eco system and human health based on

different scientific reports and materials, and demanded strict environmental regulations to control and limit the widespread use of such harmful chemicals. This book was a warning to the public and also inspired scientists. Motivated by this, the American Congress passed the National Environmental Policy Act (NEPA) in 1969 with the objective to “create and maintain conditions under which man and nature can exist in productive harmony”. In 1970, the U. S. Environmental Protection Agency (EPA) was established by President Richard Nixon for the protection of environment and human health. EPA, as an initial measure, in 1972, banned the domestic use of the pesticide DDT due to its widespread misuse and the negative impact it placed on our earth. In 1987, the *Montreal Protocol* was established by the United Nations - the first treaty in the history to get universal approval; aimed at reducing the production and consumption of ozone depleting substances. In 1990's, scientists began to recognize that pollution prevention requires much more attention than pollution control and accordingly, the Pollution Prevention Act came into effect. For the first time, the phrase “green chemistry” was coined by the staff of the EPA Office of Pollution Prevention and Toxins and by late 1990's, green chemistry and its twelve principles were defined by Paul T. Anastas and John C. Warner in their book *Green chemistry: Theory and Practice*.

## **1.1 Green chemistry**

This increasing concern regarding the environment has led to a growing need for newer technologies that produce the minimum waste and reduce or eliminate the use of toxic substances.<sup>2</sup> The most

important initiative in this context is the envisioning of *green chemistry*. Paul Anastas and John C. Warner defined green chemistry as the “utilization of a set of principles that reduces or eliminates the use or generation of hazardous substances in the design, manufacture and application of chemical products.”<sup>2,3,4</sup> Most of the chemical processes are associated with some risk factors. According to the definition of green chemistry, it is essential to either completely eliminate or to reduce the risk to an acceptable level. Generally, the environmental risk is expressed as a function of hazard and exposure.

$$\text{Risk} = f(\text{Hazard} \times \text{Exposure})^{5,6}$$

Initially, risks were reduced by controlling some of the circumstantial factors such as the use, handling, treatment and disposal of the chemicals. But with the emergence of the concept of sustainable practices, intrinsic factors such as the design and manufacture of less toxic substances, reaction pathways that reduce by-products, etc. are given due importance. In order to accomplish the concept of sustainable practices and bring them into practice, certain guidelines or criteria have to be designed. In this respect, a set of twelve principles were developed as a reference to the green practices and are summarized below.

The first and foremost among the principles of green chemistry is the prevention of waste. Waste is defined as any substance that does not have any value or loss of unutilized energy. Waste can be present in any form, and their impact on our environment solely depends on the various factors such as their nature, toxicity, quantity, and so on.

Always, it is considered better to prevent waste rather than to clean it after the formation and also utmost attention must be kept while choosing a pathway for chemical synthesis such that there is minimal or zero waste produced at the end of the synthesis or chemical process.

In this respect, in 1992, Roger Sheldon introduced a new concept namely Environmental Impact Factor or E-factor. With this approach, one could easily monitor the environmental acceptability of a manufacturing process in chemical industry.

Atom economy, is yet another important concept of green chemistry and this was introduced for the first time by Barry Trost in the year 1990. It is defined as the conversion efficiency of reactants into the final product (in terms of atoms). Atom economy, together with the terms 'selectivity' and 'yield', can be used to evaluate the greenness of a chemical process.

Wherever applicable and possible, it is necessary to employ synthetic methodologies that use and generate only substances that are non-toxic to human health and environment. In the past century, researchers have been working hard to develop new green synthetic strategies that generate non-toxic substances. Some examples of green reactions are C-H activation, olefin metathesis, enzymatic reactions, cycloaddition etc.

Design of safer chemicals is another concept of green chemistry. With the advances in science, it has become very easy to identify toxic substances and the origin of toxicity is often attributed to certain functional groups that are in no way connected to the use of that



compound. By cleverly tailoring the molecules, it is possible that toxic chemicals may be replaced with non-toxic ones, or at least less toxic ones.

Solvents are substances that are essential for the synthesis of a chemical substance but at the same time not an integral part of the compound. The conventional Volatile Organic Compounds (VOCs) used as solvents in most applications are toxic, flammable and corrosive. The reckless use of VOCs presents a serious problem and is also responsible for the pollution of land, air, and water. Recovery and reuse of these conventional solvents are highly energy intensive processes. In an effort to answer all these shortcomings, chemists started to look forward for safer solvent alternatives. Solvent-free processes and usage of alternative solvents such as supercritical fluids, ionic liquids, water etc. are some initiatives in this direction.

Some of the slow chemical reactions can be accelerated with enhanced product yield using catalysts. Green chemistry demands the use of catalysts for chemical transformations. Apart from contributing to higher yield and atom economy, the usage of catalyst can also reduce the consumption of energy to a large extent, since more than thousand transformations could be achieved before the exhaustion of a single catalyst. Replacing traditional stoichiometric strategies with catalytic processes is regarded as the simplest way to improve the efficiency. From the energy perspective, the use of microwave and ultrasound can be opted instead of the conventional heating of the reactants at very high temperatures for longer time.

The use of renewable feedstocks is another concept that needs consideration from the green chemistry perspective. Prolonged use of non-renewable starting materials ends up in the complete depletion of the same. Starting materials obtained from biological or agricultural sources can be regarded as renewable feedstocks and need to be chosen as the starting materials. Lignin, cellulose etc. are some examples for renewable feed stocks.

Utilization of derivatives for protecting some groups, which otherwise can undergo some kind of side reactions, at the given reaction conditions, cause adverse effects on our ecosystem and accordingly, their use has to be controlled.

Green chemical practices also insist on the synthesis of bio-degradable substances and demand that the degradation products must be non-toxic. The functional groups that are susceptible to hydrolysis, any type of cleavage etc. may be structurally incorporated in order to ensure that the degradation products are bio-degradable.

Accidents are very frequent in chemical industries. Bhopal gas tragedy and Love Canal incidents are some instance of the worst chemical accidents in the history of scientific development and took thousands of lives. These accidents are powerful reminders to the chemical community. Utmost attention must be there to replace hazardous chemicals by safer alternatives to prevent chemical accidents and explosions wherever possible.

Real-time monitoring using modern analytical techniques and monitoring systems must be incorporated into the industrial processes for controlling a chemical process from the beginning towards the end.

All these concepts together constitute the twelve principles of green chemistry, aimed at enabling sustainable practices in chemistry.

## **1.2 Alternative solvents**

Solvents play an inevitable role in the field of chemistry and are widely used for chemical separations and processing. The use of organic solvents such as xylene, toluene, benzene etc. in chemical processes is a major environmental concern. Apart from their high volatility, the toxic and flammable nature of these VOC's raises a major threat to the environment. Additionally, these solvents are non-renewable and non-recyclable. The use of such solvents is liable to a series of regulatory controls. Stringent environmental regulations paved the way for solvent-free processes and the use of green solvents such as water, supercritical fluids, ionic liquids, fluoruous solvents, plant based solvents etc.<sup>7,8</sup> To consider a solvent as a green alternative solvent, we need to take into account four factors, namely, their manufacture, distribution, use and disposal of the solvent. While manufacturing a solvent, the raw material used for the preparation, energy and cost requirements, recyclability of the raw material etc. needs utmost attention. The distribution and transportation of the solvent are other issues that require consideration. Easily and locally available solvents are the most preferred. The complete information (both physical and chemical properties) of the solvent must be known

before its use, since the properties such as melting point, boiling point, viscosity, density, corrosiveness etc. decides its mode of use, safety precautions, environmental, chemical and engineering considerations that must be enforced. Finally, the disposal of the solvent is an unavoidable part that requires keen attention as this stage ends up in severe damage to our ecosystem. The solvents that can be recycled and reused easily via various methods such as distillation, separation etc. stands superior to those solvents whose processing is too tedious with higher rates of economic and energy consumption. With reference to the aforementioned factors, the recyclability, cost, environmental impact, solvating power, and ease of use, of some of the customary alternative solvents are briefly discussed in the next section.

### **1.2.1 Water**

Water is a readily available, ubiquitous solvent, but purification of water is an uneconomical process. While water is used as an alternative solvent in many organic separations and synthesis, in most cases, water is unable to dissolve compounds of low polarity due to its high dielectric constant and cooperative network of hydrogen bonds.<sup>9</sup> In view of the poor solubility of most of the organic compounds in water, the use of water as an alternative solvent was restricted mostly to hydrolysis reactions. In fact, nature uses water as the solvent for the synthesis of many complex molecules in biological systems. In the recent years, researchers established that water acts as an excellent solvent for many other organic reactions such as cyclopropanation of olefins, Michael additions etc.<sup>10</sup> The high energy cost required for the removal of water is a serious limitation in using it as an alternative

solvent, due to its high heat capacity and latent heat of vaporization. Proper treatment of contaminated water is another important issue that requires an adequate consideration.

### **1.2.2 Ionic liquids**

Ionic liquids are salts that exist in liquid state and are made up of positively and negatively charged ions. These solvent systems have already replaced conventional VOC's in a variety of chemical reactions such as Friedel Crafts alkylation, reduction of aromatic rings, carbonylation etc.<sup>10</sup> Manufacture of ionic liquids is a multistep process and their manufacturing and purification are energy intensive processes. Separation and reuse of ionic liquids are not very energy intensive. Negligible vapour pressure, low viscosity, low melting point, wide liquid range and non-flammability are the most important properties that are taken into account while considering ionic liquids as green alternative solvents.<sup>9,11,12</sup> Ionic liquids are polar in nature and hence can solubilize many organic and inorganic materials. With the appropriate selection of cations and anions, the properties of ionic liquids can be tuned according to our desired needs and hence they are also known as designer solvents. Low vapour pressure of ionic liquids merely doesn't convey that they are green solvents. Most of the ionic liquids are soluble in water and have a mere chance for entering into the aquatic environment causing pollution. The environmental impact of ionic liquids is still not completely known and research works are been done in this direction.

### **1.2.3 Fluorous Solvents**

Highly fluorinated compounds such as perfluoroalkylethers, perfluoroalkenes etc. are considered as fluorous solvents and they are non-toxic, non-flammable and thermally stable.<sup>9,10</sup> They can be reused and are mostly used in biphasic systems. Much like ionic liquids, the manufacturing and purification of fluorous solvents are multi step, energy intensive process, consuming immense amount of VOC's. They have very low polarity and are generally volatile, depending on the chain length. Fluorous solvents have very high density, poor solvent strength and low solubility in water and organic solvents. Being non-polar in nature, they cannot be used in majority of the organic reactions as a solvent replacement; instead, they are used in combination with a conventional solvent to form a biphasic system. Oxidation reactions, bromination and chlorination of alcohols etc. are some of the chemical reactions wherein fluorous solvents have replaced conventional solvents. Incineration of fluoro compounds is a highly energy intensive process and can also lead to some harmful by-products which need to be treated further. These solvents persist for longer time in our environment and these bioaccumulate instead of biodegradation.

### **1.2.4 Supercritical fluids (SCFs)**

In 1822, Baron Charles Cagniard de la Tour discovered SCFs accidentally while conducting experiments related to heated fluids. In 1879, Hannay and Hogarth were the ones who demonstrated that SCFs possesses solvating power.<sup>13</sup> A substance existing at a temperature and pressure above its critical point is said to be in the supercritical state.

At the supercritical state, the substance exhibits both liquid-like and gas-like properties, which can be tuned by just varying the temperature and pressure. SCFs show gas-like molecular diffusion and liquid-like density, and the diffusion coefficient is intermediate to that of gas and liquid.<sup>13,14</sup> They have excellent ability to penetrate into porous materials much like a gas and dissolve substances as liquids do. Separation and drying via simple expansion is the foremost advantage of using SCFs. The recovered gas can be recycled and reused as such, without the need of any further purification steps. Another benefit of replacing conventional organic solvents lays on the minimum energy consumption during operation. Additionally, the thermo physical properties of SCFs such as diffusivity, viscosity, dielectric constant etc. can be tuned by simply varying the operating temperature and/or pressure. All these favourable solvent attributes of SCFs make them a good candidate as green alternative solvents.<sup>7,8,9</sup> Nowadays, SCFs are considered as greener alternatives to toxic greenhouse gases and fluids used in air conditioners, refrigerators etc. replacing ammonia, propane, sulfur dioxide and chlorofluorocarbons. Researchers began to consider SCFs as alternative reaction media by the end of 1980's. Already, attempts have been made to develop several processes using SCFs in pharmaceutical, textile and food industries.<sup>15</sup> Some of the substances that are commonly used as SCFs are methanol, ethanol, CO<sub>2</sub>, water, methane and ethane. Critical parameters of several SCFs mentioned above are provided in Table 1.1.

**Table 1.1** Critical parameters of some of the generally used SCFs.<sup>16</sup>

<b>Substance</b>	<b>Critical Temperature (<sup>0</sup>C)</b>	<b>Critical Pressure (bar)</b>
Methanol	240	79.5
Ethanol	241	63
Carbon dioxide	31.1	73.8
Water	374	220
Ethane	32.2	48.72
Propane	97	42.49

Although, methanol, ethanol, ethane etc. has been rarely used as SCFs, some applications using these SCFs are reported. For example, supercritical methanol is used as reactant for biodiesel production.<sup>17</sup> Preparation of titania/carbon nanotube composites using supercritical ethanol and metallic copper nanoparticles using supercritical ethane have been reported.<sup>18,19</sup> Among all, the most common SCFs being employed as alternative solvents for chemical separations and processing are supercritical water and CO<sub>2</sub>, respectively.

#### **1.2.4.1 Supercritical water**

Water being abundant and easily available, supercritical (sc) water also gained attention as an alternative solvent and has been used for non-catalytic Beckman and Pinacol rearrangements, etc.<sup>20,21,22</sup> It has been reported that, on varying temperature and pressure, the dielectric properties of scH<sub>2</sub>O can be switched over a wide range to achieve the polarities of common solvents in use. Also, scH<sub>2</sub>O shows enhanced



solubility and catalytic efficiency than water. Higher reaction rates, low viscosity, low surface tension, lesser extent of hydrogen bonding and higher solubility of non-polar organic compounds are some of the major features associated with the use of scH<sub>2</sub>O.<sup>20,23-25</sup> By simple adjustment of temperature and pressure, the properties of reaction medium can be varied over a very wide range of conditions. The limitations associated with the use of scH<sub>2</sub>O are its highly corrosive nature and the extreme working conditions.

### 1.3 Liquid and supercritical carbon dioxide

Utilization of liquid and scCO<sub>2</sub> as greener alternative platforms has received significant attention in the past couple of decades. ScCO<sub>2</sub> is arguably the greenest among the solvent alternatives discussed in the previous sections due to its low cost, non-flammability, non-toxicity, recyclability, abundance, moderate critical temperature and pressure (31.1 °C and 73.8 bar) and tunable solvent properties.<sup>26-29</sup> Phase diagram of CO<sub>2</sub> is shown in Figure 1.1.

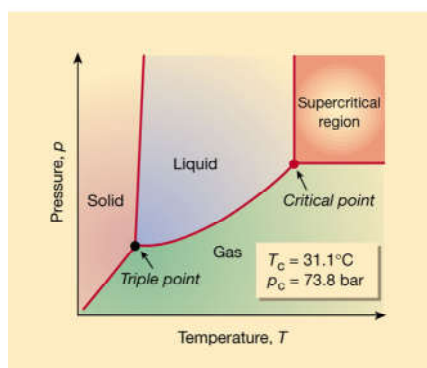


**Figure 1.1** Phase diagram of CO<sub>2</sub>.<sup>28</sup>

The ease of solvent removal is one of the major advantages associated with the use of scCO<sub>2</sub> as an alternative solvent and the products obtained after CO<sub>2</sub> processing are completely dry without any residual solvent left behind. CO<sub>2</sub> is identified as a “greenhouse” gas and accordingly, the atmospheric emission of this gas have to be reduced. By recycling CO<sub>2</sub> gas (collected as by-products from various industrial processes) and utilizing it for various chemical manufacturing and processing helps to reduce the level of emissions to the atmosphere. Also, reports say that the threshold limit value (TLV) of CO<sub>2</sub> is higher than conventional solvents such as Acetone, Chloroform, Pentane etc.

28

### 1.3.1 Solvent attributes of CO<sub>2</sub>

In order to effectively utilize CO<sub>2</sub> as a solvent, one needs to examine the solvent attributes of CO<sub>2</sub>. Generally, scCO<sub>2</sub> is considered as a feeble solvent for ionic, highly polar and high molecular weight compounds because of its low dielectric constant.<sup>29</sup>

CO<sub>2</sub> is a linear triatomic molecule belonging to the D<sub>∞h</sub> point group and thus considered as a non-polar solvent. The zero dipole moment of CO<sub>2</sub>, arising directly as a consequence of the shape of the molecule, is responsible for its very low dielectric constant. The rule of thumb for solvation is “*like dissolves like*”. So, normally one would expect that the non-polar hydrocarbons and amphiphilic systems will be soluble in the “non-polar CO<sub>2</sub>”. In fact, the dielectric constant of liquid/scCO<sub>2</sub> is even lower than that of hydrocarbons and so it was expected that CO<sub>2</sub> could be a good replacement for the hydrocarbon solvents. Contrary to these expectations, Consani and Smith showed that, in fact, many of the hydrocarbon-based molecular systems are actually insoluble in

CO<sub>2</sub>.<sup>30</sup> This led researchers to examine the microscopic aspects of solvation in more detail.

Despite the net dipole moment of the CO<sub>2</sub> molecule being zero, it has a significant quadrupole moment associated with it and on that account, CO<sub>2</sub> was often referred to as a quadrupolar solvent.<sup>31,32</sup> Dipole-quadrupole interactions were used to explain the anomalous solvent attributes of CO<sub>2</sub>. The idea about more site-specific interactions was also evoked to explain solvation in scCO<sub>2</sub>. One important study that shed more light into this is the comparison between the solvation of CO and CO<sub>2</sub> in H<sub>2</sub>O.<sup>33</sup> CO being a smaller molecule than CO<sub>2</sub> and also a molecule having a non-zero dipole moment, one would expect CO to show high solubility in H<sub>2</sub>O. But contrary to these expectations, CO<sub>2</sub> shows high solubility in H<sub>2</sub>O. This may be attributed to a profound, specific, solute-solvent interaction arising as a result of hydrogen bonding between the oxygen atom of CO<sub>2</sub> and hydrogen atom of H<sub>2</sub>O, since charge separation in CO<sub>2</sub> are on par with H<sub>2</sub>O molecule. Sato et al. has provided evidence for the solute-solvent interaction in the solvation of CO<sub>2</sub> by H<sub>2</sub>O with the aid of molecular dynamics study.<sup>34</sup> Such site-specific, solute-solvent interactions are less important between CO and H<sub>2</sub>O molecules. It was concluded that CO<sub>2</sub> can be considered as a non-polar solvent with polar attributes.<sup>33</sup>

### **1.3.2. Solvation of fluorocarbons in CO<sub>2</sub>**

By late 1980's, the usage of scCO<sub>2</sub> as an alternative solvent was almost dismissed by researchers due to the poor CO<sub>2</sub>-philicity of most of the common molecular systems.<sup>35</sup> This made researchers to think of identifying CO<sub>2</sub>-philic molecular systems that can be attached to enhance the solubility of otherwise CO<sub>2</sub>-insoluble molecules.

Interestingly, in 1992, for the first time, DeSimone et al. reported the solubility of poly(perfluoroalkyl acrylate) (Poly(FOA)) with larger number of repeating units in CO<sub>2</sub> and accordingly suggested the synthesis of polymers and copolymers using fluorinated monomers.<sup>36</sup> It was also demonstrated that the fluorocarbon systems have high solubility in CO<sub>2</sub> while the corresponding non-fluorous counterparts were completely insoluble in CO<sub>2</sub>. Thereupon, lot of research was focussed on explaining the CO<sub>2</sub>-philic nature of fluoro compounds to investigate if there is any site-specific interactions existing between CO<sub>2</sub> and the fluorinated compounds with the aid of FT-IR, <sup>1</sup>H and <sup>19</sup>F NMR, etc. A research team lead by Yee et al. investigated the CO<sub>2</sub>-philic nature of these compounds using FT-IR spectroscopy, but couldn't observe any interactions but rather could conclude that the high repulsive nature of fluorocarbon-fluorocarbon interactions is responsible for its high solubility.<sup>37</sup> Later, Dardin et al. examined the solubility of n-hexane (C<sub>6</sub>H<sub>14</sub>) and perfluoro-n-hexane (C<sub>6</sub>F<sub>14</sub>) in CO<sub>2</sub> with the aid of <sup>1</sup>H and <sup>19</sup>F NMR technique, although they could not observe any specific interaction between C<sub>6</sub>H<sub>14</sub> and CO<sub>2</sub>, but could observe a small chemical shift in the C<sub>6</sub>F<sub>14</sub> spectra, which they attributed to van der Waals interactions between C<sub>6</sub>F<sub>14</sub> and CO<sub>2</sub>.<sup>38</sup> Kazarian et al. also investigated the interactions between poly(vinylfluoride) and CO<sub>2</sub> and could observe a small splitting in CO<sub>2</sub> bending mode of vibration and hence concluded that weak CO<sub>2</sub>-F interactions are responsible for its solubility in CO<sub>2</sub>.<sup>39</sup> The discrepancies in NMR results for different compounds compared were reported to be due to structural and electronic differences between these molecules.<sup>40</sup> Even now, there are conflicting views among the researchers regarding the solvation of fluorinated compounds in scCO<sub>2</sub>. It is largely believed that the non-directional, dispersive

interactions are largely responsible for the high miscibility of fluoro compounds with liquid and scCO<sub>2</sub>. Since fluorocarbons are miscible with liquid and scCO<sub>2</sub>, researchers considered fluorination and the attachment of fluorocarbon moieties to other molecules for the design of functional CO<sub>2</sub>-philes such as surfactants. It was also considered that the extent of CO<sub>2</sub>-philicity is a function of the extent of fluorination. Later, Raveendran et al., using computational quantum chemistry, studied the effect of step-wise fluorination on the CO<sub>2</sub>-philicity of methane and concluded that in partially fluorinated molecules, the F atom acts as a weak Lewis Base and interacts with the electron deficient carbon atom of CO<sub>2</sub>, and the hydrogen acquires a positive charge and interacts with the electron rich oxygen atoms in CO<sub>2</sub>.<sup>41</sup> The results indicated that there could be a turnover concentration of fluorine atoms, beyond which one may expect a reduction in the CO<sub>2</sub>-philicity.

### **1.3.3 Polar attributes of scCO<sub>2</sub>**

Previous studies indicated that one needs to have a detailed, microscopic understanding of the solvation phenomena in CO<sub>2</sub> for enabling the utilization of scCO<sub>2</sub> as an alternative solvent. In fact, CO<sub>2</sub> is a charge-separated molecule with a partial negative charge on the electronegative oxygen atoms and a partial positive charge on the carbon atom. Thus the carbon atom can act as a weak Lewis Acid (LA) and the oxygen atoms as weak Lewis Base (LB) making it a solvent system wherein LA-LB type interactions can govern the solvation in it.<sup>32</sup> A comparison of the atomic charges and bond dipoles on individual atoms of H<sub>2</sub>O and CO<sub>2</sub> were reported by Raveendran et al.<sup>33</sup> and is shown in Figure 1.2. It reveals that the charge separations in

both the molecules resemble very closely. It must be borne in mind that charges are only an abstract representation of the electron density distribution in the molecule. In fact, one observes significant difference in the solvent behaviour of CO<sub>2</sub> and water. Water, with its extensive networks of cooperative hydrogen bonds can act as an excellent solvent for polar units. In fact, these hydrogen bond networks break down when water is brought to supercritical conditions leading to a low dielectric constant. A faster, intra-chain, proton transfer mechanism was suggested in such situations to explain the observed reaction selectivity and enhanced reaction rates in such situations.<sup>22</sup>

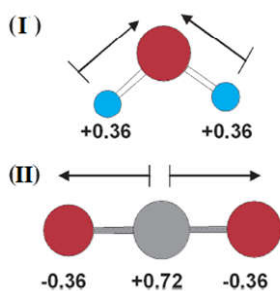


**Figure 1.2** Illustration of bond dipoles and atomic charges on atoms of (I) H<sub>2</sub>O and (II) CO<sub>2</sub>.<sup>33</sup>

Based on the *ab initio* quantum chemical calculations on several carbonyl containing prototype molecules, Raveendran et al<sup>42</sup> suggested that carbonyl containing compounds may be solvated in CO<sub>2</sub>.

Interaction between CO<sub>2</sub> and sp<sup>3</sup> C atom of methanol and dimethyl ether were also reported.<sup>43,44</sup> For ester groups, both ether oxygen and the carbonyl group contribute to the solvation in CO<sub>2</sub>.<sup>45</sup> The same was responsible for the solubility of certain polymers in liquid/scCO<sub>2</sub>.<sup>46,47</sup>

Raveendran et al. also demonstrated that for systems such as Methyl Acetate, the oxygen atom in CO<sub>2</sub> can also form a cooperative C–H···O hydrogen bond with electron deficient hydrogen atoms attached to the  $\alpha$ -carbon atom attached to the carbonyl group (Figure 1.3).<sup>42</sup>

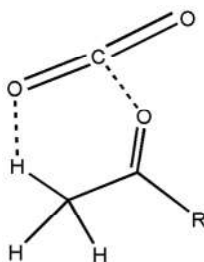


**Figure 1.3** Schematic of LA-LB interactions between the carbonyl oxygen atom and carbon atom of CO<sub>2</sub> molecule, and also cooperative C–H···O hydrogen bonding between oxygen atom of CO<sub>2</sub> and the C <sub>$\alpha$</sub> H bond.<sup>33</sup>

In support of the theoretical calculations, they also reported a blue-shift in the frequency of the C-H stretching mode and a red-shift in the frequency of the carbonyl stretching mode, respectively, in the Raman spectrum of the Acetaldehyde-CO<sub>2</sub> complex.<sup>48</sup> Other molecular systems such as phenol<sup>49</sup> and CH<sub>3</sub>F<sup>41,50</sup> were also observed to be capable of forming both conventional and non-conventional hydrogen bonds with CO<sub>2</sub>.

### 1.3.4 Design of non-fluorous CO<sub>2</sub>-philes

The high cost and low environmental acceptability of fluorocarbon-based compounds were the major limiting factors in further development using this class of CO<sub>2</sub>-philes and the applications were restricted to areas where fluoro compounds are used generally. As an initial attempt to develop non-fluorous CO<sub>2</sub>-philes, Sarbu et al. investigated the solubility of non-fluorous polymers in scCO<sub>2</sub>.<sup>51</sup> In one of the pioneering studies, Kazarian et al. had demonstrated using IR spectroscopy that there exists site-specific interactions between CO<sub>2</sub> and carbonyl groups.<sup>39</sup> This observation was followed by many works in which polymers were incorporated with oxygen containing functional groups to enhance its solubility in CO<sub>2</sub> for example, Kilic et al. studied the phase behaviour of oxygen containing polymers in CO<sub>2</sub>.<sup>52</sup>

Later, guided by theory, Raveendran et al. demonstrated that acetylation of naturally occurring poly-hydroxy systems such as carbohydrates can be used as a method for the development of an inexpensive, environmentally benign and renewable class of CO<sub>2</sub>-philes.<sup>53</sup> In fact, these compounds are widely used in food, pharmaceutical applications, etc. It was shown that peracetylated sugars such as D-Glucose pentaacetate ( $\alpha$  and  $\beta$  forms),  $\beta$ -D-galactose pentaacetate, Sucrose octaacetate, and acetylated cyclodextrins are all highly miscible with liquid and scCO<sub>2</sub>.<sup>53-57</sup> Crystallization of some of these carbohydrates was also demonstrated by Raveendran et al.<sup>58</sup> Absorption of CO<sub>2</sub> by some of the aforementioned sugar acetates were studied using quartz crystal microbalance.<sup>59</sup> In 2006, Wallen et al.



reported the change in crystallinity of some sugar acetates and acetylated cyclodextrins using Sum Frequency Generation (SFG) spectroscopy and Differential Scanning Calorimetry (DSC) technique.<sup>60</sup> Another work of Enick et al. included the study of global phase behaviour of  $\beta$ -D-maltose octaacetate, validating the LA-LB and cooperative hydrogen bond interactions between carbonyl group of sugar acetates and CO<sub>2</sub>.<sup>61</sup>

Another strategy employed to overcome the poor solvent strength of CO<sub>2</sub> is to identify surfactants that form thermodynamically stable water-in-CO<sub>2</sub> reverse microemulsions.<sup>62</sup> Initially, it was observed that surfactants used in hydrocarbon solvents are not suitable for scCO<sub>2</sub>; instead certain CO<sub>2</sub>-philes are to be identified.<sup>30,63,64</sup> Initially, fluorocarbon,<sup>65,66</sup> silicone<sup>67-69</sup> and fluorinated analogues<sup>70,71</sup> of AOT surfactants were identified. Later on, researchers were successful in identifying non-fluorinated surfactants, capable of stabilizing water-in-CO<sub>2</sub> microemulsions. Also, Eastoe et al.<sup>72</sup> synthesized environment friendly, CO<sub>2</sub>-philic O-surfactants by adding oxygen into the surfactants, thereby sustaining the stability of water in CO<sub>2</sub> emulsions and their design was based on acetylated sugars. Based on reports regarding various interactions between CO<sub>2</sub> and polymers, certain polymers were expected to be soluble in scCO<sub>2</sub>.<sup>39,47,73</sup>

#### **1.4 Applications of liquid and scCO<sub>2</sub>- A brief summary**

Supercritical CO<sub>2</sub> has already made inroads into many areas in industry. Historically, extraction of natural products using scCO<sub>2</sub> is considered as the oldest and the most developed industrial application,

with wide applications especially in food industry.<sup>78</sup> Among the various extractions carried out using scCO<sub>2</sub>, decaffeination of caffeine is the first commercialized one.<sup>78</sup> Extraction of hops during the beer brewing process is yet another important application using scCO<sub>2</sub>. Other examples for extractions using scCO<sub>2</sub> includes, extraction of fats and oils, extraction of cholesterol, lipids etc.<sup>79-81</sup> Later, scCO<sub>2</sub> was also applied for extractions in pharmaceutical, forensic and nutraceutical industry.<sup>82</sup> In addition to extraction, SCF chromatography is another SCF technology that has been commonly used as an alternative to conventional liquid chromatographic separation and this technique has found application in food and pharmaceutical industries.

ScCO<sub>2</sub> has also gained much attention in the area of polymer synthesis and processing. As already mentioned, DeSimone et al. has synthesised fluoropolymers for the first time, using CO<sub>2</sub> as a solvent, based on its very high solubility in CO<sub>2</sub>.<sup>36</sup> Synthesis of CO<sub>2</sub>-soluble surfactants were reported by many groups, since surfactants plays a significant role in the synthesis of polymers and other polymer processing includes extractions, coatings, drug delivery and so on.<sup>83</sup> Nowadays, scCO<sub>2</sub> is regarded as the most viable and promising alternative solvent for polymerization and processing.<sup>84-88</sup> CO<sub>2</sub> is known to plasticize a variety of amorphous polymers and is able to significantly reduce their glass transition temperatures. Preparation of polymer composites and control of their morphology are still major challenges in biomaterials processing.<sup>89,90</sup> Howdle and co-workers have reported that scCO<sub>2</sub> can be used to synthesize polymeric composites incorporating guest materials without any loss of activity

of the polymer.<sup>91</sup> Application of scCO<sub>2</sub> in the production of polymer systems for drug delivery is already well established.<sup>92</sup>

SCF technology also presents possibility in the field of photolithographic technology wherein no solvent of any kind, whether organic/aqueous are used in coating, in any of the developing steps.<sup>83,93</sup>

Nanochemistry, a recently emerged and fast growing branch of chemistry, is always grateful to supercritical fluid technologies since numerous novel works are reported in this area.<sup>94-96</sup> Precipitation of particles into micro- and nano- particles can be easily achieved using supercritical fluid technologies instead of conventional methods such as spray-drying, freeze-drying etc.<sup>97,98</sup> Many drawbacks associated with the conventional methods such as solute degradation, residual solvent concentration, poor control on particle size, structural changes etc. can be rectified or completely eliminated by replacing them with scCO<sub>2</sub>. Rapid expansion of supercritical solutions (RESS), supercritical antisolvent precipitation etc. are some of the SCF techniques proposed for the particle formation especially for pharmaceutical applications wherein solubility and bioavailability of pharmaceutical compounds can be increased by size reduction.<sup>99</sup> In pharmaceutical industry, SCFs are mainly utilized for the purpose of micronization, preparation of solid dispersions and polymorphic control.<sup>100,101</sup>

By now, dyeing processes using scCO<sub>2</sub> as dyeing solvent is a sought after process in textile industry.<sup>102,103</sup> Disadvantages associated with conventional dyeing process such as generation of huge amount of

waste water, energy-intensive drying process etc. can be eliminated. Low viscosity and high diffusion rate of scCO<sub>2</sub> facilitates CO<sub>2</sub>-dye mixture to penetrate into the material. Likewise, it is well established that liquid/scCO<sub>2</sub> can be used for dry-cleaning applications. It is considered as the ideal and sustainable alternative to perchloroethylene (PER) in dry-cleaning process.<sup>104</sup> Supercritical drying of materials, particularly in the case of mesoporous/ supermicroporous materials, is another important application of SCFs.<sup>105</sup> SCF technology is considered as the best alternative to conventional drying processes wherein the final product is efficiently dried without the requirement for high temperature. Decontamination of soil using scCO<sub>2</sub> is yet another application which has gained considerable attention and is considered as an attractive alternative to conventional method involving extraction with liquid solvents.<sup>106</sup>

ScCO<sub>2</sub> has also found applications in the field of microelectronics as cleaning agents and is mainly applied for organic contamination removal.<sup>107</sup> SCFs have also been explored as reaction media where phase-transfer catalysis (PTC) is employed.<sup>108</sup> PTC is an important and effective method to conduct heterogeneous reactions with the aid of a catalyst. In 1996, Dillow and co-workers reported the first example of a PTC reaction carried out in scCO<sub>2</sub>.<sup>109</sup> This was followed by a series of PTC reactions carried out in scCO<sub>2</sub>.<sup>110</sup> In some particular cases, co-solvent is used in order to ensure complete dissolution in scCO<sub>2</sub>.

SCF technology have also found interesting applications in the area of synthetic organic chemistry.<sup>111</sup> Hydrogenation reactions such as homogeneous catalytic, asymmetric and continuous hydrogenation etc.

are very common and frequently reported reactions in scCO<sub>2</sub>.<sup>112,113</sup> Hydroformylation reactions, much similar to hydrogenation reactions, which are traditionally carried out in liquid solvent media are nowadays replaced with scCO<sub>2</sub>.<sup>114</sup> Photochemical and radical reactions such as free radical halogenation reactions and thermally initiated radical reactions, are also performed in scCO<sub>2</sub>.<sup>115</sup> Diels-Alder cycloaddition, Friedal-Crafts alkylation, Heck reactions etc. are some common name reactions carried out in scCO<sub>2</sub> medium.<sup>111,116,117</sup> Researchers have also identified that scCO<sub>2</sub> medium may be used to perform oxidation reactions such as catalytic aerobic oxidation and oxidation by alkyl peroxide.<sup>118</sup> Palladium mediated coupling reactions in scCO<sub>2</sub> are also reported.<sup>119</sup>

Owing to the interesting features of scCO<sub>2</sub>, significant interests have been developed in the preparation of environmentally friendly coatings.<sup>120</sup> The use of CO<sub>2</sub> as a solvent or co-solvent in the coating related applications has gained much more attention due to the environmental concerns over the adverse effect of conventional solvents. Some processing as well as commercial profits are also claimed for the use of CO<sub>2</sub> in coating applications. Solvent properties of CO<sub>2</sub> are much improved at higher liquid densities and at the same time viscosities and interfacial tension are observed to be lower than conventional solvents; enabling them to easily facilitate the transport of solvent to the imperfections on the surface to be covered, which is highly beneficial for the coating on etched surfaces.<sup>121</sup>

## 1.5 Present work

The present work targets the utilization of liquid/scCO<sub>2</sub> as a green alternative solvent for various coatings/processing making use of inexpensive CO<sub>2</sub>-philes. It is expected that the integration of these CO<sub>2</sub>-philes with liquid/scCO<sub>2</sub> would pave the lane for newer applications in the field of textiles, paper, wood, agricultural and pharmaceutical industries. In this work, we are investigating the possibility of utilizing a combination of liquid/scCO<sub>2</sub> and CO<sub>2</sub>-philes for coatings/chemical processing applications.

In this work, we have employed three CO<sub>2</sub>-philes, viz.,  $\alpha$ -D-Glucose pentaacetate (AGLU), Sucrose octaacetate (SOA) and Poly(ethylene glycol) (PEG; MW 1500). The first two belongs to the class of sugar acetates and the last one belongs to the class of oxygenated polymers. Factors responsible for their CO<sub>2</sub>-philic nature have already been discussed.

The five acetate groups attached to the Glucose ring plausibly involves in strong intermolecular interactions between the acetate groups and thus results in significant lattice energy resulting in high melting point for these systems. Lattice energy is observed to be lower for SOA as evidenced by its low melting point in spite of its very high molecular weight. Interestingly, after treatment with CO<sub>2</sub>, SOA forms a glass while AGLU forms a crystalline material. In fact, it has been reported by a team of researchers that the CO<sub>2</sub>-treated SOA has a glass transition at around 25.8 °C.<sup>60,122</sup> In the case of PEG, which is generally hydrophilic, the CO<sub>2</sub>-induced deliquescence may be due to

the LA–LB interactions between the carbon atom of the CO<sub>2</sub> molecule and ether oxygen of PEG. Upon CO<sub>2</sub> treatment PEG transforms from a semi crystalline state to an amorphous state.<sup>122</sup>

*This thesis is divided into eight chapters:*

- Chapter 2 summaries the specifications of various materials used, detailed description of scCO<sub>2</sub> facility, methodologies and characterization techniques implemented for the present research work.
- Chapter 3 furnishes the results of our investigation on the sizing and desizing of cotton and polyester yarns using CO<sub>2</sub>-philes as the size material and liquid/scCO<sub>2</sub> as alternative solvent. Sizing of yarns were also carried out in Acetone and Ethyl Acetate medium and compared.
- Chapter 4 presents the results of sizing of paper using CO<sub>2</sub>-philes as the size material and liquid/scCO<sub>2</sub> as alternative solvent.
- Chapter 5 deals with the study of the impregnation/coating of wood with SOA using scCO<sub>2</sub> medium.
- Chapter 6 discusses the preparation of composites of Urea with sugar acetates using scCO<sub>2</sub> for sustained release of Urea and the kinetics of release of Urea from those composites. The results are compared with the release kinetics for composites prepared using Ethyl Acetate medium.

- Chapter 7 presents the application of scCO<sub>2</sub> as solvent for the preparation of drug-excipient composites using Atenolol as the drug with the model CO<sub>2</sub>-philic systems as excipients. The results are compared with the composites prepared using Ethyl Acetate medium.
- Chapter 8 summarises the highlights of the work and presents future scope and perspectives of extending these applications to an industrial level.



## CHAPTER 2

# **MATERIALS AND METHODS**

---

### **2.1 Introduction**

The appropriate choice of the materials together with the adopted experimental conditions plays a vital role in deciding the extent of solution to a research problem. In the CO<sub>2</sub>-based processes, control of pressure and temperature are the two important factors which may determine the morphology and texture of CO<sub>2</sub>-processed materials. This chapter describes the materials used throughout the work, detailed experimental set up of the supercritical CO<sub>2</sub> facility, experimental procedures and finally a brief description of various characterization techniques employed for the present work.

### **2.2 Materials**

All the chemicals used are of analytical grade and are used as received without any further purification. List of chemicals used for this research work are provided in Table 2.1.

**Table 2.1** List of chemicals used and their purity.

<b>Material</b>	<b>Abbreviation</b>	<b>Company</b>	<b>Purity</b>
Carbon dioxide	CO <sub>2</sub>	Chemix gases	SCF grade
Sucrose octaacetate	SOA	Sigma Aldrich	98%
Alpha-D-Glucose pentaacetate	AGLU	Sigma Aldrich	99%
Poly(ethylene glycol) (M.W.1500)	PEG	Sigma Aldrich	Bio ultra-grade
Urea	UR	Hi-Media	99%
Atenolol	AT	Sigma Aldrich	≥98%
Acetone	AC	Nice chemicals	99%
Ethyl Acetate	EA	Nice chemicals	≥99%

Three different CO<sub>2</sub>-philes viz., SOA, AGLU and PEG are used in the present work in light of their environmentally benign features. SOA and AGLU are biocompatible, inexpensive and renewable materials. PEG is widely used in food, cosmetic and other various industries due to its benign attributes such as low cost, biocompatibility and low volatility. Detailed description of these three CO<sub>2</sub>-philes and their structures are provided in Figure 2.1.

**Sucrose octaacetate (SOA)**, an acetylated derivative of Sucrose, has a molecular weight of 678.59 g/mol and melts at 83 °C. It is widely used as a bitterant and also as an inert agent in pesticides and herbicides. SOA is an excellent CO<sub>2</sub>-phile which is highly miscible with CO<sub>2</sub> and at 35 °C, SOA begins to melt at 26 bar and at 50 bar SOA is in a

complete melt state. SOA is observed to be completely soluble in liquid and scCO<sub>2</sub>.

**Alpha-D-Glucose pentaacetate (AGLU)**, an acetylated derivative of D(+)-Glucose, where in five hydroxyl groups are replaced by acetate groups, has a molecular weight of 390.34 g/mol and melts at 109-111 °C. Alike SOA, AGLU is also a CO<sub>2</sub>-phile showing high miscibility with CO<sub>2</sub>, i.e. at 35 °C, AGLU begins to melt at 54 bar and is in a complete melt state at 65 bar. Similar to SOA, AGLU is also observed to be completely soluble in liquid and scCO<sub>2</sub>.

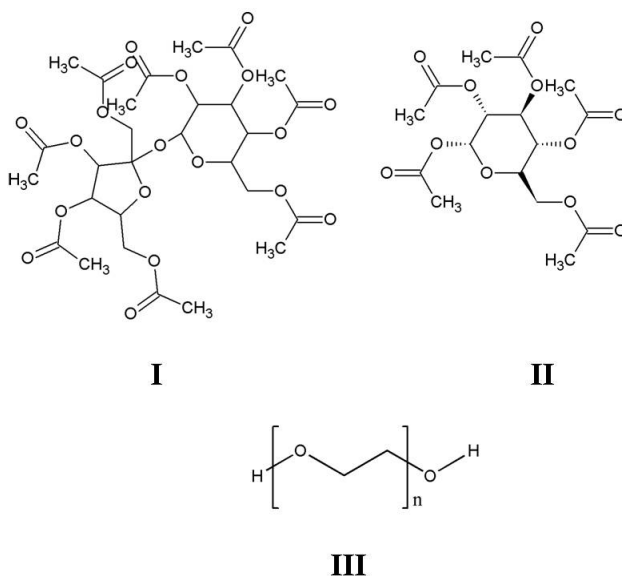


**Figure 2.1** Structure of the CO<sub>2</sub>-philes used (I) SOA, (II) AGLU, and (III) PEG.

**Poly(ethylene glycol) (PEG)** (also known as polyethylene oxide) is a polyether compound with numerous applications, depending on its molecular weight. In this work, we have used PEG of molecular

weight 1500, considering its miscibility with CO<sub>2</sub>. PEG-1500 melts at 45-50 °C, whereas in CO<sub>2</sub>, at 35 °C PEG begins to melt at 78 bar and PEG is observed to be in a liquid state at 90 bar.

In the present work, we are mainly focussing on different coatings/processing applications using liquid and scCO<sub>2</sub>. Sizing of yarn and paper, and impregnation/coating of wood are carried out using liquid/scCO<sub>2</sub> as alternative solvents. Also, composites of Urea and composites of Atenolol are prepared for their controlled release studies, which have many applications in agricultural and pharmaceutical industry, respectively.

### **Yarn**

Cotton and polyester yarns (CY and PY) required for the sizing process are provided by Madura Coats Pvt. Ltd.

### **Paper**

A 5 cm×1 cm normal uncoated paper is used as reference paper for the sizing process.

### **Wood**

Match size pieces of white pine wood species with typical dimensions are used for the impregnation/coating of wood using CO<sub>2</sub>.

### **Urea (UR)**

Urea, also known as carbamide is the most widely used nitrogenous fertilizer (Figure 2.2) and the molecular formula of Urea is CO(NH<sub>2</sub>)<sub>2</sub> (M.W.= 60.056 g/mol; m.p.=132.7 °C).

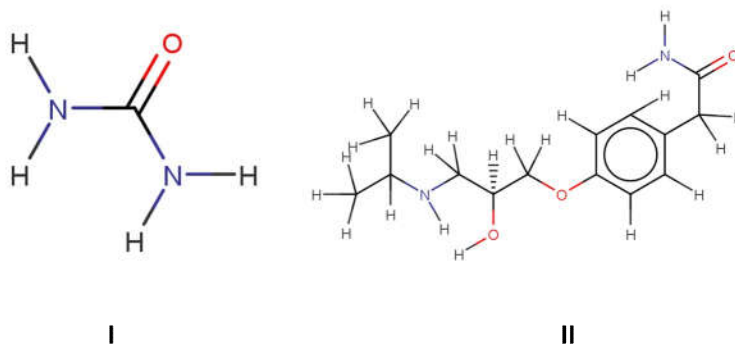


**Figure 2.2** Structures of (I) Urea and (II) Atenolol.

### Atenolol (AT)

Atenolol is a drug that belongs to a class known as beta-blockers (Figure 2.2) and these drugs are used to treat high blood pressure (hypertension) and to reduce the chest pain (angina) Molecular formula of Atenolol is  $C_{14}H_{22}N_2O_3$  (M. W.= 266.336 g/mol; m. p. =163  $^{\circ}C$ ).

## 2.3 Experimental

### 2.3.1 Supercritical $CO_2$ facility

The  $CO_2$  processing of all materials mentioned in this work are carried out in supercritical  $CO_2$  facility. The major components of this facility are a  $CO_2$  cylinder,  $CO_2$  pump, view cell, back pressure regulator (BPR) and a water bath (temperature controller). The main part of the cell is a SCF-VCI model high pressure column type view cell with two sapphire windows (to facilitate the visual observation of the interior) of inner dimension 10 dia  $\times$  12.5 mm and an inner volume of 10  $cm^3$ . Maximum operating pressure and temperature allowed are 25 MPa and 80  $^{\circ}C$ . The cell is fitted with three openings, one for introducing  $CO_2$  and other for emptying  $CO_2$  via BPR and the third one to introduce

temperature controller. Apart from these, the view cell is equipped with a magnetic stirrer to ensure uniform mixing and exposure of the cell contents with CO<sub>2</sub>. Jasco PU-4380 model CO<sub>2</sub> pump is used to compress and deliver liquid CO<sub>2</sub>. Jasco BP- 4340 model BPR is used to maintain constant pressure inside the view cell and also for venting out CO<sub>2</sub> either manually or by setting time program. A temperature controller (ESCY Enterprises) maintains the desired temperature in the view cell. The schematic of the experimental setup and the photographic image of scCO<sub>2</sub> facility is provided in Figure 2.3.

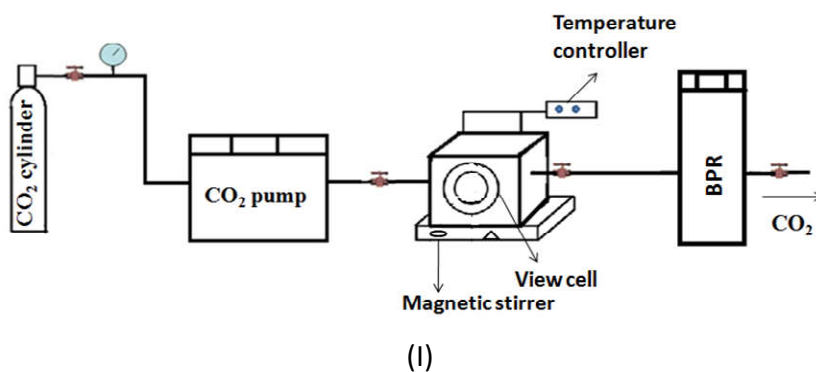


**Figure 2.3** Schematic diagram (I) and photographic image (II) of the scCO<sub>2</sub> facility.

The working procedure of scCO<sub>2</sub> facility is as follows: Once the valve of the CO<sub>2</sub> cylinder is open, CO<sub>2</sub> gas is pumped to the CO<sub>2</sub> pump, where it is liquefied in order to prevent cavitation and passes to the view cell. The CO<sub>2</sub> processing of the material is carried out in the view cell and finally CO<sub>2</sub> is vented out using the BPR outlet. All the experiments in the present work are carried out at a controlled flow rate of 2 ml/min. Prior to each experiment, the cell is brought to desired temperature and the view cell is closed and purged with CO<sub>2</sub>. In all the experiments performed, CO<sub>2</sub> is vented out at a constant rate of 1 bar/min.

## **2.3.2 Experimental procedure for various applications**

### **2.3.2.1 Sizing of yarns using liquid/scCO<sub>2</sub>**

Sizing of cotton and polyester yarns (CY and PY) are carried out with three different size compounds namely SOA, AGLU and PEG. The sizing procedure is detailed below.

In a typical experiment, the cell is loaded with 0.5 g of the size compound. About 30cm of the yarn is introduced from the top of the cell. The cell is brought to the desired temperature (25 °C for SOA and AGLU; 35 °C for PEG). Thereafter, CO<sub>2</sub> is introduced into the view cell followed by raising the pressure of the system to the desired value (65 bar for SOA and AGLU; 90 bar for PEG). Yarn is immersed in the CO<sub>2</sub> solution of the size for 5 minutes followed by venting out CO<sub>2</sub> using the BPR. The sized yarns obtained are removed and characterized.

### **2.3.2.2 Desizing of sized yarns in scCO<sub>2</sub>**

SOA, AGLU and PEG sized yarns are desized by the following experimental procedure.

The cell is loaded with sized yarn from the top and brought to a desired temperature of 35 °C. Thereafter, CO<sub>2</sub> is introduced into view cell, and CO<sub>2</sub> pressure inside the cell is raised to 90 bar. The cell is maintained at this temperature and pressure for 5 minutes. Finally, CO<sub>2</sub> is vented out using the BPR. The desized yarn obtained is taken out and characterized.

### **2.3.2.3 Sizing of yarns using Ethyl Acetate and Acetone**

Sizing of CY and PY with SOA in EA and AC were carried out by the following method.

0.5g of SOA is dissolved in 5ml of EA/AC with stirring to prepare a homogeneous solution of the size. 30 cm long yarn is taken and drawn out of the prepared size solution. The sized yarn obtained is dried by evaporation of solvent at room temperature for two days. The sized yarn obtained is analyzed.

### **2.3.2.4 Sizing of paper using liquid/scCO<sub>2</sub>**

Sizing of paper is carried out with three different size compounds namely SOA, AGLU and PEG. The sizing procedure is detailed below.

In a typical experiment, the cell is loaded with 0.5 g of the size compound and the paper to be sized is suspended from the top of the cell. The cell is brought to the desired temperature (25 °C for SOA and AGLU; 35 °C for PEG). Thereafter, CO<sub>2</sub> is introduced into the view



cell followed by raising the pressure of the system to the desired value (65 bar for SOA and AGLU; 90 bar for PEG). Paper is immersed in the CO<sub>2</sub> solution of the size for 5 minutes followed by venting out CO<sub>2</sub> using the BPR. The sized papers obtained are removed and characterized.

### **2.3.2.5 Impregnation/coating of wood**

Initially, the cell is loaded with 0.5 g of SOA and the wood pieces, followed by pressurizing the cell with CO<sub>2</sub>. The cell is brought to the desired temperature of 35 °C. Thereafter, CO<sub>2</sub> is introduced into the view cell followed by raising the pressure of the system to the desired value of 80 bar. Wood is immersed in the CO<sub>2</sub> solution of the impregnating material for 30 minutes, followed by venting out CO<sub>2</sub> using the BPR. The samples are taken out for further characterizations.

### **2.3.2.6 Preparation of composites of Urea (UR) in scCO<sub>2</sub>**

Initially the cell is loaded with UR and the coating material (SOA/AGLU) in the weight ratio 1:20, followed by bringing the cell to a desired temperature of 35 °C. Upon attaining the desired temperature, CO<sub>2</sub> is introduced into the view cell to attain the desired pressure of 80 bar. Once the desired pressure is achieved, the components inside the cell are stirred for 30 minutes to ensure effective mixing of UR and the coating material. Finally, CO<sub>2</sub> is vented out using the BPR and the samples are collected for further characterizations.

1:10 and 1:50 composites of UR: SOA/AGLU are also prepared, via the same procedure.

### **2.3.2.7 Preparation of composites of Urea in Ethyl Acetate**

UR and the coating material (SOA/AGLU) are mixed in the weight ratio 1:20 and placed inside a beaker. To this, 10 ml of EA is added and the mixture is homogeneously mixed by continuously stirring for 30 minutes. Finally, the EA is evaporated off with the help of a rotary evaporator and the samples are collected for further studies.

### **2.3.2.8 Preparation of composites of Urea with combination of coating materials in scCO<sub>2</sub>**

SOA and AGLU are mixed in the weight ratios 80:20, 60:40, 50:50, 40:60 and 20:80 and then mixed with UR in the weight ratio 20:1. This mixture is introduced into the view cell and the cell is brought to a desired temperature of 35 °C. Thereafter, CO<sub>2</sub> is introduced into the view cell followed by raising the pressure of the system to 80 bar. Once the desired pressure is achieved, the components inside the cell are stirred for 30 minutes. Finally, CO<sub>2</sub> is vented using the BPR and the samples are collected for different studies.

### **2.3.2.9 Preparation of Atenolol (AT)-excipient composites in scCO<sub>2</sub>**

Initially the cell is loaded with AT and the excipient (SOA/AGLU/PEG) in the weight ratio 1:20, followed by bringing the cell to a desired temperature of 35 °C. Thereafter, CO<sub>2</sub> is introduced into the view cell followed by raising the pressure of the system to the desired value (80 bar for SOA and AGLU; 90 bar for PEG). Once the set pressure is attained, stirring is carried out for 30 minutes to ensure homogeneous mixing of the drug and the excipient. Finally, CO<sub>2</sub> is vented out using the BPR and the samples are collected for further characterizations.

1:10 and 1:50 AT-excipient composites are also prepared by following the same procedure.

### **2.3.2.10 Preparation of Atenolol-excipient composites in Ethyl Acetate**

AT and the excipient (SOA/AGLU/PEG) are mixed in the weight ratio 1:20 and placed inside a beaker. To this, 10 ml of EA is added and the mixture is homogeneously mixed by continuously stirring for 30 minutes. Finally, the EA is evaporated off with the help of a rotary evaporator and the samples are collected for further studies.

## **2.4 Characterization techniques**

The following are the instruments used for the characterization and analysis during the research work.

SEM	Scanning Electron Microscope
	Stereo Microscope
UTM	Universal Testing Machine
ATR-FTIR	Attenuated Total Reflectance-Fourier Transform Infrared Spectrometer
FT-Raman	Fourier Transform Raman Spectrometer
UV-Vis	Ultraviolet-Visible- Spectrophotometer
AFM	Atomic Force Microscope
Contact angle	Goniometer
XRD	X-ray Diffractometer
TG	Thermogravimetric Analyzer

### **2.4.1 Field Emission Scanning Electron Microscopy (FE-SEM)**

SEM is used for producing high resolution images of a sample surface and is done by scanning the sample with a focused beam of high energy electrons. FE-SEM technique has found wide applications in defect analysis, elemental analysis, characterization of size, shape, distribution of additives, thickness measurements of coatings etc.

In the present study, Carl Zeiss Gemini SEM-300 instrument is used for the surface scanning of the samples.

### **2.4.2 Stereo Microscope**

Stereo microscope is an optical microscope used for low magnification applications (up to 100X), wherein the light reflected from the surface of an object is used rather than light transmitted through it. Stereo microscopes are generally used to carry out close work such as watch making, dissection etc. and to study surfaces of solid specimens.

In this work, optical microscopic images are captured using LEICA M-80 stereo microscope.

### **2.4.3 Universal Testing Machine**

The Universal testing machine (UTM), also known as universal tester is used to perform many standard tensile and compression test on materials. Tensile test is performed by clamping the specimen on each of its ends and is pulled apart until it breaks. This tells us the tensile strength, elongation and Young's modulus for the specimen. The major

application of UTM is to test the tensile strength and compressive strength of materials.

In the present study, Shimadzu AG-Xplus 10kN UTM served the purpose of testing the mechanical properties of samples.

#### **2.4.4 Fourier Transform Infrared (FTIR) Spectroscopy<sup>123, 124</sup>**

FTIR spectroscopy is a vibrational spectroscopic technique applied for the identification of the compounds and also has many other applications such as identification of the transition phases, widely used in the fields of toxicology, molecular genetics etc.

ATR-FTIR spectra are recorded using Jasco FTIR-4700 spectrophotometer equipped with an ATR cell.

#### **2.4.5 Fourier Transform Raman (FT-Raman) Spectroscopy<sup>123,124</sup>**

Raman spectroscopy is a vibrational spectroscopic tool complementary to IR spectroscopy. It is a simple, non-destructive characterization technique that provides complete information about the rotational, vibrational and all other low energy modes in a molecule. Raman spectroscopy has many applications such as to identify the molecules and their chemical bonding, investigating the phase transitions, to identify the defects in crystals etc.

In the present experiments, a Bruker MultiRaM FT-Raman spectrophotometer with laser excitation 1064 nm is used for recording Raman spectra of the samples in the Retro-Raman (180 °scattering) mode. A liquid nitrogen – cooled Ge detector is used as the detector.

#### **2.4.5 UV-Visible Spectroscopy (UV-VIS)<sup>123, 124</sup>**

UV-Vis spectroscopy deals with the study of interaction of UV-Vis radiation with the molecules. This technique is based on the absorption of light and hence is also referred as absorption spectroscopy. UV-Vis spectrophotometer is the instrument used to measure the UV-Vis spectra. This spectroscopic technique has found wide applications such as to study the reaction kinetics, to determine the concentration of unknown sample etc.

Thermo Scientific Evolution-201 UV-Visible spectrophotometer is used for recording the UV-Vis spectra of the samples in the range 200-800 nm.

In particular, the method adopted for determining the release profiles of UR and AT using UV-Visible spectrophotometer are discussed below.

##### **Urea release studies**

About 3.5 mg of the composite is dispersed in 3.5 ml of distilled water in a cuvette and is placed in UV-Visible spectrophotometer. Absorbance is measured in the kinetics mode at regular time interval of 20 minutes at  $\lambda_{\text{max}}$  of 197 nm, till the absorbance value of UR stabilizes at maximum absorbance.

##### **Atenolol In-vitro release studies**

About 3.5 mg of the composite is dispersed in 3.5 ml of distilled water in a cuvette and the cuvette is placed in UV-Visible spectrophotometer.

Absorbance is measured in the kinetics mode at regular time interval of 20 minutes at  $\lambda_{\text{max}}$  of 224 nm, till the absorbance value of AT stabilizes at maximum absorbance.

#### **2.4.6 Atomic Force Microscopy (AFM)**

AFM also known as scanning force microscopy, is one among the various scanning probe techniques and is used to get detailed and distinct three dimensional images of the specimen surfaces with resolution ranging from nanoscale to atomic scale. The surface roughness, three dimensional topographic maps of the surface, morphology of the particles, pore size, surface area, volume distribution etc. can be inferred from the AFM data.

In the present experiment, contact mode AFM images were recorded using WITec GmbH Alpha-300RA atomic force microscope.

#### **2.4.7 Contact angle measurements**

Contact angle is defined as the angle formed between the outline tangents of the drop deposited on the substrate and the surface of the substrate. Surface contact angle goniometer is the simplest and convenient instrument which is used for measuring the contact angle. Depending upon the contact angle, the substrates may be labeled as hydrophobic ( $> 90^{\circ}$ ), superhydrophobic ( $> 150^{\circ}$ ), hydrophilic ( $< 90^{\circ}$ ) and superhydrophilic ( $< 30^{\circ}$ ). Information related to wettability, adhesion properties etc. are also available from the contact angle measurements.

Contact angle measurements are carried out using Digidrop contact angle goniometer (GBX Digidrop).

#### **2.4.8 X-Ray Diffraction (XRD)**

X-ray diffraction technique is a non-destructive technique used to study the crystal structure and lattice parameters of a molecule. Crystallite size, degree of crystallinity, lattice parameters, crystal phase, etc. can be determined with the help of X-ray diffractometer.

In the present study, Rigaku miniflex-600 diffractometer with  $\text{CuK}\alpha$  radiation with  $\lambda=1.5404 \text{ \AA}$  is used to measure the X-ray diffraction pattern of the samples and the sample is scanned in the  $2\theta$  range of  $5-90^\circ$ .

#### **2.4.9 Thermogravimetry (TG)**

In thermogravimetric analysis (TGA), the quantity and rate of change in weight of the substance is recorded as a function of time or temperature in a controlled atmosphere. This simplest thermo analytical method is primarily used to determine the thermal stability of materials up to  $1000^\circ\text{C}$  and the composition of materials. This method can also be employed to calculate the weight loss or weight gain that a substance undergoes upon oxidation, decomposition and dehydration.

In the present work, PerkinElmer STA-8000 thermal analyzer is used to carry out thermogravimetric analysis and the samples were analyzed at a constant heating rate of  $10^\circ\text{C}$  from  $30^\circ\text{C}$  to  $500^\circ\text{C}$ .



#### 2.4.10 Cobb<sub>60</sub><sup>\*</sup> measurement

Cobb<sub>60</sub>, a measure of the quantity of water absorbed by the paper in a specified time of 60 seconds, was determined by a variant of the standard method<sup>125</sup> (ISO 535:2014) and hence denoted as Cobb<sub>60</sub><sup>\*</sup>. Since the inner dimension of the view cell used in the present system is smaller, we could not use a paper of cross sectional area of 100 cm<sup>2</sup> for Cobb<sub>60</sub> measurement. According to our experimental procedure, amount of water absorbed on a definite area of 3.85×10<sup>-3</sup> dm<sup>2</sup> was measured. Any one side of the paper is exposed to a water pressure of 1 cm height for 60 s at temperature 31 °C.

Cobb<sub>60</sub><sup>\*</sup> is calculated as:

$$\text{Cobb}_{60}^* = \frac{m_f - m_i}{S}$$

Where, m<sub>i</sub> = Mass of paper before exposure to water

m<sub>f</sub> = Mass of water after exposure to water

S = Cross sectional area of the cylinder

Arithmetic mean of replicate test results of Cobb<sub>60</sub><sup>\*</sup> values are calculated.



## CHAPTER 3

# SIZING AND DESIZING OF COTTON AND POLYESTER YARNS

---

### 3.1 Introduction

Textiles industry is one of the oldest industries in our country and its main objective is to convert fiber to yarn and then, to fabric. The conversion of yarn into a fabric is a tedious, multi-step process. The important step in the conversion of yarn into fabric is ‘weaving’ and the weaving process requires a loom and also, before the commencement of weaving, the yarn is subjected to a sequence of processes namely winding, warping, sizing, looming and pirning; finally leading to the production of woven yarn. There is a high chance for the breakage of warp yarn on the weaving machine<sup>126</sup> since the yarns will have to withstand huge cyclic strain, friction between the yarns, flexing, abrasion etc. These actions can be overcome by the sizing of yarn, which is an important and necessary process executed in the textiles industry.

Sizing is defined as the process in which the yarns to be used as a warp in weaving process is impregnated with some material to improve its strength, elasticity, abrasion resistance, smoothness, reduce friction, reducing the hairiness of the yarn and to remove the projecting fibres.<sup>127</sup> Not all materials can enhance the strength of the yarn. The degree of increase in the strength of the yarn and the other factors mentioned above, depends upon the adhesive force between the yarn

and the size material, penetration of size into the yarn, and the encapsulation efficiency of the yarn and all these factors varies from one yarn to another. Other major factors which have to be considered while selecting the size materials are, they should be cheap, easily washable, abundant, environmentally viable and finally, should not result in the degradation/ exfoliation of the yarn. Different methods are adopted for the sizing process depending on the type of the fabric used, thickness of the yarn and the type of weaving machinery used. Commonly used natural sizing agents are starch/starch derivatives, cellulose derivatives like carboxymethyl cellulose, methylcellulose etc. and protein based starches like glue, gelatin etc. whereas synthetic sizing agents used in textile industry are polyvinyl alcohol (PVA), styrene/ maleic acid copolymers, polyacrylates etc. Among the aforementioned sizes, starch and PVA are the most commonly used<sup>128</sup> and PVA is the most appropriate candidate for the spun polyester blends whereas both starch and PVA may be used as the size for the cotton fabrics. Sizing can be done either with hand or with the help of a sizing machine. Conventional method of sizing involves drawing the yarn through a concentrated, aqueous (or organic) dispersion of the size and then drying it.<sup>129</sup> This consumes tremendous amount of water and is a highly energy intensive process. This is problematic, especially in developing countries like India where the textiles industry, and, in particular, the cotton industry is ranked as the second largest employment provider.

Desizing is another important process in the textile industry in which the size is removed from the warp yarn after the fabric is woven.

Desizing, in general, involves a desizing agent which either degrades or solubilizes the size from the fabric. There are different types of desizing processes and they may be classified into enzymatic, acid, oxidative, fermentative and removal of water soluble size. Generally, the size material is removed from the fabric by washing with water, generating lots of waste water and the causing contamination of the natural water reservoirs down the line. So it may be concluded that the sizing and desizing processes carried out in textiles industry generates huge amount of waste water which cannot be discharged unless free from contamination, resulting in ecological issues and also results in massive utilization of energy. The cost of water and the cost to treat the waste from it requires tremendous consideration.

In spite of the immense progress in the textile industry, there exists a series of concerns regarding environmental issues which may be reformed by replacing such environmentally unfriendly technologies with greener alternatives.

As part of the textile industry efforts to reduce or eliminate the consumption of water in all areas of textiles processing such as yarn preparation, sizing, desizing, dyeing etc., SCF technology has been proven as an alternative for these commercial textile applications. In 1996, Fulton and coworkers<sup>129,130</sup> proposed that the CO<sub>2</sub>-solvent platform can serve as an alternative medium for the sizing and desizing of yarn using fluoropolymers as the size compounds. However, this wonderful method couldn't take off as an economically viable method in the textile industry, plausibly due to the high cost of the

fluoropolymers and other potential environmental issues associated with the fluorinated size compounds.

Herein, we present (Figure 3.1) a top to bottom green route for the sizing and desizing of yarns using liquid and supercritical carbon dioxide as the process medium and non- fluorous CO<sub>2</sub>-philes as the size material.

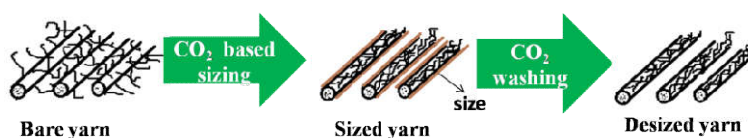


**Figure 3.1** Pictorial representation for the sizing and desizing of yarn

In this work, we demonstrate a completely green strategy for the sizing and desizing of yarns, both cotton and polyester (CY and PY), with highly CO<sub>2</sub>-philic size materials such as SOA, AGLU, and PEG using CO<sub>2</sub> medium. The sugar acetates such as AGLU and SOA melt under moderate pressures of gas phase CO<sub>2</sub> and are completely miscible with liquid and scCO<sub>2</sub> and the dense CO<sub>2</sub> solutions of these compounds can be easily used for the sizing of the yarns. On the other hand, the low molecular fragments of PEG (MW = 1500) melt at 35 °C under pressures of CO<sub>2</sub> (~90 bar) and expands further, although the CO<sub>2</sub>-melt of PEG is not completely miscible with liquid or scCO<sub>2</sub>. Thus, one can easily develop a CO<sub>2</sub>-melt strategy for the sizing of yarn by drawing the yarn through the CO<sub>2</sub>-melt of PEG. The ease of solvent removal

makes these strategies inherently dry and green processes, without requiring any further drying. It is demonstrated herein that the CO<sub>2</sub>-based sizing and desizing has the potential to be developed into an ideal zero-pollution technology with wider implications for the textile industry. It should also be noted that, all the size materials used are inexpensive and environmentally benign and can be completely recycled along with the solvent.

### **3.2 Results and Discussion**

As discussed in the previous section, the main objective of this work is to examine the possibility of sizing of CY and PY using CO<sub>2</sub>-philes such as SOA, AGLU, and PEG. It is relevant to investigate how these size compounds binds with two entirely different classes of yarns, CY and PY. It is also important to note that these size compounds behaves differently after CO<sub>2</sub> treatment and is already discussed in Chapter 1. Hence, it is also important to investigate how the CO<sub>2</sub>-induced modifications on these CO<sub>2</sub>-philes are going to manifest on the sizing properties. The method adopted for sizing and desizing process are detailed in Chapter 2. The desizing of sized yarns are carried out using scCO<sub>2</sub>. The choice of liquid CO<sub>2</sub> for sizing and scCO<sub>2</sub> for desizing is primarily due to the higher rate of diffusion in the supercritical state that can help in faster and improved wash of the size compounds from the sized yarn.

The optical microscopic images of bare CY along with those after sizing with SOA (CY-SOA), AGLU (CY-AGLU) and PEG (CY-PEG) are shown in Figure 3.2. It is very clear that in CY-SOA, the CY has a

very smooth, transparent, reasonably uniform, thick, and a glassy coating of SOA is observed. The individual microfibers of CY are buried underneath the SOA coating. This may be attributed to the glass formation of SOA upon CO<sub>2</sub>-treatment.<sup>60,122</sup> In the case of CY-AGLU, the AGLU coating has discontinuous and powdery features with the individual microfibers protruding out of the coated yarn. A thick and uniform coating was noticed for PEG, however, the PEG coating has a viscous liquid-like appearance even after the CO<sub>2</sub> removal, plausibly due to its low lattice energy.

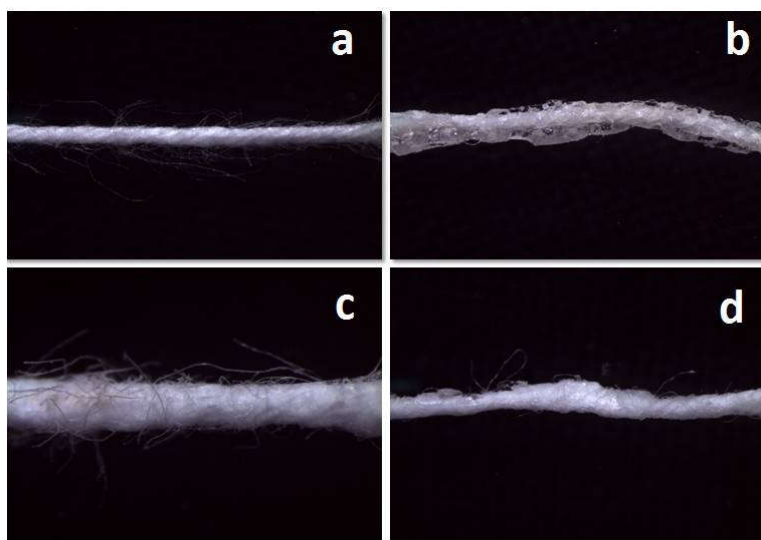


**Figure 3.2** Optical microscopic images of (a) bare CY b) CY-SOA c) CY-AGLU and d) CY-PEG

Similar sizing experiments are also carried out for PY. The optical microscopic images of bare PY, PY coated with SOA (PY-SOA), AGLU (PY-AGLU), and PEG (PY-PEG) are provided in Figure 3.3. It



is observed that the size material forms almost similar coatings on PY as observed in the case of CY.

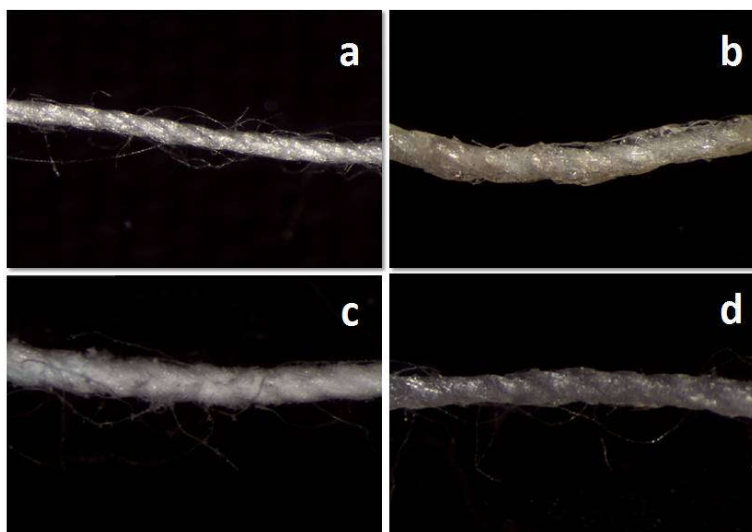


**Figure 3.3** Optical microscopic images of a) bare PY b) PY-SOA c) PY-AGLU and d) PY-PEG.

While SOA forms a smooth, glassy, and transparent coating on PY, AGLU forms a white, powdery coating on PY. The SOA sizing appears to be of much superior quality as compared to both AGLU and PEG. In the case of PEG, the coating is more of a semi-solid type as observed in the “starching” using water. While SOA provides a thick glassy coating with stronger protection to the yarn, the waxy coating formed by PEG might be of some use from a mechanical perspective, by reducing friction during the weaving process. In the case of PY, both SOA and PEG give smooth, transparent/translucent coatings with complete coverage of the individual microfibers of the yarn while the AGLU coating is less effective.

In order to evaluate the nature of the coatings more closely, SEM images of the unsized and sized yarns are recorded to examine the degree of encapsulation and the uniformity of the coating. The SEM image of bare CY, CY-SOA, CY-AGLU and CY-PEG are presented in Figure 3.4. In the case of bare CY, the individual fibers are clearly visible. SOA forms a very smooth coating on CY with some pores observed, which may be plausibly due to the bubble formations as a result of the evolution of CO<sub>2</sub> from the CO<sub>2</sub>- melt of SOA. On the other hand, AGLU has successfully penetrated into the yarn structure, but appears to be just a filler material without much binding to the yarn. In the case of CY-PEG, a thick coating is observed with none of the individual fibers protruding out.

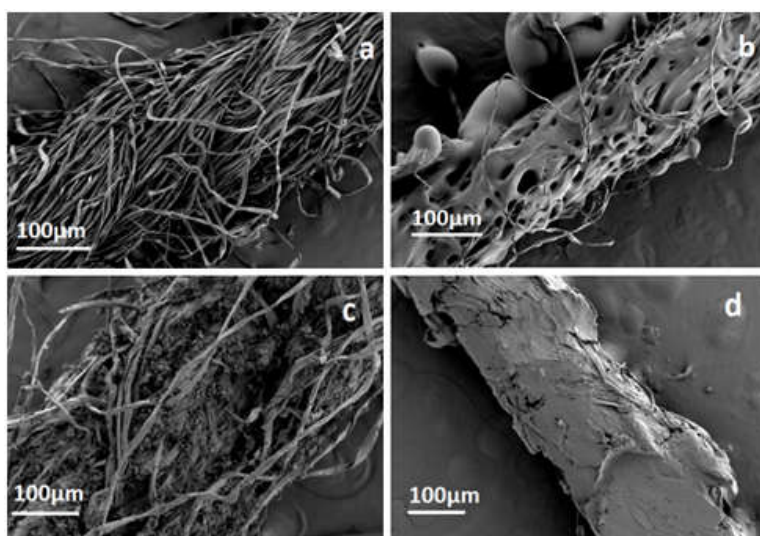


**Figure 3.4** FE-SEM images of a) bare CY b) CY-SOA c) CY-AGLU and d) CY-PEG.

SEM of PY, PY-SOA, PY-AGLU and PY-PEG are provided in Figure 3.5 and a smooth, uniform coating is observed for PY-SOA without any of the microfibers being projected outside. SOA appears to strongly adhere to the yarn surface and has also penetrated between the individual fibers. Coating with AGLU is not very effective, in terms of the encapsulation efficiency. In PY-AGLU, individual fibers are clearly visible even after the coating. Both SOA and PEG encapsulate the PY better than AGLU. Among the trio, SOA was found to be superior to its counterparts in terms of coating on PY.

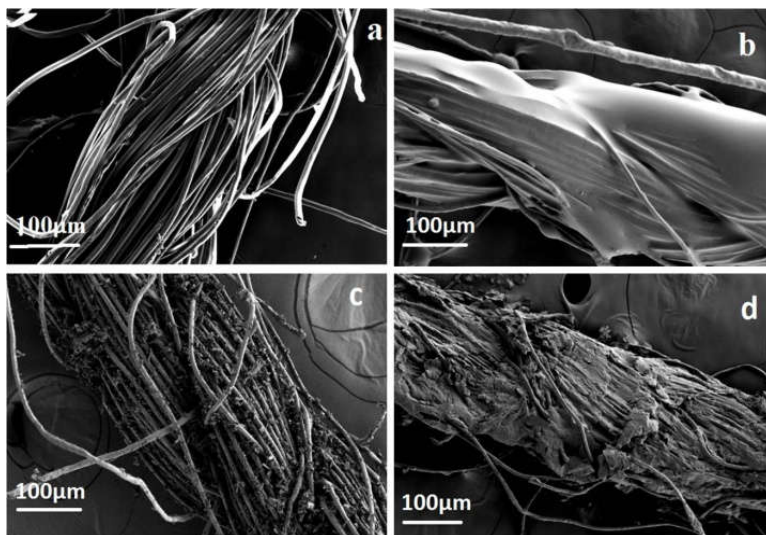


**Figure 3.5** FE-SEM images of (a) bare PY (b) PY-SOA (c) PY-AGLU and (d) PY-PEG.

Mechanical properties such as tensile strength, percentage elongation, and Young's modulus before and after abrasion are measured for CY, CY-SOA, CY-AGLU, CY-PEG, PY, PY-SOA, PY-AGLU, and PY-PEG to make an assessment on how sizing has improved the suitability of the yarns for the weaving process and the results are summarized in

Table 3.1. The abrasion process is carried out by adopting a procedure developed by Fulton et al., i.e. by pulling the yarn three times over a 90° edge with a corner radius of 0.5 mm.<sup>130</sup> Sizing with all the three size candidates resulted in an increase in the tensile strength, for CYs and PYs. Among these, tensile strength is found to be the highest for the CY and PY sized with SOA, followed by AGLU and finally, PEG. The tensile strength is almost doubled for the CY-SOA while an enhancement of 60% is observed for PY-SOA than their corresponding bare yarns.

From the data, it is also evident that the percentage elongation of all the sized yarns is higher than that of their corresponding bare yarns. The results also reveal that although all the three size compounds stiffened the yarns, SOA showed the best response as a size compound, for CY and PY.

**Table 3.1** Mechanical properties of bare and sized yarns.

<b>Yarn</b>	<b>Tensile strength (N/ mm<sup>2</sup>)</b>	<b>Percentage elongation</b>	<b>Young's modulus (N/ mm<sup>2</sup>) before abrasion</b>	<b>Young's modulus (N/ mm<sup>2</sup>) after abrasion</b>
CY	232.0	10.7	17.8	15.8
CY-SOA	472.4	15.0	31.7	26.4
CY- AGLU	362.9	11.7	31.0	17.6
CY- PEG	271	14	19.3	16.2
PY	723.6	16.1	45.0	41.6
PY-SOA	1156.5	16.4	72.1	65.7
PY-AGLU	1019.2	16.6	61.1	48.4
PY- PEG	871.9	16.8	54.0	49.3

In all the three cases, abrasion process caused a reduction in the Young's modulus, although the abrasion had minimal effects in the case of yarns sized with SOA. In the case of CY-AGLU and PY-AGLU, the stiffness of the yarn has been reduced significantly after abrasion. This may be due to the poor surface coverage of the size on the surface of the yarn as evidenced from the SEM images. Yarns sized with SOA and PEG shows complete surface coverage and hence, one would expect similar stiffness characteristics and abrasion resistances in both the cases. However, there are significant differences between these two size compounds. In the case of SOA, the stiffness of the yarn has increased considerably after sizing, and it also shows high resistance to abrasion, plausibly due to the formation of the glassy SOA coating and improved binding of the size with the yarns. On the other hand, although the surface coverage of the PEG on the yarn is observed to be good, the waxy nature of the coating results in low stiffness and abrasion resistance as compared to SOA. It can be summarized from the UTM measurements that, while all the three CO<sub>2</sub>-philes considered here are suitable size candidates for the textile industry in terms of mechanical properties, SOA is the most suitable size material in terms of the quality of the coating and mechanical properties. The optical microscopy and SEM studies show that the hairiness of the yarns has been reduced upon sizing due to improved surface coverage of the size materials on the yarns. In this case also, SOA provides the best protection to the yarn as observed from optical and SEM studies.

Likewise, it is interesting to note that while AGLU and SOA are equally miscible with liquid and scCO<sub>2</sub>, SOA forms a much better and smooth coating on the yarn. As can be seen from the optical microscopic images, the SOA forms a transparent and continuous coating on the yarn, removing the hairiness of the yarn. The mechanical properties are also much more superior for the SOA-coated yarns. One plausible reason is the formation of the SOA glass after CO<sub>2</sub>-treatment, while such glass formation is absent in the case of AGLU. Better controls on such coatings can be achieved by superior process controls in the engineering designs. In any case, SOA, being the cheapest and the most easily available among the sugar acetates, provides a strong basis for the transformation of the process into an industrial technology.

Finally, sizing was gravimetrically estimated by measuring the mass of the bare yarn prior to and after the sizing process. Finally, the yarn was washed with scCO<sub>2</sub> to remove the size compound and reweighed. An increase in the mass of the yarn upon coating is observed (Table 3.2). If the mass of the desized yarns are observed to be same as that of their corresponding bare yarn, then one could say that the desizing process is complete and effective. Difference between the mass of the bare yarn and desized yarn represents the amount of size compound that was not completely removed on washing with CO<sub>2</sub>. From the mass determination studies, it can be noted that the desizing is complete in the case of SOA and AGLU-sized yarns whereas, it is incomplete for PEG-sized yarns, which may be plausibly due to low miscibility of PEG in scCO<sub>2</sub> when compared to SOA and AGLU.

**Table 3.2** Mass determination studies of bare, sized and desized yarns.

<b>Yarn</b>	<b>Mass of the bare yarn (g)</b>	<b>Mass of the sized yarn (g)</b>	<b>Mass of the desized yarn (g)</b>
CY-SOA	0.0351	0.1143	0.0354
PY-SOA	0.0115	0.0385	0.0118
CY-AGLU	0.0338	0.1089	0.0340
PY-AGLU	0.0102	0.0258	0.0104
CY-PEG	0.0372	0.1158	0.0401
PY-PEG	0.0108	0.0356	0.0129

The SEM images of the desized CYs and PYs are shown in Figure 3.6 which clearly illustrates that the size compound is washed off from the SOA and AGLU-sized yarns, although minute traces of SOA and AGLU are visible in both CY and PY. The desizing process is observed to be very effective for SOA and AGLU-sized yarns and not for PEG-sized yarns. Unlike SOA and AGLU, sizing of yarn using PEG is achieved by melt processing and hence did not result in the complete removal of PEG from PEG-sized yarns upon desizing.

The FE-SEM results for the desizing of yarns are supporting well with the mass determination studies wherein the mass of the unwashed substance is observed to be higher for PEG.

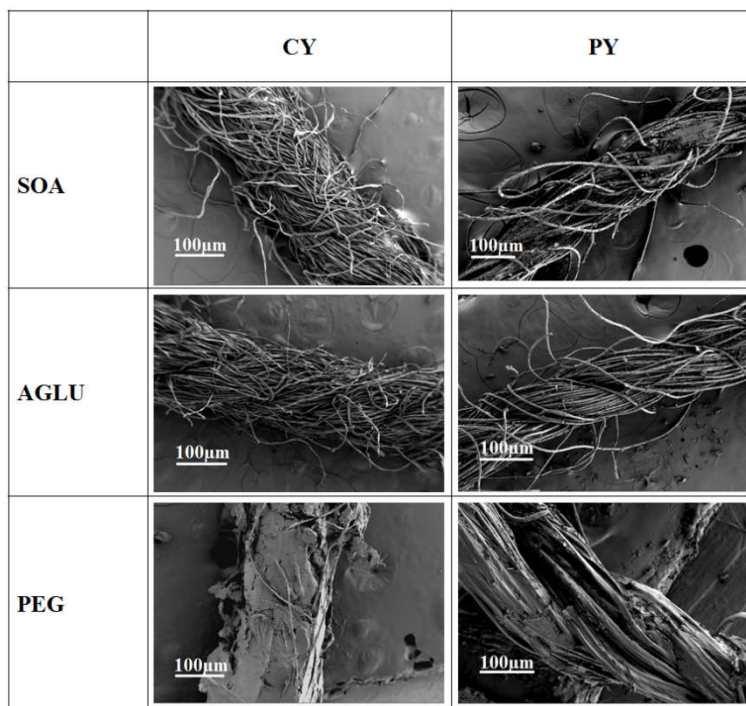


**Figure 3.6** FE-SEM images of the desized yarns

We have also carried out a study to make a comparison between the CO<sub>2</sub>-solvent system and the conventional solvents such as Acetone (AC) and Ethyl Acetate (EA) for the sizing process with SOA as the size material. The optical microscopic and SEM images of CY sized with SOA using EA (CY-SOA-EA) and AC (CY-SOA-AC) are provided in Figure 3.7. Although SOA is highly soluble in both AC and EA, SOA does not bind effectively with the yarns as observed for the yarns sized with SOA in CO<sub>2</sub> solvent system. A non-uniform, irregular coating is observed for CY processed in conventional solvents.



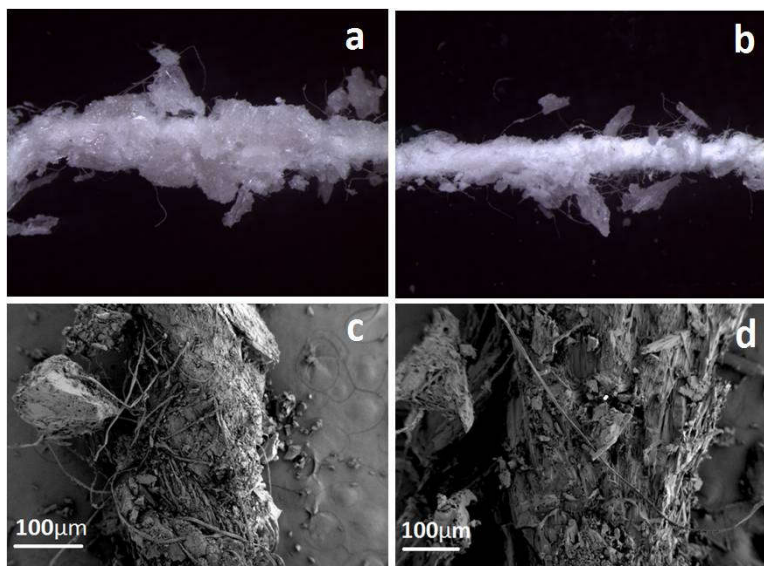


**Figure 3.7** Sizing using conventional solvents: (a) & (b) Optical microscopic images of CY-SOA-EA and CY-SOA-AC; (c) & (d) FE-SEM images of CY-SOA-EA and CY-SOA-AC.

Likewise, the optical microscopic and SEM images of PY sized with SOA using EA (PY-SOA-EA) and AC (PY-SOA-AC) are presented in Figure 3.8 and it was observed that the results are similar to those observed for sizing of CY with SOA using conventional solvents. Sizing was not observed to be effective for PY in conventional solvents medium. Also, there is no noticeable decrease in the hairiness of CY and PY after sizing with SOA in EA and AC medium.

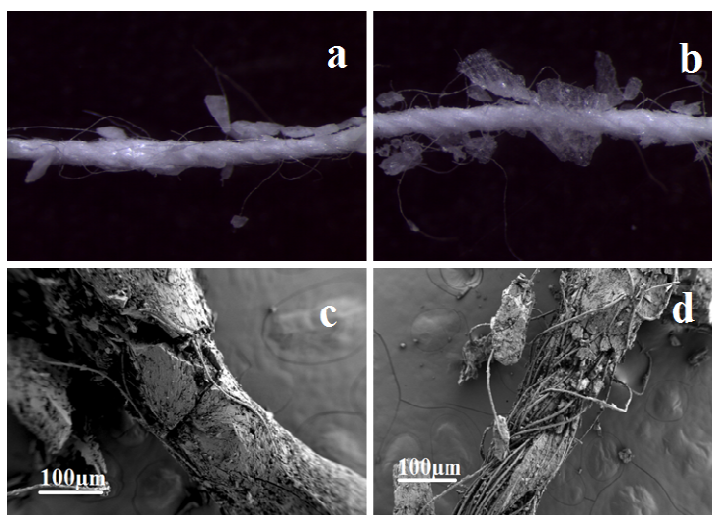


**Figure 3.8** Sizing using conventional solvents: (a) & (b) Optical microscopic images of PY-SOA-EA and PY-SOA-AC; (c) & (d) FE-SEM images of PY-SOA-EA and PY-SOA-AC.

Mechanical properties of CY and PY sized with SOA in conventional solvent media (EA and AC) are measured and shown in Table 3.3. The results show that tensile strength, percentage elongation and Young's modulus of the sized yarns are higher than their corresponding bare yarns.

**Table 3.3** Mechanical properties of CY and PY sized with SOA in conventional solvents (EA and AC).

Yarn	Tensile strength (N/mm <sup>2</sup> )	Percentage elongation	Young's modulus (N/mm <sup>2</sup> )
CY	232.01	10.75	17.78
CY-SOA-EA	430.83	12.73	31.5
CY-SOA-AC	401.46	12.15	29.73
PY	723.62	16.14	45.07
PY-SOA-EA	1198.45	17.3	69.4
PY-SOA-AC	1130.32	18.2	62.14

Upon comparing the mechanical properties of CY and PY sized with SOA in CO<sub>2</sub> and conventional solvent medium, one could notice that the mechanical properties are more or less similar. In specific, for PY, tensile strength and percentage elongation are observed to be slightly higher for the one sized in EA medium, whereas for CY, all the mechanical properties are observed to be higher for the yarns sized using CO<sub>2</sub> solvent medium. Hence, conventional solvents can be replaced by CO<sub>2</sub> since the latter is found to be much superior in terms of coating and hairiness, although mechanical properties are observed to be improved for yarns sized with SOA in CO<sub>2</sub> as well as in conventional solvent medium.

### **3.3 Summary and Conclusions**

In this work, we have investigated the possibility of utilizing liquid and scCO<sub>2</sub> as a green alternative medium for the sizing and desizing of CY and PY for the textile industry using inexpensive, non-fluorous, CO<sub>2</sub>-philes. We have considered three size compounds, viz., AGLU, SOA, and PEG, by virtue of their CO<sub>2</sub>-philicity. The sized yarns are then characterized using optical microscopy and SEM techniques to investigate how effective the sizing was. The samples are also analyzed to evaluate the improvement in mechanical properties of the yarn upon sizing. Among the systems studied, SOA is found to be the most ideal candidate as the size material for the CO<sub>2</sub>-based processing. Sizing of CY and PY with SOA resulted in a smooth, uniform, and glassy coating. It also showed improved mechanical properties.

Finally, desizing of the sized yarns using scCO<sub>2</sub> were carried out and analyzed using mass determination and SEM studies. Finally, as a comparative study, sizing of yarn with SOA is performed in conventional solvents and analyzed.

Overall, the results clearly indicate that the combination of SOA (as an inexpensive and environmentally benign size material) and liquid/scCO<sub>2</sub> can be effectively utilized for the sizing process and can be developed into a transformational technology for the textiles industry with zero pollution since both the size and the solvent can be easily and completely recycled. Since SOA is a very inexpensive agricultural product, the technology can be made economically viable.

### **4.1 Introduction**

Paper is a multifaceted material with a layered network structure and is made up of a network of cellulose fibers derived from wood.<sup>131</sup> Paper possess wide applications primarily for writing and printing, and then for packaging etc. Surface sizing of paper has been a very common practice followed in paper industry to improve the quality of paper. With respect to sizing, paper can be classified into three categories namely unsized, weak sized and strong sized papers. The first category of papers have got lower water resistance (papers used for blotting), the second category is somewhat absorbent (newsprint paper) whereas the third class of papers have got the highest water resistance (coated papers). Apart from these three classes of paper (based on sizing), there are two types of sizing i.e. surface sizing and internal sizing. Surface sizing is applied only to highest grade paper whereas internal sizing can be applied to all papers. Higher mechanical strength, smoothness, water resistance, decreased surface porosity and improved print quality, can be achieved by sizing of paper.<sup>132,133</sup> The compounds selected for sizing should result in a low energy coating on the paper, at the same time should also meet all the requirements of the sizing of paper. Earlier times, alum was used as the size material. Later on many works has been carried out and the researchers identified sizing materials such as starch, Poly vinyl alcohol and rosin.<sup>134</sup> Recently,

alkyl ketene dimer (AKD) and alkenyl succinic anhydride (ASA) are being widely used to hold hydrophobic molecules on the paper surface.

The use of water as the medium for sizing generally causes damage to the paper surface due to its high surface tension and also generates lots of waste water causing environmental concerns. On the other hand, the use of volatile organic solvents presents the more serious problem of atmospheric contamination. Cost-effectiveness and environmental concerns associated with sizing need consideration while designing and adopting newer strategies.

The use of the CO<sub>2</sub>-solvent system for sizing was originally conceived by Fulton and co-workers,<sup>130</sup> which is discussed in Chapter 3. However, the fluorocarbon-based size materials used in their work are rather expensive and are also often associated with potential environmental issues, limiting the industrial scale implementation of this strategy. When it comes to paper, fluorocarbon coating will also make the paper unsuitable for several applications. Generation of super hydrophobic surfaces using AKD by rapid expansion of supercritical CO<sub>2</sub> is reported.<sup>135,136</sup> The disadvantage of using fluorocarbons, can possibly be overcome by the use of the carbonyl-based CO<sub>2</sub>-philic materials such as acetylated sugars and polymers such as PEG.

In this work, we demonstrate that we can easily employ liquid/scCO<sub>2</sub> as a solvent system for the sizing of paper in an industrially viable manner by combining the CO<sub>2</sub>-solvent platform with an inexpensive, renewable, and non-toxic but more importantly, highly CO<sub>2</sub>-philic size materials such as SOA, AGLU and PEG (M.W. 1500). Finally we are

comparing the efficiency of all the three CO<sub>2</sub>-philes for the sizing of paper. The experimental procedure adopted for the sizing of paper is described in Chapter 2. Finally, unsized reference paper (RP) and the sized paper (SP) samples are characterized and their sizing performances are compared.

## **4.2 Results and Discussion**

As a preliminary study to confirm the presence of the size compound on the surface of the paper, gravimetric estimation is carried out, i.e. measuring the mass of the paper before and after sizing. The mass of the paper upon sizing increased from 0.0079 g to 0.0196 g, 0.0089 g to 0.0235 g and 0.0082 g to 0.0149g for SOA, AGLU and PEG, respectively, confirming the presence of the size material on the surface of the paper.

### **4.2.1 FT-IR-ATR studies**

Vibrational spectroscopic studies can serve as a non-destructive method for differentiating the reference and the treated samples by virtue of the additional bands corresponding to the size material on the treated one.<sup>137</sup> The FT-IR-ATR spectra of RP, SOA, AGLU, PEG and all the sized papers are provided in Figure 4.1. The FT-IR-ATR spectra of RP shows two strong bands at 1104 cm<sup>-1</sup> and 1029 cm<sup>-1</sup> corresponding to glycosidic C-O-C stretching vibration and C-OH stretching vibrations of primary alcoholic group of cellulose, respectively. The band at 1054 cm<sup>-1</sup> can be ascribed to the C-OH stretching vibrations of secondary alcoholic groups of cellulose. The band at 1160 cm<sup>-1</sup> corresponds to C-C stretching (asymmetric ring

breathing mode) in cellulose/hemicelluloses constituent of paper.<sup>138-141</sup> In the case of pure SOA, two prominent bands are visible at  $1748\text{ cm}^{-1}$  and  $1236\text{ cm}^{-1}$ , corresponding to the C=O stretching and C-O stretching, respectively. Apart from the cellulose peaks, the two intense bands of SOA are visible in the spectra of SOA-sized paper which is an indication of the efficient surface sizing of paper with SOA.

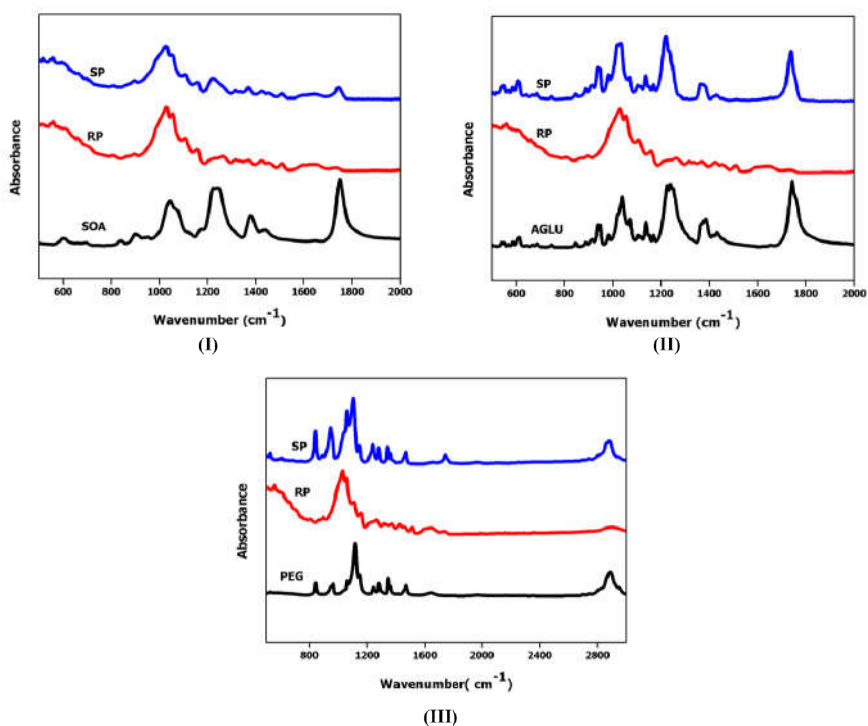


**Figure 4.1** FT-IR-ATR spectra of a) size compound, b) RP, and c) SP for (I) SOA, (II) AGLU, and (III) PEG.

Intense bands of AGLU are appearing at  $1741\text{ cm}^{-1}$  and  $1236\text{ cm}^{-1}$ , corresponding to C=O and C-O stretching, respectively. Apart from the cellulose peaks, one also observes the intense bands of AGLU on the



surface of the paper sized with AGLU, revealing that the sizing process is complete.

For PEG, the intense bands are observed at  $1112\text{ cm}^{-1}$ ,  $1343\text{ cm}^{-1}$  and  $2893\text{ cm}^{-1}$  corresponding to C-O-H stretching, C-H bending and stretching, respectively. These intense bands of PEG are observed on the spectra of PEG coated paper indicating the presence of PEG on the surface of the paper.

The FT-IR-ATR spectra results reveal that the size materials have been successfully incorporated into the paper surface.

#### **4.2.2 FT- Raman studies**

Similar to FT-IR-ATR spectroscopy, Raman spectroscopy is also a non-destructive technique for differentiating RP and SP, and also to confirm the presence of the size compound on the surface of the paper.

FT-Raman spectra of RP, size materials and the sized papers are provided in Figure 4.2. The peaks around  $1097\text{ cm}^{-1}$  and  $2898\text{ cm}^{-1}$  are characteristic peaks of cellulose. The presence of a peak at  $1464\text{ cm}^{-1}$  is typical of cellulose.<sup>142,143</sup> The intense bands of SOA are appears at  $1743\text{ cm}^{-1}$  and  $2939\text{ cm}^{-1}$  corresponding to the acetate carbonyl groups and various C-H vibrational modes of acetate groups. In the case of SOA-coated paper, one could observe the bands of RP and although weak, the notable presence of some of the prominent peaks of SOA, confirming the coating of SOA on the paper surface. The absence of the intense band  $2898\text{ cm}^{-1}$  of cellulose in the SOA coated paper may

be attributed to the merging of the C-H stretching band of SOA with the cellulose peak at  $2898\text{ cm}^{-1}$ .

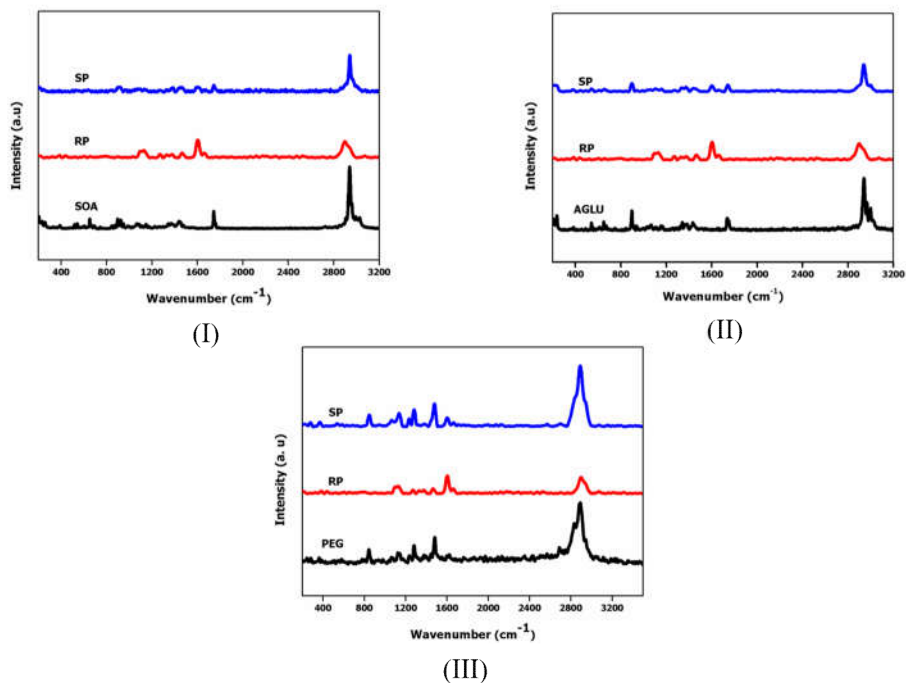


**Figure 4.2** FT-Raman spectra of a) size compound, b) RP, and c) SP for (I) SOA, (II) AGLU, and (III) PEG.

Likewise for AGLU, the highest intense bands are appearing at  $898\text{ cm}^{-1}$ ,  $1735\text{ cm}^{-1}$  and  $2939\text{ cm}^{-1}$  corresponding to the  $\beta$ -anomeric link (C-1-H) bending vibration, C=O stretching and C-H stretching vibrations. The intense bands of AGLU and RP are appearing in the FT-Raman spectra of AGLU coated paper confirming the presence of AGLU on the surface of the paper.

In the case of PEG, the intense bands are appearing at  $839\text{ cm}^{-1}$ ,  $1279\text{ cm}^{-1}$ ,  $1481\text{ cm}^{-1}$  and  $2888\text{ cm}^{-1}$  corresponding to PEG skeletal vibrations,  $\text{CH}_2$  twisting vibration,  $\text{CH}_2\text{-CH}_2$  symmetric bending vibration and  $\text{CH}_2$  symmetric stretching vibrations, respectively. Apart from the bands corresponding to RP, the prominent bands of PEG are also visible on the Raman spectra of PEG sized paper, confirming the effective sizing of paper with PEG. The absence of intense band at  $2888\text{ cm}^{-1}$  in the spectra of PEG coated paper may be due to the merging of the intense band at  $2888\text{ cm}^{-1}$  of PEG and that at  $2898\text{ cm}^{-1}$  of the RP.

Both the vibrational spectroscopic techniques (FT-IR-ATR and FT-Raman) confirms the presence of the size material on the surface of the paper.

#### **4.2.3 SEM studies**

Scanning electron microscopy can be applied as a technique to qualitatively evaluate the uniformity of coating of the size material on the paper surface.<sup>144</sup> The FE-SEM images of RP and the papers sized with three different  $\text{CO}_2$ -philes viz. SOA, AGLU and PEG are provided in Figure 4.3.

Network of cellulose microfibrils are clearly visible in the SEM image of the bare paper whereas the FE-SEM images of all the three sized papers clearly reveals the permeation of size into the paper. In the case of SOA, one could observe a very smooth surface for the sized paper. Image also affirms a more closed and a less porous structure to the SOA sized paper. The cellulose fiber interspaces are filled by SOA,

providing it a smooth and glossy surface. One generally observes a macroscopically smooth surface for SOA-coated paper. It was shown earlier by Wallen et al.<sup>60</sup> that the SOA can in fact form a glass upon treatment with CO<sub>2</sub>. The glassy SOA almost covers the fibrous rough surface of the bare paper suggesting possible improvement in the smoothness of the paper as a result of the SOA sizing. Since SOA fills up most of the void spaces in the paper after sizing, the plasticity of the material is also likely to be improved.

In the case of AGLU sized paper, the cellulose microfibrils are clearly visible, indicating poor binding of AGLU with the paper surface. Also, crystallites of AGLU are visible on the surface, i.e. AGLU seems to be just like a filler material without complete surface coverage.

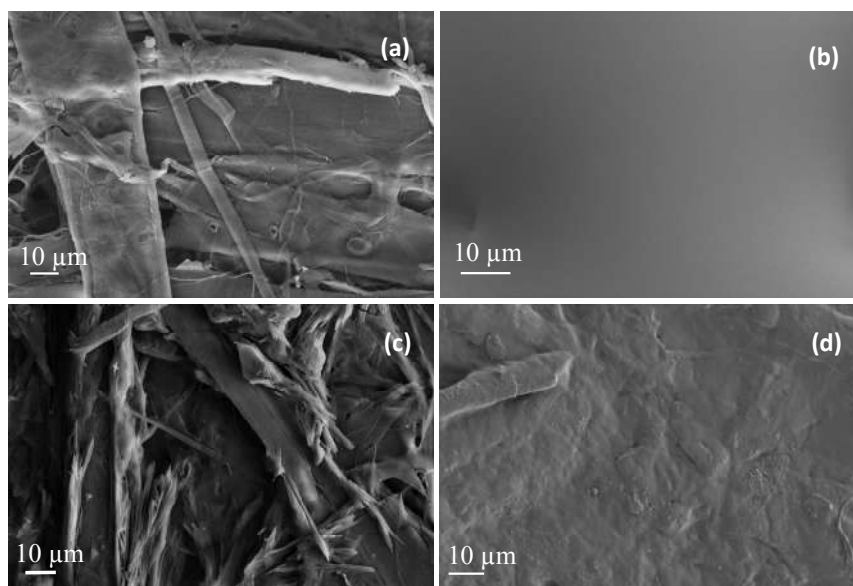


**Figure 4.3** SEM images of (a) RP, (b) SOA-coated paper, (c) AGLU-coated paper and (d) PEG-coated paper.

Sizing of paper using PEG also results in a very smooth coating due to transformation of PEG from a semi crystalline state to a waxy state after treatment with CO<sub>2</sub>.<sup>122</sup> PEG is well entrapped between the cellulose microfibrils on the paper surface and none of the cellulose fibers are visible. Although a reasonably uniform coating is observed in the case of paper sized with PEG. Sizing of paper with SOA is found to be superior in terms of uniformity and constancy of coating.

#### **4.2.4 AFM studies**

AFM can be used as a good tool to study the surface roughness of paper. The atomic force microscopy images of RP and the sized papers are presented in Figure 4.4. Bundles of microfibrils corresponding to the very fine structure of cellulose fibers are clearly visible in the AFM image of the bare paper and the 3-D image shows large number of projections, which refers to the non-uniform rough surface of the bare paper.<sup>145, 146</sup>

For SOA coated paper, microfibrils are not visible and also in fact the 3-D image shows a very smooth coating of SOA on the paper surface with projections less than that of the bare paper indicating a smoother surface.

Cellulose fibers are clearly visible in the AFM image of AGLU coated paper. Projections along with the cellulose fibers are observed in the 3-D image indicating a poor coating of AGLU on the paper surface. AGLU instead of forming a smoother coating, AGLU particles are as such lying on the surface of paper, leading to a rough surface, as observed from the SEM image.

Cellulose fibers are not that visible for the PEG coated paper, since PEG forms a very smooth coating on the paper as already discussed. 3-D image of PEG coated paper shows large number of projections but individual microfibrils are not visible unlike to that observed in the case of AGLU.

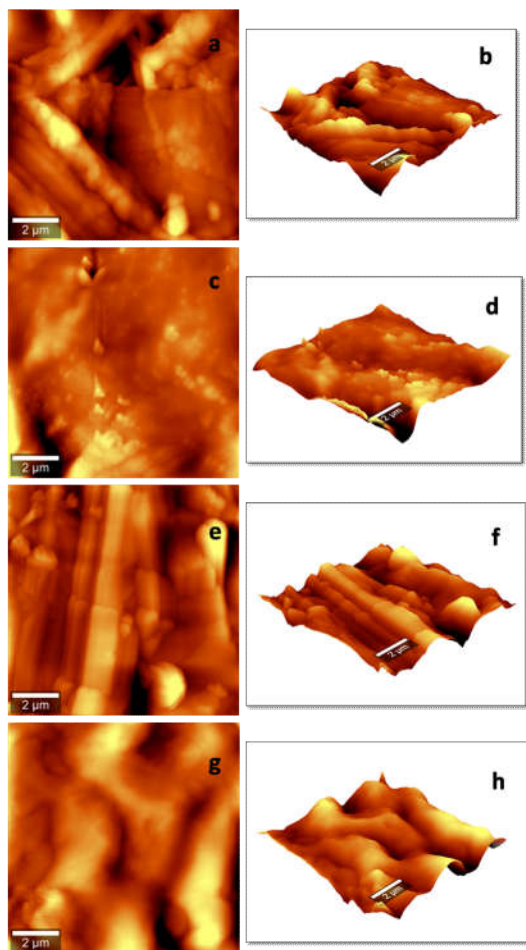


**Figure 4.4** AFM images of (a) and (b) RP; (c) and (d) SOA-coated paper; (e) and (f) AGLU-coated paper; and (g) and (h) PEG-coated paper.

From these results, it may also be concluded that the AFM results are in well accordance with the SEM results.

The surface roughness parameters obtained from AFM analysis is provided in Table 4.1. Comparison of the roughness factors SA and SQ for RP and SPs affirms that the RP exhibits higher values of roughness factors than papers sized with SOA, AGLU and PEG indicating a much smoother surface upon coating.

**Table 4. 1** Topographic parameters obtained by AFM.

<b>Paper</b>	<b>SA (nm)</b>	<b>SQ (nm)</b>
Bare	116.7	150.5
SOA-coated paper	74.9	105.7
AGLU-coated paper	113.7	145.3
PEG-coated paper	46.6	59.5

Higher roughness factor of RP may be due to the unpolished and crude surface of unsized paper. The higher values of roughness factors for RP may also be attributed to the distinct fibers visible in its 3D image. AGLU, in accordance with the SEM results shows higher surface roughness factors than SOA and PEG. These surface roughness factor results are in concordance with the SEM and AFM results wherein the SEM and AFM images shows a very smooth coating for SOA and PEG, but a non-uniform coating in the case of AGLU. Also, one could observe from the surface roughness factors that the surface roughness

of PEG is less than that of SOA, which may be due to the waxy coating observed for PEG sized paper.

#### **4.2.5 Hydrophobicity studies**

By virtue of the acetylation, all the hydroxyl groups of Sucrose and Glucose are replaced by the more hydrophobic acetate groups. Although one cannot expect the hydrophobicity of systems coated with long n-alkyl chains (which will also lead to their self-assembly), it is very likely that the coating with the sugar molecules decorated with acetate groups can yield the paper surface moderately hydrophobic. Such a moderate hydrophobicity will have several implications to the characteristics of the paper surface.<sup>147</sup> This property can easily be verified by measuring the contact angle that a dropping water droplet makes on the surface, with the help of a goniometer assembly. Spreading contact angle is influenced by surface roughness and in addition to the introduction of hydrophobicity to the surface, the surface roughness also can direct the degree to which the water droplet spreads, upon sizing.<sup>147,148</sup> Photographs of the water drop impact on reference and sized papers samples are shown in Figure 4.5.

Also, the contact angles at different time frames for RP, SOA, AGLU and PEG-sized papers are shown in Table 4.2. In the case of SOA-coated paper, static contact angle was found to be  $70.8^{\circ}$  and it remained almost constant even at the 72<sup>nd</sup> frame. From this observation, it can be summarized that water wetting resistance or hydrophobicity of the SOA-coated paper is superior. It can be seen that even though the contact angle is well below  $90^{\circ}$ , the surface retains its



non-wetting nature. It is also observed that the drop does not stick to the surface and easily falls off when the paper is tilted. It may be hypothesized that the observed behaviour is arising out of two reasons.

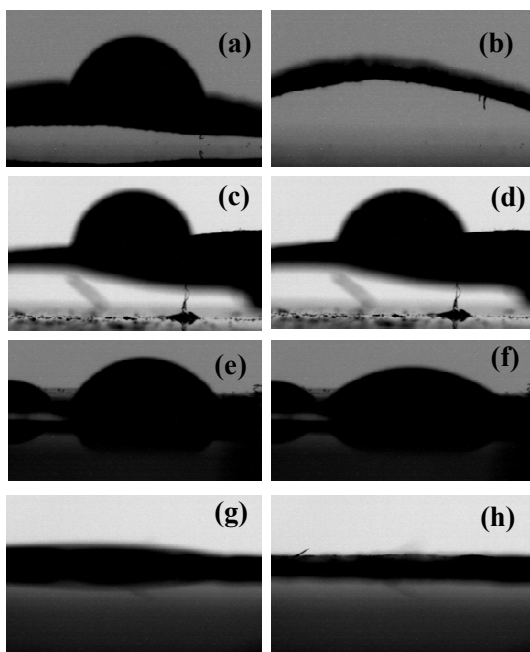


**Figure 4.5** Photographs of drop impact on (a) and (b) RP; (c) and (d) SOA-coated paper; (e) and (f) AGLU-coated paper and, (g) and (h) PEG-coated paper at 0<sup>th</sup> and 72<sup>nd</sup> frame.

Firstly, the acetylated sugar has a fundamentally hydrophobic nature which predicts that the surface should be hydrophobic. However, the carbonyl groups of the acetate groups can form hydrogen bonds with the water molecules of the drop causing a reduction in the observed surface tension. It may also be plausible that the surface of the paper is having a microscopic roughness created by the evolution of CO<sub>2</sub> from the CO<sub>2</sub>- melt and thereby resulting in an enhancement in the contact

area between surface and the water drop. It is also likely that there could be some pockets of unsized cellulosic regions which in comparison with the largely hydrophobic regions will give rise to a hydrophobic surface with an apparent contact angle less than 90°. Although SOA is hydrophobic, contact angle of paper could not be increased to a large extent due to the very smooth coating of SOA on the paper as it is already reported in literature that smoother surface results in lower contact angle.<sup>148-150</sup>

**Table 4.2** Variation in the contact angles for different frames depending on time for RP, SOA, AGLU and PEG-coated papers.

<b>Frame (ms)</b>	<b>RP</b>	<b>SOA-coated paper</b>	<b>AGLU-coated paper</b>	<b>PEG-coated paper</b>
0	41.9	70.8	53.5	19.8
2	39.7	70.8	53.1	19.7
4	38.2	70.6	49.7	19.6
6	34.5	70.4	48.3	17.3
8	28.2	70.4	46.8	16.3
10	27.6	70.0	45.4	0
72	0	67.1	29.9	0

For AGLU coated paper, one observes a static contact angle of 53.5° which is well below the static contact angle observed for SOA and at the 72<sup>nd</sup> frame, contact gets reduced to 29.9°. Since both SOA and AGLU are hydrophobic, normally one would expect similar water wetting properties, but contrary to our presumption, water wetting property is poor than that of SOA. This decrease in contact angle may be attributed to the non-uniform and inconsistent coating of AGLU on

the paper surface. Major portion of the cellulose, even after coating with AGLU is still exposed to water since coating with AGLU was observed to be not that effective.

PEG being hydrophilic, one observes a very low static contact angle of  $19.8^\circ$  and it suddenly reduces to zero at the very 10<sup>th</sup> frame itself. Apart from the hydrophilic nature of PEG, the smoother paper surface obtained upon PEG coating, results in the reduction of contact angle below that of the reference paper. From the AFM results, one observed very low surface roughness factors for PEG, which is in accordance with the very low contact angle of PEG-coated paper.

Also, the water retention capacity of RP and the SPs are studied by the  $\text{Cobb}_{60}^*$  measurement, which is the measure of water absorbed by the paper in one minute and the  $\text{Cobb}_{60}^*$  values of RP and SPs are provided in Table 4.3. The detailed experimental procedure for  $\text{Cobb}_{60}^*$  measurement is discussed in Chapter 2 and it is observed that the  $\text{Cobb}_{60}^*$  value of SOA-coated paper is much lower than RP. SOA being hydrophobic, it forms a water resistant coating on paper and this might be responsible for the lower  $\text{Cobb}_{60}^*$  value of SOA-coated paper.

**Table 4.3**  $\text{Cobb}_{60}^*$  values for RP, SOA, AGLU, and PEG-coated papers.

Paper	$\text{Cobb}_{60}^*$ (g/m <sup>2</sup> )
RP	552
SOA-coated paper	146
AGLU-coated paper	456
PEG-coated paper	583

One observes higher Cobb<sub>60</sub><sup>\*</sup> value for AGLU compared to that of SOA, which reveals higher water absorbance capacity of AGLU-coated paper and this may be plausibly due to the poor binding of AGLU with the paper resulting in poor surface coverage of the size material on the paper surface. In the case of PEG, Cobb<sub>60</sub><sup>\*</sup> value is noticed to be higher than RP, indicating that the water absorbance capacity of PEG-coated paper is even higher than that of RP. This may be attributed to the hydrophilic nature of PEG and also results are in support with the contact angle measurement values wherein, water wetting resistance is observed to be least for PEG-coated paper.

#### **4.2.6 Mechanical properties**

Finally, the mechanical properties of the RP and SPs are recorded and are shown in Table 4.4. The tensile strength of the paper sized with SOA increased from 6.4187 N/mm<sup>2</sup> to 10.2596 N/mm<sup>2</sup>, i.e. nearly a 60 percent increase. Sizing of paper with SOA is found to be superior in terms of all the mechanical properties. Generally, from the SEM and AFM results, one would expect PEG to have many folds higher value of tensile strength than that of AGLU, but contrary to our assumption, only a small difference in tensile strength is observed. This may be ascertained to the waxy nature of the PEG coating.

**Table 4.4** Mechanical properties of RP, SOA, AGLU and PEG-coated papers.

<b>Paper</b>	<b>Tensile strength (N/mm<sup>2</sup>)</b>	<b>Percentage elongation</b>	<b>Young's modulus (N/mm<sup>2</sup>)</b>
RP	6.4	4.8	1.3
SOA-coated paper	10.2	2.9	3.6
AGLU-coated paper	7.6	2.5	3.2
PEG-coated paper	7.9	4.3	1.9

Also, the increase in the tensile strength after coating with all the three size compounds may be due to the fact that the microfibrils in the cellulose which are highly protected in the sized paper when compared to the RP.

### **4.3 Summary and Conclusions**

The objective of this work was to validate the enabling of the use of liquid CO<sub>2</sub> as a green solvent platform for sizing of paper. The use of inexpensive and CO<sub>2</sub>-philic size materials such as SOA, AGLU, and PEG in combination with liquid/scCO<sub>2</sub> provides an economically viable, green, and inherently dry process for the sizing of paper. Different characterization techniques such as FT-IR and Raman spectroscopic technique, AFM and SEM studies are carried out to differentiate and characterize the bare and the sized papers. Sizing

efficiency in terms of hydrophobicity is also measured. Mechanical properties of the bare and coated papers are measured.

From the various results, it may be concluded that, among the three size compounds utilized for the sizing of paper, SOA is found to be the best candidate. SOA is found to be superior to AGLU and PEG in terms of uniformity of coating, surface coverage, smoother surface, roughness parameters, water wetting resistance property, water absorbing property and mechanical properties.

AGLU, although successfully incorporated into the paper surface as observed from the IR and Raman studies, this seems to be just like a filler material and is not completely covering the paper surface. Non-uniform, discontinuous coating is observed for the paper sized with AGLU. Water absorbance and water wetting resistance properties did not increase significantly.

In the case of PEG, uniform, smooth coating with complete surface coverage is observed. But due to its hydrophilic nature, water wetting resistance is noticed to be even lower than that of the bare paper.

### **5.1 Introduction**

Wood is an “ecofriendly” raw material with innumerable applications in different sectors and the term “ecofriendly” can be justified only if wood remains non-toxic from the beginning towards the end of each application. Wood is primarily composed of cellulose, hemicellulose and lignin. Apart from these components, wood consists of many hydroxyl groups that absorb water molecules. These hydroxyl groups are responsible for the hygroscopic nature of wood. Shrinkage and swelling of wood upon absorption and desorption of water is a major concern in the wood industry and other branches of industry wherein wood is used as the major raw material. As a remedy to this issue, over the years, the chemical modification of wood is a common practice followed in the wood industry.<sup>151</sup> Chemical modification of wood improves the properties of wood such as thermal stability and resistance to degradation. One of the most preferred methods for chemical modification of wood is acetylation,<sup>151</sup> wherein hydroxyl groups are replaced by acetyl groups thereby resulting in the decrease in absorption and desorption of water.<sup>152</sup> This process also in turn results in improved dimensional stability of wood and resistance against weathering and microbial attacks. Untreated wood undergoes degradation very fast and the most common method universally followed is the use of Chromated Copper Arsenate (CCA).<sup>153</sup> Conventional methods for the chemical modification of wood have

many drawbacks such as poor environmental acceptability and difficulty in drying the wood after treatment with liquid and handling the treatment liquids. Apart from these, the solvents used are viscous suspensions, incapable of smoothly flowing through this semi-porous solid resulting in depthless penetration. Taking into consideration, all the negative impacts of conventional wood impregnation methods, researchers are making attempts to find an alternative method for the modification of wood.

For the past few decades, the use of scCO<sub>2</sub> as a green alternative solvent is gaining interest due to its environmentally benign solvent properties and is replacing the conventional solvents in majority of the chemical processes as discussed in the introductory chapter. Likewise, scCO<sub>2</sub> has achieved considerable attention in the field of wood processing.<sup>154-156</sup> As mentioned in Chapter 1, scCO<sub>2</sub> exhibits both liquid and gas like properties. It has very high density like that of a liquid and hence results in easier dissolution of the impregnating substance into the wood matrix and has very low surface tension and exhibits gas like viscosity which enables it to easily penetrate into the fine microcapillary network in the wood.<sup>156</sup> Recently, acetylation of wood using scCO<sub>2</sub> has been reported.<sup>157,158</sup> Another added advantage of using scCO<sub>2</sub> based impregnating techniques is that the entire process is dry and the wood does not remain wet all through the process. Superior ability of scCO<sub>2</sub> to penetrate the wood has already been reported and numerous works has been reported regarding the impregnation of wood with various biocides and pesticides using scCO<sub>2</sub> as the carrier.<sup>159,160</sup>

Besides the aim to improve the properties of wood through chemical modification, the other major objective that we have focused is the



protection of wood from the wood destroying animals such as termites, wood boring beetles, carpenter ant etc. However, wood is very much susceptible to attacks from these organisms and hence wood has to be impregnated with protective materials that prevent the destruction of wood from these species. The search for environmentally friendly and economically viable wood protecting agents are in progress and the research efforts to emerge together the environmentally benign, CO<sub>2</sub>-philic wood protecting substances with scCO<sub>2</sub> is the current research interest. Herein this work we have chosen SOA as the coating material. SOA, has been commercially used as an inert agent in insecticides and pesticides. SOA is also popularly used as a bitterant and is considered as an aversive agent, used in several coating applications to prevent children from consuming it.<sup>161</sup> Apart from the environmentally benign features of SOA ( discussed in Chapter 1), studies also reveals that SOA can also be used in agriculture sector in plant protection since it is observed to possess antifungal activity.<sup>162</sup> SOA, due to its very high miscibility with CO<sub>2</sub>, together with the above mentioned features, is an excellent impregnating substance for the modification of wood. SOA deliver bitterant taste to the wood and hence protect it from ‘wood destroying insects’. Also, SOA-modified wood find applications in preparation of toys so that children can be prevented from biting the toys.

The primary aim of this work is to check the viability of impregnation/coating of wood with SOA using scCO<sub>2</sub> as a green alternative solvent. Detailed experimental procedure adopted for the impregnation/coating of wood is discussed in Chapter 2. Further, the modified wood is examined to investigate the homogeneity and nature

of coating of SOA on the wood and the effect of impregnation on thermal and dimensional stability of wood.

## 5.2 Results and Discussion

The electron microscopic and optical microscopic images of untreated and treated wood samples are provided in Figure 5.1. Pits, empty voids and distinct cavities are clearly visible in the electron and optical microscopic image of untreated wood.<sup>163</sup> Likewise, untreated wood wall is observed to have a very rough surface. In the case of SOA-impregnated wood, one would observe a very smooth and comparatively uniform coating of SOA, filling up all the void spaces and pits of the wood vessel walls.

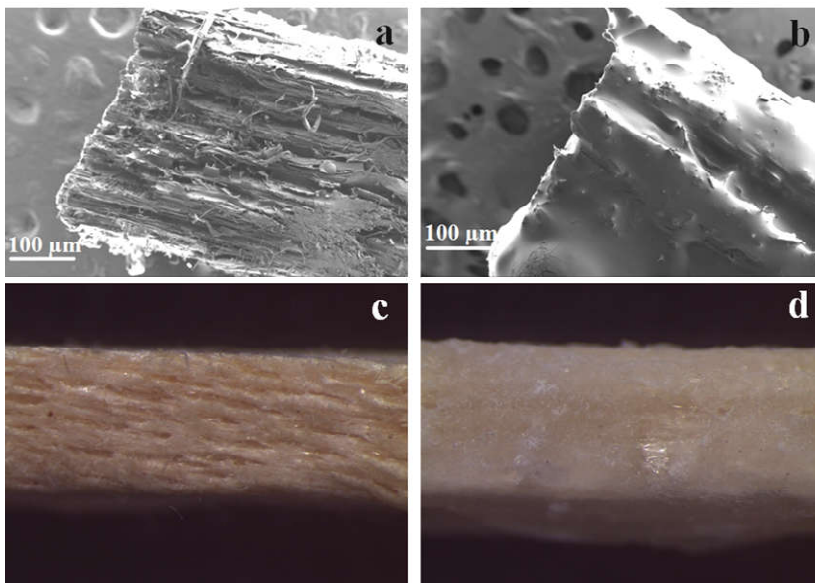


**Figure 5.1** FE-SEM images of a) untreated wood b) treated wood, and optical microscopic images of c) untreated wood d) treated wood.

Upon impregnation, the waxy wood surface has been replaced with a smoother surface. It may be concluded from the morphological studies that the impregnation of wood with SOA in CO<sub>2</sub> medium resulted in a uniform coating with good surface coverage. Hence, SOA based impregnation/coating can be applied for coating applications on wood especially for protection against wood destroying species and in the manufacturing of toys and other items, thereby preventing children from biting it.

Further, the treated and the untreated wood samples are analyzed using FT-IR-ATR and FT-Raman spectral techniques to confirm the presence of SOA on the wood surface after the coating process.

The FT-IR-ATR spectra of SOA, untreated and treated wood are shown in Figure 5.2. For SOA sample, the peaks at 1743, 1216 and 1032 cm<sup>-1</sup> corresponds to C=O, C-O and C-O (six membered ring) stretching bands, respectively. The untreated wood sample shows a prominent band in the region 3000 to 3600 cm<sup>-1</sup>, corresponding to OH stretching vibration. The band in the region 2800-3000 cm<sup>-1</sup> can be assigned to C-H stretching vibrations. Another strong band at 1732 cm<sup>-1</sup> corresponds to C=O stretching, the band at 1238 cm<sup>-1</sup> may be ascribed to C-O stretching, the bands at 1507 and 1593 cm<sup>-1</sup>, may be assigned to aromatic skeletal vibrations (C=C) of lignin, a major component of wood. The less intense bands observed at 1030, 1372 and 1458 cm<sup>-1</sup> may be assigned to cellulose, lignin and hemicellulose.<sup>164,165</sup>

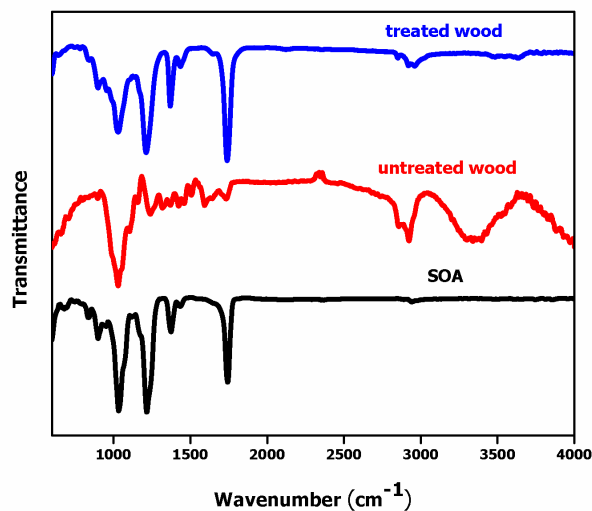


**Figure 5.2** The FT-IR-ATR spectra of a) SOA, b) untreated wood, and c) treated wood.

For treated wood, the two most prominent bands appears at 1739 and 1212  $\text{cm}^{-1}$  corresponding to C=O and C-O stretching vibrations in SOA and wood as well. The C=O stretching vibrational bands corresponding to untreated wood and SOA, merged and appeared at 1739  $\text{cm}^{-1}$  for the treated wood sample. The band at 1030  $\text{cm}^{-1}$  may be assigned to vibrations in wood. Apart from the intense bands of wood, the treated wood sample showed the intense bands of SOA, revealing the presence of SOA or successful coating of SOA on the wood surface.

The FT-Raman spectra of SOA, untreated and treated woods samples are presented in Figure 5.3. For SOA, the two strong bands at 2940 and 1743  $\text{cm}^{-1}$  may be ascribed to C-H and C=O stretching vibrations of the acetate moiety.

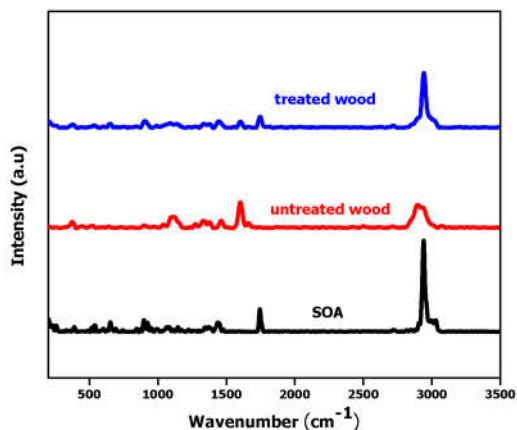


**Figure 5.3** FT-Raman spectra of a) SOA, b) untreated wood, and c) treated wood.

The untreated wood shows two prominent bands at  $1602\text{ cm}^{-1}$  arising from the phenyl groups in lignin, a major component of wood and a very strong peak at  $2896\text{ cm}^{-1}$  with a shoulder peak at  $2939\text{ cm}^{-1}$  corresponding to C-H vibrations in cellulose, lignin and hemicellulose.<sup>166</sup> The treated wood sample showed a prominent peak at  $2941\text{ cm}^{-1}$  and this may be due to the overlapping of the C-H stretching band of untreated wood and SOA samples in this region. Since the treated wood sample showed the prominent stretching bands of wood as well as SOA, we could infer the presence of SOA on the surface of the wood. The FT-Raman results are in good correlation with the FT-IR-ATR results, both the results reveals the successful impregnation/coating of wood with SOA.

The diffractions patterns for untreated and treated wood samples are presented in Figure 5.4. The untreated wood sample, a semi crystalline

material, shows two diffractions rays at  $2\theta$  of  $22^\circ$  and  $16^\circ$ , that can be assigned to cellulose crystal planes  $I_{002}$  and  $I_{101}$ , respectively.<sup>165</sup> These two diffraction rays are typical of cellulose.

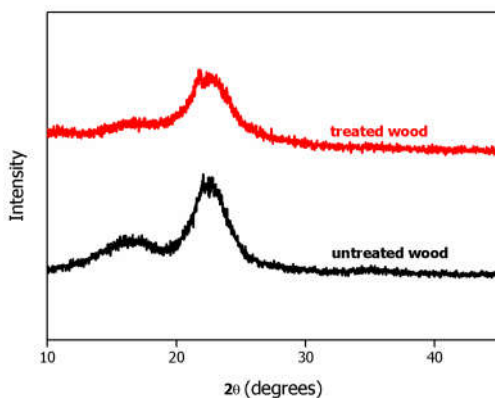


**Figure 5.4** X-ray diffractograms of untreated and treated wood samples.

Normally, one would expect the presence of diffraction peaks of SOA on the XRD diffractogram of treated wood and there by expects an increase in the crystallinity of wood. But contrary to our assumption, no noticeable change in the crystallinity of wood is observed. This may be due to the fact that, SOA after treatment with  $\text{CO}_2$  and on rapid depressurization, transforms to an amorphous state.<sup>60, 122</sup>

The thermogravimetric analysis of untreated and treated wood samples were carried out and the corresponding thermogravimetric curves and their derivative thermogravimetric (DTG) curves are shown in Figure 5.5. Untreated wood showed first degradation in the temperature range  $50\text{-}115^\circ\text{C}$  and this is may be due to the loss of water and moisture

from the wood. In the same temperature range, no weight loss is observed for treated wood which clearly indicates that the water and moisture uptake is reduced upon impregnation with SOA. Hydrophobic nature of SOA may be responsible for the lower uptake of water by the SOA-coated wood.

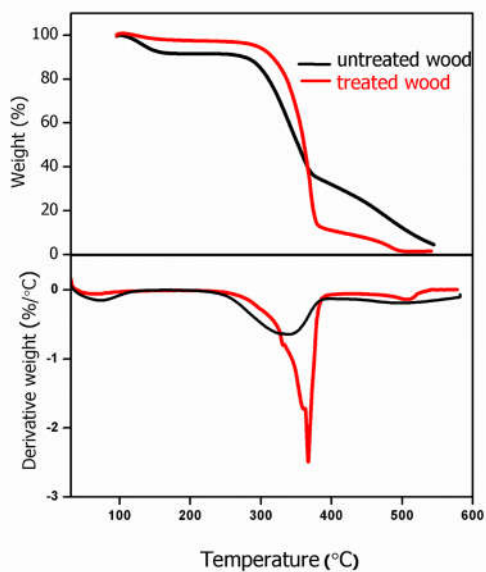


**Figure 5.5** TGA and DTA curves of untreated and SOA-treated wood samples.

The untreated wood began to degrade at a temperature of 269 °C ( $T_{\text{onset}}$ ) with a major decomposition peak at 335 °C ( $T_{\text{max}}$ ) as observed from the DTG curve. Likewise, the treated wood started degradation at 298 °C with a major decomposition peak at 367 °C. On comparing the  $T_{\text{max}}$  and  $T_{\text{onset}}$  values of both the samples, it is very well evident that the thermal stability of the treated wood is enhanced. Also, the residual weight of untreated wood is approximately 5.17 % and that of treated

wood is 1.6 % at 577 °C. Since the residual mass left over is observed to be lower for the treated wood, we can reduce the wastage into the environment to a larger extent. Since the treated wood shows lower weight loss (lower water uptake on impregnation) with higher degradation temperature, it is thermally stable than the untreated wood sample.

### **5.3 Summary and Conclusions**

Summarizing, we have investigated the viability of using SOA and scCO<sub>2</sub> for the impregnation of wood. SEM and microscopic images clearly revealed that the impregnation was successful since, the pores and pits present on the wood surface was completely covered by a smooth, hydrophobic, glassy SOA coating. The FT-IR-ATR and FT-Raman spectra confirms the presence of SOA on the surface of the wood, since the treated wood sample showed the vibrational stretching bands of SOA and wood. XRD results suggests no noticeable changes in the crystallinity after coating with SOA in scCO<sub>2</sub>. Thermal studies shows a significant increase in the thermal stability of the wood after coating with SOA. Overall, the properties of wood improved after impregnating with SOA in scCO<sub>2</sub> medium. The impregnation/coating of wood carried out in scCO<sub>2</sub> medium is a complete dry process and the solvent and SOA can be recycled and reused. As already discussed, SOA being a bitterant, SOA impregnated wood finds many applications in various fields.



## CHAPTER 6

# **COMPOSITES OF UREA WITH CONTROLLED RELEASE PROFILES**

---

### **6.1 Introduction**

The use of fertilizers is a very common practice followed in agricultural sector since soil does not provide all the essential nutrients required for the plants for its optimal growth and productiveness. Cultivable land available has diminished due to urbanization, industrialization, land degradation from heavy flooding etc. These factors are responsible for lower agricultural production. Over the years, a tremendous increase in the use of fertilizers was noticed, in order to meet the world food demand through increased agricultural production. Some efficient measures are to be implemented to meet the challenge of global food security. So we need to look forward for such systems that enhance production with little or minimal environmental burden.

#### **6.1.1 Controlled and Slow Release Fertilizers**

Controlled and slow release fertilizers (CRFs and SRFs) releases the nutrient in a controlled, slow manner and releases the nutrient as and when required by the plants.<sup>167-169</sup> These fertilizers ensures efficient nutrient uptake by reducing the loss of nutrients via leaching, runoff, volatilization etc. thereby improving the crop yield. The basic difference between CRFs and SRFs is that the rate, pattern and the duration of release of CRFs are well controlled and for SRFs the rate,

pattern and duration of release are not controlled and these varies with the change in the climatic and soil conditions. According to the Association of American Plant Food Control Officials (AAPFCO), controlled and slow release fertilizers contains a plant nutrient that are of the two forms : (a) the one that delays the availability and uptake for the plant as well as its utilization after application, (b) the one which is available to the plant for a period longer than the ‘rapidly available nutrient fertilizer’.<sup>168</sup> Likewise, CRFs are also described as fertilizers coated with a natural, or semi-natural, and environmentally benign macromolecule material such that the nutrient is released in a slow pace such that a single uptake could meet the essential nutrient requirement for model plant growth.<sup>167,169</sup>

### **6.1.2 Classification of CRFs**

CRFs are broadly classified into three categories.<sup>167,168,170</sup>

1. The first category (organic compounds) can further be subdivided into naturally occurring organic compounds and synthetically produced organic compounds. The latter consists of the condensation products from Urea and aldehyde. This can be further divided into biologically decomposing compounds such as Urea-acetaldehyde and chemically decomposing compounds such as isobutyledene-diUrea.
2. The second category consists of water soluble fertilizers in which certain physical barriers control the nutrient release. Fertilizers coming under this class appears as granules coated with a hydrophobic polymer or as matrices in which the active

water soluble nutrient are dispersed in a continuum via hydrophobic polymers that leads to controlled nutrient dissolution and the latter is less common compared to the former one. The former one, i.e., coated CRFs are further classified into those coated with organic materials and those coated with inorganic materials. Likewise, the materials used for the preparation of matrices can be sub categorised into hydrophobic materials and gel-forming polymers which are hydrophilic in nature.

3. The third category includes inorganic low solubility compounds such as metal ammonium phosphates and partially acidulated phosphate rock.

### **6.1.3 Advantages and disadvantages of CRFs**

The use of CRFs are considered advantageous in many aspects, especially, their use reduces toxicity due to high ionic concentrations associated with the fast dissolution of the fertilizer. Due to reduced toxicity and salt content of fertilizers, they can be utilized for a prolonged time; thereby reducing the frequency of usage. Also, use of CRFs meets the complete nutrient requirement of the plant. They also reduce the loss of nutrients which occur either by evaporation, loss of ammonia, loss of nitrate nitrogen etc. CRFs also lead to the reduction in gas emissions.

Use of CRFs are also known to have some drawbacks. Lack of a standardized method for the determination of controlled release of fertilizer is a major disadvantage. Consequently, the laboratory results

and actual results upon field applications shows large differences. Various coatings such as urea-formaldehyde, urea-sulfur, urea-polymer coatings etc. possess one or the other drawbacks, say, in the case of urea-formaldehyde, it was noticed that some portion of nitrogen was getting released very slowly or sometimes not at all. Likewise, use of urea-sulfur fertilizers resulted in increased acidity of the soil and also they released the nutrient very fast at its initial stages, causing damage to the plant itself. Polymer-based coatings resulted in the deposition of undesired residues of synthetic substituents into the soil. Besides all these, the cost requirements are too high for the manufacture of CRFs.

#### **6.1.4 Controlled release Urea fertilizers**

Urea is probably the most vital and widely used fertilizer due to its high nitrogen content (46%), ease of application, and low cost of production.<sup>171</sup> The major drawback associated with the application of urea is the fast and premature decomposition, disabling the efficient absorption of nitrogen by the plant. Before the plant absorbs the nutrient, evolution of ammonia occurs via the action of water, volatilization, urease enzyme etc.<sup>172</sup> Urea undergoes various physico-chemical and biological transformations when applied to soil and produces various plant available nutrients.<sup>167</sup> Plants require very small amount of nutrient in its initial stages and higher amounts for its upcoming stages of growth. Also, higher chances for leaching, surface run off and vaporization of Urea need to be considered. Consequently, major amounts of the nutrient will be absorbed by the plant at its initial stage of growth. Approximately, 40 to 70% of nitrogen escapes to the environment and only remaining nitrogen uptake takes place.<sup>171</sup>

Globally, the current scenario is to go in tune with the raising agricultural production and over the years, research efforts were focused in this direction and their paramount aim was to develop highly efficient, biodegradable and low cost-fertilizers. This issue is addressed by the development of CRFs and SRFs.

The first and the foremost method adopted for controlled release of Urea was sulphur-coating. In one of the adopted procedures, Urea was initially coated using wax which acts as a sub-coating, followed by spraying with sulfur and finally, plasticizers (such as polyethylene) were adhered to the sulfur surface to prevent cracking of the coated surface.<sup>173</sup> In another procedure, Urea was coated with molten sulfur using spouted fluidized bed under temperature pressure conditions.<sup>174</sup> Urea was also coated using an outer polymer coating and an inner sulfur coating.<sup>175</sup> This double coating provided more resistance to abrasion and cracks while handling it. A three layer method of Urea coating using sulfur is also reported.<sup>176</sup> All these sulfur coated Urea showed significantly good results with respect to controlled release. However, the major disadvantage associated with the use of sulfur is that it is much prone to brittleness and formation of microscopic pores due to the crystalline nature of sulfur. Also, it takes much time for the disintegration of sulfur into the soil and may end up in the acidification of soil. On account of these, researchers began to investigate the viability of using polymer-based coatings for Urea. The use of solvents for spray-coating of polymer on Urea was too hazardous and this was replaced with aqueous polymer solutions.<sup>177</sup> Also, Urea was coated with polyurethane. Although expensive, the coating was observed to be

very thin, and these thin coatings are reported to be superior and the entire Urea was released in forty to fifty days.<sup>178</sup>

Certain polymers with excellent swelling capacity and the ability to withstand high osmotic pressure were also used as coating materials for Urea. Han et al. developed three different coatings for Urea namely Ca-Mg Phosphate, polyolefin, polyolefin plus dicyanamide.<sup>179</sup> All three were observed to act as good CRFs. The feasibility in using Poly(lactic acid-co-ethylene terephthalate) as a coating material for Urea was investigated and the research group concluded that morphology played a vital role in deciding extent of controlled release.<sup>180</sup> Coating of Urea granules using Polyhydroxy butyrate and ethyl cellulose combination shows fast release of Urea, in approximately five minutes, which is too low for its application in agricultural sector.<sup>181</sup>

Polymer-based coatings, in spite of their ability to supply nutrients with respect to the plant needs and being inert against microorganisms, their usage has been reduced due to continuous use of solvents and the complications in the coating methods. Super-absorbent polymer materials, known for their ability to absorb water, was used for the preparation of controlled release Urea.<sup>182</sup> Double coated Urea<sup>183</sup> such as inner coating of starch and outer coating of Acrylic acid and Acrylamide, inner coating of urea-formaldehyde and outer coating of cross-linked poly(acrylic acid)/organo-attapulgite composite, inner layer of polystyrene and outer layer of cross-linked poly(acrylic acid), all these were identified to act as moderately good controlled release Urea fertilizers. Triple layer polymer coatings of Urea using

Polyethylene, Poly(acrylic acid-co-acrylamide) and Poly (butyl methacrylate) was also studied and good results were observed.<sup>184</sup>

However, upon realizing the importance of environment conservation together with stringent environmental protection rules, the use of all the above mentioned CRFs reduced tremendously since most of them were observed to be non-biodegradable, toxic and highly expensive. This was followed by the discovery of a large number of environmentally friendly coatings.<sup>185-189</sup> Even today, some of the commercially available fertilizers have coatings made from polyurethane, alkyl resin etc, which are highly non-biodegradable and may adversely affect the soil properties. Therefore, utmost attention must be kept while choosing coating materials for fertilizers and must assure that the coating material applied is environmentally benign in all aspects.

Starch being inexpensive, abundant and biodegradable, is an alternative choice for the design of CRFs. The hydrophilic nature of starch limits its application, but upon pertinently modifying starch with various materials, it may be used for this purpose. Different starch-based coatings discussed are dual coating using starch and Isobutylidendiurea,<sup>190</sup> coating using a solution of starch, polyethylene glycol and acrylic acid etc.<sup>191</sup> These starch-based coatings couldn't gain much attention in this sector since it was not found to be compatible with the plant needs. Controlled release of Urea using lignin was also investigated.<sup>192</sup> Neem and neem oil based controlled Urea fertilizer<sup>167</sup> has gained considerable interest in recent years since it was scientifically proven that neem is an effective nitrification

inhibitor. Neem coated Urea is one among the widely used commercial Urea fertilizer. Likewise, still researchers are in search for suitable green coatings for Urea.

In this study, we present a novel and benign procedure for the preparation of composites for the controlled release of Urea (UR) wherein the UR is coated with CO<sub>2</sub>-philes such as SOA and AGLU, using scCO<sub>2</sub> as the green solvent platform. Similar composites were also prepared using Ethyl Acetate (EA) medium. Specifically, four systems are studied in this chapter viz. AGLU-UR-EA, AGLU-UR-CO<sub>2</sub>, SOA-UR-EA, and SOA-UR-CO<sub>2</sub>. The abbreviations mentioned are described in the following order: coating material-Urea-solvent used, and represents the encapsulation of Urea in a particular coating material using a particular solvent.

In general, we have used a weight ratio of 1:20 for the preparation of composites of UR and the coating material. Apart from this, weight ratios of 1:10 and 1:50 were also prepared to study the effect of concentration of UR in the release kinetics of UR from the composites prepared. Detailed experimental procedures for the preparation of the composites of UR in CO<sub>2</sub> and EA medium are detailed in Chapter 2.

## **6.2 Results and Discussion**

Initially, we are studying the change in crystallinity of the coating material and UR upon composite formation and also the extent of dispersion of UR in the coating material. It is pertinent to study these changes in order get a clear idea of the UR release kinetics from different matrices.



### 6.2.1 XRD studies

The X-ray diffraction patterns of UR, AGLU, SOA, and the four composites namely AGLU-UR-EA, AGLU-UR-CO<sub>2</sub>, SOA-UR-EA, and SOA-UR-CO<sub>2</sub> are shown in Figure 6.1.

One expects that the XRD peaks of UR will vanish if UR is dispersed completely at a molecular level. On the other hand, if the crystals of UR are coated with the coating materials, the XRD pattern for UR crystals will survive in the XRD.

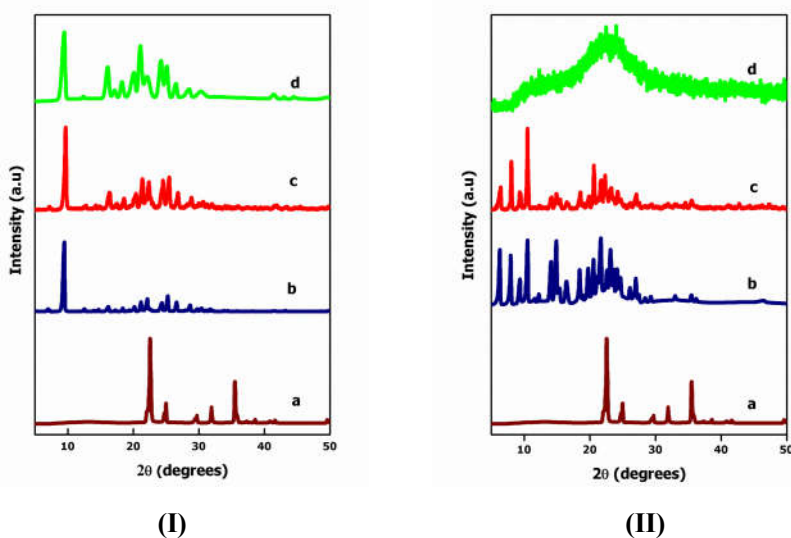


**Figure 6.1** XRD pattern for UR, AGLU, SOA, and the different composites prepared using EA and CO<sub>2</sub>: (I) (a) UR (b) AGLU (c) AGLU-UR-EA, and (d) AGLU-UR-CO<sub>2</sub>; (II) (a) UR (b) SOA (c) SOA-UR-EA, and (d) SOA-UR-CO<sub>2</sub>.

In the case of AGLU-UR composites prepared using EA and CO<sub>2</sub>, none of the peaks of UR are present, indicating that UR is completely dispersed in the AGLU matrices. It has already been reported by our

group that upon CO<sub>2</sub> treatment the crystallinity of AGLU is reduced to a microcrystalline level.<sup>122</sup> A small decrease in the lattice order is also observed for the AGLU-UR composites prepared in EA, when comparing with that of the XRD data of pure AGLU. To conclude, although both the composites prepared are observed to be still crystalline, a decrease in the order of crystallinity is observed when compared to that of pure AGLU.

Similar studies were carried out for SOA-UR composites prepared in CO<sub>2</sub> and EA medium. Interestingly, the UR peaks are completely absent in both the SOA-UR composites, revealing that UR is molecularly dispersed in their matrices. Again, our results remains concordant with the earlier reports that SOA upon CO<sub>2</sub> treatment transforms to an amorphous glassy state.<sup>60,122</sup> In this case, the XRD data shows an amorphous state for SOA-UR composites prepared in CO<sub>2</sub> medium. No noticeable changes are observed in the degree of crystallinity of SOA in the SOA-UR composite prepared using EA, except that the UR is molecularly dispersed in SOA.

On comparing the XRD data, one would expect a faster release of UR from composites prepared using AGLU, as the composites remains almost crystalline with only a slight decrease in the long range order. The composite of SOA prepared in CO<sub>2</sub> medium is expected to show a slow release, since the UR is encapsulated in a glassy and hydrophobic matrix.

### **6.2.2 Raman spectroscopic studies**

Vibrational spectroscopy is one of the most useful methods for probing the molecular environments using the characteristic peak positions as

well as the line widths. While the peak positions and the shifts observed provides information regarding the nature of binding, the line widths provides information about the local disorder in the lattice. IR and Raman spectroscopic methods provide complementary information in this regard. FT-Raman serves as a non-destructive vibrational spectroscopic tool that provides information from this perspective. It is pertinent to know how such physicochemical factors affect the release kinetics of UR from the composite.

From a structural perspective, the XRD results have already shown that the SOA remains crystalline after treatment with conventional solvents such as Acetone and Ethyl Acetate while the sample turns into a glassy state after treatment with CO<sub>2</sub>.<sup>122</sup> The investigation particularly focuses on the changes for the two spectral bands, viz., the carbonyl peak around 1740 cm<sup>-1</sup> and the C-H stretching peak around 2940 cm<sup>-1</sup>. The FT-Raman spectra of AGLU and AGLU-UR-CO<sub>2</sub> in the carbonyl and C-H stretching regions are provided in Figure 6.2.

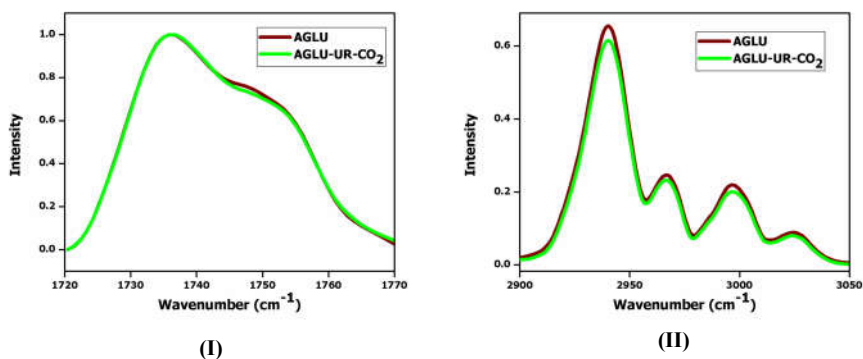


**Figure 6.2** FT-Raman spectra of AGLU and AGLU-UR-CO<sub>2</sub> in different regions: (I) 1720-1770 cm<sup>-1</sup> and (II) 2900-3050 cm<sup>-1</sup>.

No significant changes are observed, neither in the Raman spectral band positions or their line widths indicating that there are no significant changes in the physicochemical states of AGLU. In fact, the results reveal that the crystallinity of AGLU in the composite remains the same even after CO<sub>2</sub> processing. A detailed study of the UR peaks is also carried out to investigate to probe any plausible interaction between UR and AGLU, in AGLU-UR-CO<sub>2</sub> composite. No noticeable shifts in the UR peaks are observed.

Similar studies are also carried out on SOA and SOA-UR-CO<sub>2</sub> composite. The FT-Raman spectra of pure SOA and the SOA-UR-CO<sub>2</sub> composite, in the two important regions are provided in Figure 6.3.

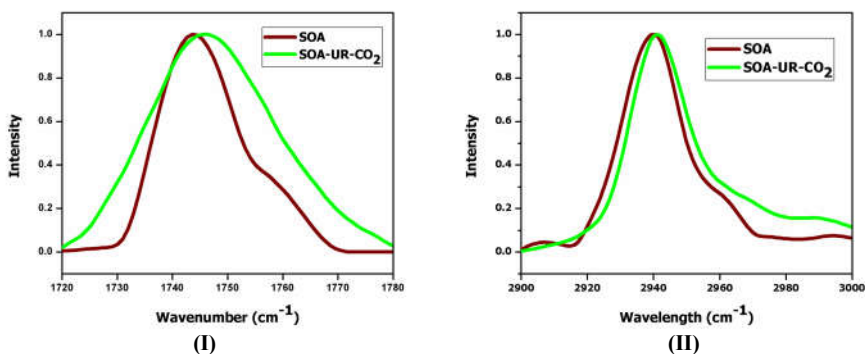


**Figure 6.3** FT-Raman spectra of SOA and SOA- UR-CO<sub>2</sub> in different regions: (I) 1720-1780 cm<sup>-1</sup> and (II) 2900-3000 cm<sup>-1</sup>.

It is clearly evident that notable peak shifts took place at both carbonyl and C-H stretching frequencies. Line width of both the bands are increased indicating a decrease in the short range order, as shown by the XRD results, showing an amorphous state for the CO<sub>2</sub>-treated sample. A correlation between the line width and the order is directly

related to the Heisenberg's uncertainty relationship between energy and excited state life time. In a disordered lattice, the vibrational relaxation is faster and thus one would expect broader lines.

Apart from the lattice expansion, notable shifts in peak positions are also observed. The carbonyl stretching band has been blue shifted by  $3\text{ cm}^{-1}$  from  $1743$  to  $1746\text{ cm}^{-1}$ . Similarly, the C-H stretching mode is blue shifted by  $2\text{ cm}^{-1}$  from  $2939$  to  $2941\text{ cm}^{-1}$ . Both these may be attributed to the higher degree of disorder wherein the average intermolecular distances are rendered longer. Also, the solvent  $\text{CO}_2$  molecules are not retained in the system.

Finally, we are investigating whether any of the UR bands have undergone any physical or chemical changes on composite formation. The FT-Raman spectra of UR and SOA-UR- $\text{CO}_2$  composite in the vibrational frequency region of  $900$  to  $1030\text{ cm}^{-1}$  is provided in Figure 6.4. The most intense band of UR, at  $1011\text{ cm}^{-1}$  corresponding to symmetrical CN stretching, is observed to be red-shifted by  $2\text{ cm}^{-1}$ .

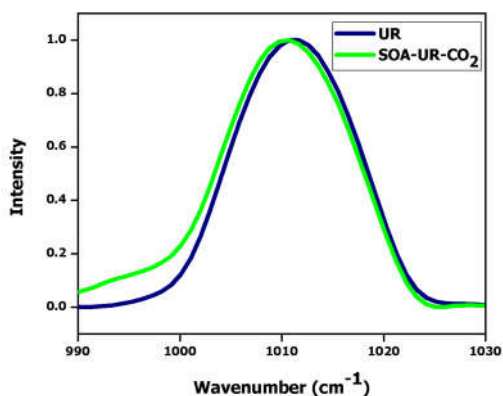


**Figure 6.4** FT-Raman spectra of UR and SOA-UR- $\text{CO}_2$ :  $990$  to  $1030\text{ cm}^{-1}$  vibrational frequency region.

This red shift signifies stronger binding between UR and SOA in the composite prepared.

### 6.2.3 Optical microscopic studies

Optical microscopic images give a clear idea regarding the visible changes in morphology that took place after composite preparation. Optical microscopic images of AGLU-UR and SOA-UR composites prepared in CO<sub>2</sub> medium are provided in Figure 6.5. The optical microscopic image of AGLU-UR-CO<sub>2</sub> composite shows a white crystalline powder and SOA-UR-CO<sub>2</sub> shows a transparent, glassy substance.

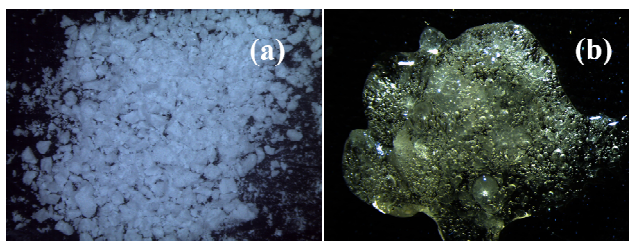


**Figure 6.5** Optical microscopic images of (a) AGLU-UR-CO<sub>2</sub> and (b) SOA-UR-CO<sub>2</sub>.

The bubbly appearance may be due to the rapid evolution of the encapsulated CO<sub>2</sub> from the surface, when the system is brought to the ambient conditions.

### 6.2.4 SEM Studies

Scanning electron microscopic studies provides more understanding of the variations in physical state and morphology of the different systems under study. Herein, since both the CO<sub>2</sub>-philes, AGLU and SOA, are hydrophobic, the surface morphology of the systems also will have a significant effect on the surface area of the materials and

thereby affects the access of water molecules to the UR. This will directly influence the kinetics of UR release. The FE-SEM images of AGLU, SOA, UR, AGLU-UR-EA, AGLU-UR-CO<sub>2</sub>, SOA-UR-EA and SOA-UR-CO<sub>2</sub> are presented in Figure 6.6.

From the SEM image of UR, we could infer that UR is existing in the form of granules of different sizes (Figure 6.6 (a)). Pure AGLU is observed as aggregates of crystals of different particle size and shape (Figure 6.6 (b)). AGLU-UR composite prepared in EA shows an agglomerated morphology with network of particles (Figure 6.6 (c)) and AGLU-UR prepared in CO<sub>2</sub> also shows similar networked structure (Figure 6.6 (d)). The SEM image of pure SOA shows crystallites of different shape and size (Figure 6.6 (e)). It is interesting to observe that the SOA-UR-EA morphology (Figure 6.6 (f)) is slightly different from that of pure SOA, with a more aggregated structure.

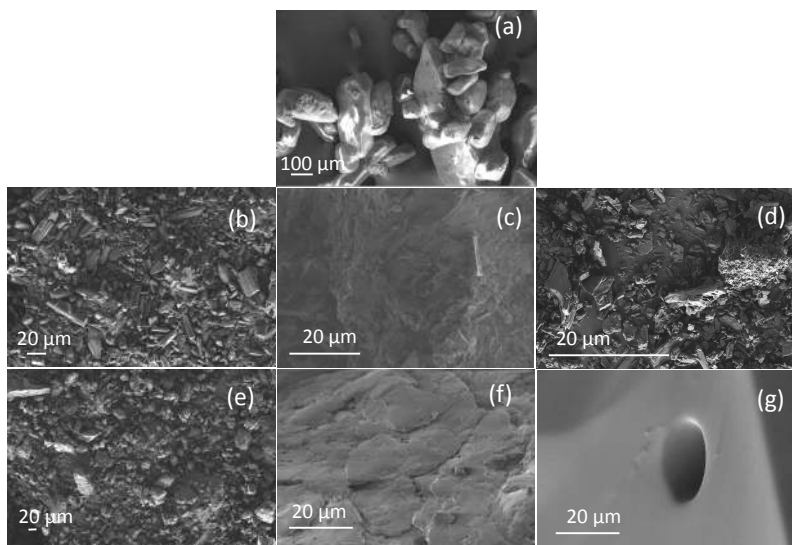


**Figure 6.6** FE-SEM images of a) UR, b) AGLU, c) AGLU-UR-EA, d) AGLU-UR-CO<sub>2</sub>, e) SOA, f) SOA-UR-EA, and g) SOA-UR-CO<sub>2</sub>.

The SEM image of SOA-UR-CO<sub>2</sub> (Figure 6.6 (g)) shows a very smooth surface. The hole observed on the surface is due to the evolution of the entrapped CO<sub>2</sub>. This smooth surface observed is consistent with the glassy nature of the composite observed from the optical microscopic image.

### **6.2.5 Urea release kinetics**

The structural modifications, change in lattice order, site-specific binding between UR and the coating material, and the microenvironments are expected to affect the kinetics of release of Urea. As we have seen earlier, AGLU retains its crystallinity and lattice order after CO<sub>2</sub>-treatment while SOA transforms into a glass. In the next sections, we will investigate how this is going to reflect on the results of our studies on the UR-release kinetics from these composites when dispersed in aqueous medium, as in the case of a natural environment.

The release kinetics of UR from AGLU-UR-EA and AGLU-UR-CO<sub>2</sub> are presented in Figure 6.7. It can be seen that UR release from both the composites appears to be very similar, the complete release taking place within an approximate time span of 20 hours. About 80 % of UR gets released within a span of 10 hours.



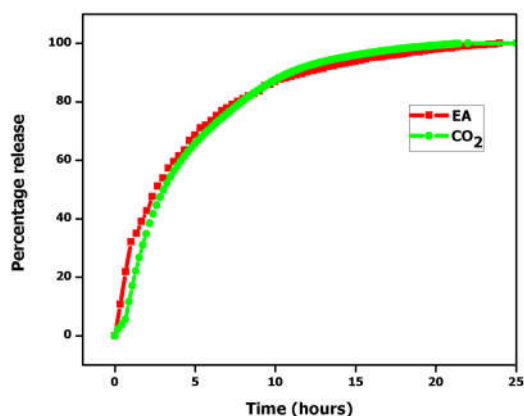


**Figure 6.7** The release kinetics of UR from AGLU-UR composites prepared in EA and CO<sub>2</sub>.

We have also seen that for both the composites AGLU-UR-EA and AGLU-UR-CO<sub>2</sub>, the AGLU is in the crystalline state, although the crystallite sizes vary slightly. In such cases, one would expect that the Urea molecules will be pushed out to the exterior of the AGLU crystal surface, making it easier to be accessed by the surrounding water molecules.

The kinetics of release of UR from SOA-UR composites prepared in EA and CO<sub>2</sub> are presented in Figure 6.8.

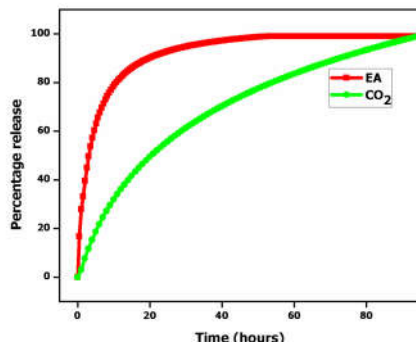


**Figure 6.8** The release kinetics of UR from SOA-UR composites prepared in EA and CO<sub>2</sub>.

The SOA-UR composites prepared in CO<sub>2</sub>, show a very slow release of UR. It is observed that it takes nearly 93 hours for complete, spontaneous, release of UR, when dispersed in aqueous medium. Unlike in the case of AGLU, the SOA-UR-EA has a completely different release profile when compared to SOA-UR-CO<sub>2</sub>. In the former, the release is significantly faster, where most of UR is getting released within about 20 hours. The observed differences may be attributed to the structural differences between the two systems; the most important being that SOA-UR-CO<sub>2</sub> is a glass while SOA-UR-EA is a crystalline material. It is likely that the UR molecules are entrapped and immobilized in the SOA glass matrix, making it difficult to diffuse out into water, which is made still more difficult by the hydrophobic nature of SOA. Additionally, SOA-UR-CO<sub>2</sub> has a smoother surface and plausibly lesser surface area, making the solvent accessible area even lesser. On the other hand, in the case of SOA-UR-EA, SOA is crystalline and therefore the UR molecules are tethered to the surface of the SOA crystal, making it easier to be diffused into the

aqueous medium. This explains the observed differences between the release kinetics of the two systems.

### **6.2.6 Effect of concentration of Urea**

The change in concentration of UR may have a significant role in deciding the release kinetics. In a system containing UR and the coating material, three types of interactions need consideration. These are UR-UR interactions, host-host interactions and UR-host interactions, respectively. When the amount of UR increases, UR-UR interactions may become more notable, making the UR-host interaction cross-section smaller, leading to a faster release of UR. Conversely, when the amount of UR is lesser, UR-host interactions predominate, resulting in sustained slow release of UR. Also, when the amount of UR is lesser, UR can be more efficiently encapsulated within the matrix, leading to slower release kinetics.

In order to investigate the effect of concentration on the UR release, we employ UR-coating material composites (processed using CO<sub>2</sub>) of three different weight ratios viz., 1:10, 1:20 and 1:50, respectively. The release kinetics of UR from AGLU matrix with three different UR-AGLU weight ratios is provided in Figure 6.9. It is observed that three weight ratios show slight variations in the release kinetics. One observes a faster release in the order 1:10 > 1:20 > 1:50 weight ratio. This trend observed may be due to the fact that, as the concentration of UR decreases, UR can be more efficiently encapsulated in the matrix, leading to slower release profile.

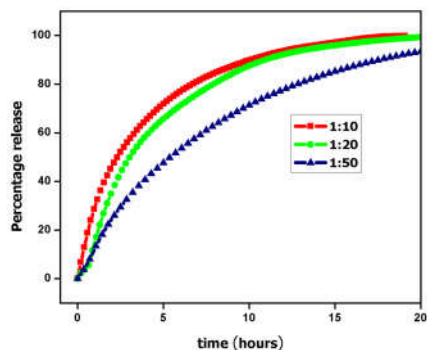


**Figure 6.9** Release kinetics of UR from AGLU matrix with different UR-AGLU ratios.

The release kinetics of UR from SOA matrix with three different UR-SOA weight ratios is provided in Figure 6.10. One observes only less significant changes in the release kinetics.

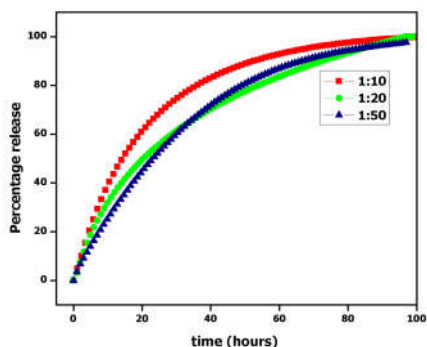


**Figure 6.10** Release kinetics of UR from SOA matrix with different UR-SOA weight ratios.

Almost similar UR release kinetics from three different UR:SOA ratios can be attributed to the glass formation observed in SOA composites. UR is encapsulated within the glassy SOA matrix, and hence it is very difficult for UR to come out, resulting in slower release. Also, SOA being hydrophobic, it not only forms a glass, but a hydrophobic glass

is formed. Due to this hydrophobic coating, solvent access to UR is very less, making the release slower.

### **6.2.7 Combinatorial approach for tailoring the UR release**

So far, we have chosen AGLU and SOA separately as the coating materials for Urea. Composites of AGLU-UR and SOA-UR were prepared in EA and CO<sub>2</sub>. Initially, changes in crystallinity were studied using XRD data, UR-coating material interactions were studied using FT-Raman spectroscopic techniques. Morphological changes of the composites were compared using optical microscopic and SEM studies. Finally, the release kinetics of these composites were determined using UV-spectroscopic technique. We also discussed the different factors affecting the release kinetics of UR.

Different release kinetics were observed for AGLU-UR and SOA-UR composites depending on different physico-chemical characteristics of the composites. UR release from AGLU matrix took place in 20 hours whereas UR release from SOA took place in 93 hours. As discussed in the introduction part, plants require nutrient at its different stages of growth, and this varies from plant to plant depending on its life span. This led to the idea of tailoring the UR release kinetics by taking different compositions of AGLU and SOA composites. Likewise, we decided to combine AGLU and SOA in 5 different weight ratios, viz., 80:20, 60:40, 50:50, 40:60 and 20:80, in the CO<sub>2</sub>-solvent system. The composite of UR are prepared with these five different AGLU-SOA compositions in the weight ratio 1:20 in CO<sub>2</sub> medium. The detailed experimental procedure for the preparation of composites is provided in Chapter 2. Both AGLU and SOA are hydrophobic, but AGLU-UR composite is observed to be crystalline whereas SOA-UR composite is

noticed to be an amorphous glassy solid, so one would expect that the combination of AGLU and SOA would be a hybrid of these two coating materials.

### 6.2.7.1 XRD studies

Previous studies from our research group<sup>122</sup> had demonstrated that AGLU retains its crystalline nature after CO<sub>2</sub>-treatment whereas the SOA forms a glass after CO<sub>2</sub>-treatment. Similar observations were recorded by us with reference to AGLU-UR-CO<sub>2</sub> and SOA-UR-CO<sub>2</sub> composites, it is expected that the XRD patterns would vary significantly for the composites with varying ratios of AGLU and SOA. The XRD patterns corresponding to the composites with different combinations of AGLU and SOA are exhibited in Figure 6.11.

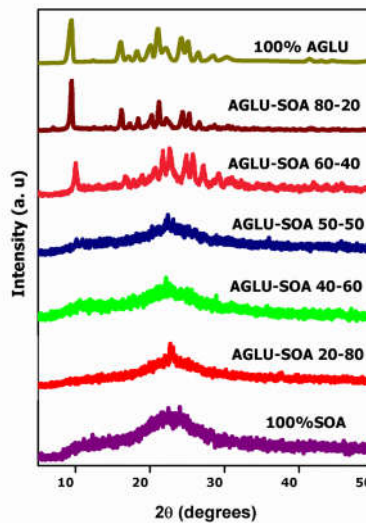


**Figure 6.11** XRD patterns for the different composites of UR with varying compositions of AGLU and SOA (a) 100% SOA (b) SOA:AGLU 80:20 (c) SOA:AGLU 60:40 (d) SOA:AGLU 50:50 (e) SOA:AGLU 40:60 (f) SOA: AGLU 20:80 (g) AGLU 100 %.

As one systematically moves from 100 % AGLU to 100 % SOA, XRD pattern shows a clear sequence from highly crystalline to highly amorphous nature. The composite with 100% AGLU, as already observed is crystalline in nature. When 20% SOA is introduced to it, a fall in crystallinity is observed and this keeps continuing. For the composite of UR prepared with AGLU:SOA (50:50), the intensity of the peaks of AGLU is decreased and a broad band, which is a characteristic of the amorphous SOA forms the background. Eventually, one observes a broad band characteristic for 100 % glassy SOA.

#### **6.2.7.2 SEM studies**

SEM studies provide insights into various morphological changes; specifically the crystallinity, homogeneity, surface roughness/smoothness etc. of the coating materials. These are the factors which determine the extent of UR encapsulation in the matrix, which directly affects the release kinetics. Information regarding the solvent access to UR by the solid composites may also be indicated by the SEM studies. The SEM images of the composites of UR prepared with different combinations of AGLU and SOA are shown in Figure 6.12.

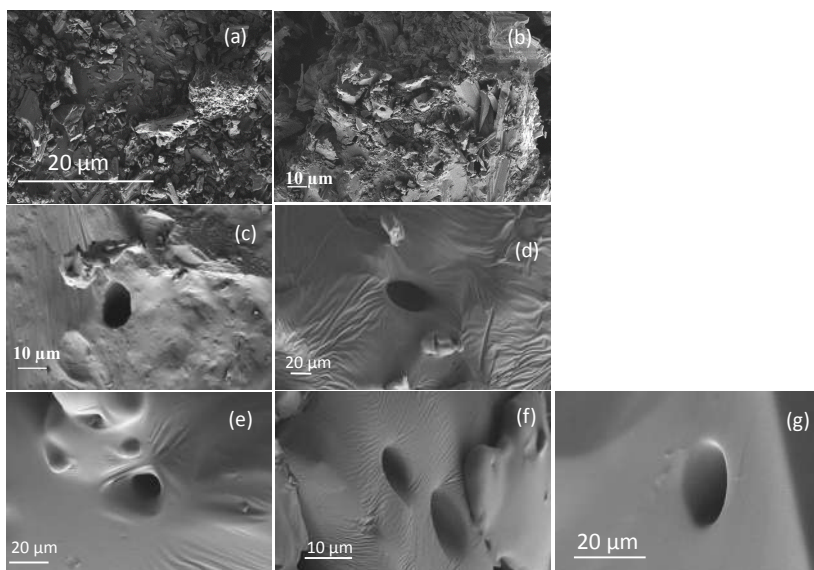


**Figure 6.12** SEM images of the composites of UR with various combinations of AGLU and SOA. (a) 100% AGLU (b) AGLU:SOA 80:20 (c) AGLU:SOA 60:40 (d) AGLU:SOA 50:50 (e) AGLU:SOA 40:60 (f) AGLU:SOA 20:80 (g) 100% SOA.

As already discussed in the previous section, AGLU-UR composite shows a networked structure with crystalline particles of different shape and size. A much more agglomerated structure is observed for AGLU:SOA (80:20) composite with a small increase in surface smoothness. In AGLU:SOA (60:40), a tremendous increase in surface smoothness is observed, although it possess an agglomerated structure. In the next three combinations of AGLU:SOA, the surface smoothness kept increasing and a glassy state began to appear. We could infer that, as SOA concentration kept increasing, the surface smoothness improved. Finally, as already discussed, 100 % SOA showed a complete smooth glassy surface. In none of the SEM images of the



composites, UR granules were observed, attributing to complete miscibility of UR in the composites.

### **6.2.7.3 Urea release kinetics**

Release kinetics depends on various factors which we have already discussed in the previous sections. Individually, we have studied the UR release kinetics from AGLU and SOA matrices upon CO<sub>2</sub> and EA processing and the factors which decided the release kinetics. Herein, we are investigating the UR release kinetics from different combinations of AGLU-SOA composites and relating it with the XRD and SEM studies. The release kinetics of UR from the various composites of AGLU and SOA are presented in Figure 6.13.

Just by looking at the figure, one could observe a particular trend in the UR release kinetics. AGLU-UR composite took 20 hours for the complete release of Urea from its matrix whereas SOA-UR composite took 93 hours for the complete UR release. It is well evident that in composites with higher SOA concentration, UR is very slowly released from the matrix. Likewise, the composites with higher AGLU concentrations, showed release behaviour much like that of AGLU-UR composites, i.e., a fast release kinetics. From this observation one could infer that the release kinetics depends on the concentration of the individual coating materials. 100 % AGLU shows a faster release, and as one gradually adds SOA to this, release rate is slowed down.

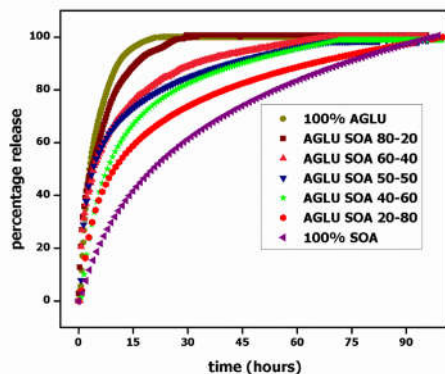


**Figure 6.13** Release kinetics of UR from composites prepared using varying amounts of AGLU and SOA.

As the concentration of AGLU increases, the UR release is observed to be faster, plausibly due to the rupture of the glass formed by SOA. From this particular trend observed in the release kinetics, one could easily tune the UR release kinetics according to our needs. In fact, one observes a very good correlation between the extent of glass formation and the UR release kinetics. The higher the degree of glass formation, the slower would be the release, with the UR being completely immobilized inside.

### 6.3 Summary and Conclusions

In the present chapter, we have investigated the possibility of utilizing CO<sub>2</sub> and two non-fluorous CO<sub>2</sub>-philes, viz., SOA and AGLU, for the preparation of Urea composites for controlled release of Urea, one of the prominent issues in agriculture. The XRD and FT-Raman studies of UR, CO<sub>2</sub>-philes and composites were recorded, followed by the

study of release kinetics. We investigated the kinetics of release of UR in relation to the physicochemical and structural changes of the sugar acetates used. It is observed that SOA forms a glass upon processing with CO<sub>2</sub> with significant impact on the release kinetics. For the composite SOA-UR-CO<sub>2</sub>, the UR is completely encapsulated and immobilized in the hydrophobic SOA glass, making its release rather slow, within a span of 93 hours. On the other hand, in all other composites where the sugar acetates retained their crystallinity, the UR release is very fast. This must be due to the fact that in the crystalline excipient systems, the UR molecules are pushed out to the exterior of the acetate crystallites allowing the solvent molecules to access them easily. Effect of concentration on the Urea release profile is also investigated. Finally, we tried to tune the release kinetics by combining two coating materials and preparing their composites with different weight ratios. XRD, release kinetics and SEM results of the new composites prepared are discussed.

The coating materials and the solvent used in this work are environmentally benign in all aspects. SOA, AGLU and CO<sub>2</sub> are of low cost and readily available. This CO<sub>2</sub>-based glassification strategy has the potential to be commercialized for the preparation of UR composites with tunable release kinetics, with immense applications in the field of agriculture.



## CHAPTER 7

# **PREPARATION OF DRUG-EXCIPIENT COMPOSITES FOR CONTROLLED DRUG RELEASE: THE CASE OF ATENOLOL**

---

### **7.1 Introduction**

Supercritical Fluid (SCF) technology has emerged as a promising technology in the field of pharmaceuticals during the last few decades. In this chapter, we report the results of our investigations on how supercritical CO<sub>2</sub> can be used as a solvent for the homogeneous mixing of drug and excipient to prepare drug-excipient composites. Essentially, the drug and a CO<sub>2</sub>-philic excipient are mixed together and then the CO<sub>2</sub> is vented out to obtain drug-excipient composites with little residual solvent in it. Before proceeding further, it is worth understanding the basics of drug formulation, beginning from the various components of a drug.

#### **7.1.1 Components of medication**

The drug is essentially composed of two components namely the excipient and the Active Pharmaceutical Ingredient (API). According to World Health Organization (WHO), API is “a substance used in a finished pharmaceutical product (FPP), intended to furnish pharmacological activity or to otherwise have direct effect in the diagnosis, cure, mitigation, treatment or prevention of disease, or to have direct effect in restoring, correcting or modifying physiological functions in human beings”.<sup>193</sup> There are also cases like multiple therapies, wherein more than one API is present, to treat different

symptoms and act in different ways. The excipient is defined as a “substance(s) other than the API which has been appropriately evaluated for safety and is included in a drug delivery system to either aid processing of the system during manufacturing or protect, support or enhance stability, bioavailability or patients compliances or assist in product identification and enhance any other attributes of overall safety and effectiveness of drug product during storage or use”, by the International Pharmaceutical Excipients Council.<sup>194,195</sup> Rarely, the excipients also possess pharmacological activity. Excipients are also classified as binders, fillers, lubricants, glidants, compression aids, colors, sweeteners etc., based on their functions.<sup>196</sup>

### **7.1.2 Amorphous Solid Dispersions**

Oral drug delivery is regarded as the most easy, simple and widely accepted method for drug administration. However, in many cases, this method is found to be inefficient for a number of reasons, such as poor bioavailability of drugs. In fact, the most important problem in a drug formulation is the poor bioavailability and dissolution rate of poorly water soluble drugs. Several approaches have been employed to overcome these issues, such as the preparation of solid dispersions, crystallization, nanosuspensions, lipid-based drug delivery systems etc. Among these, solid dispersions have gained considerable interest as the most effective approach for improving the bioavailability and the dissolution rate. Sekiguchi and Obi were the first ones to describe solid dispersion in the year 1961.<sup>197</sup> In general solid dispersions can be defined as the dispersion of one or more pharmaceutical ingredients in a carrier or matrix at solid state.<sup>198</sup> The matrix can be amorphous or

crystalline. Based on the arrangement, solid dispersions can be broadly classified into three categories viz. eutectics, amorphous precipitations in crystalline matrix and solid solutions.<sup>198,199</sup> Eutectic mixtures are composed of two components that are completely miscible in the liquid state and also, often, to a less extent, in the solid state. They are generally prepared by melt fusion method. The second category, is similar to eutectic mixture and the only difference is that the drug is precipitated in the amorphous state. In solid solutions, both the components crystallize together in a single phase system and are generally prepared by solvent evaporation or co-precipitation methodologies.

With reference to Biopharmaceutical Classification System (BCS), drugs are classified into four categories.<sup>198</sup> Solid dispersion strategy is the most promising technology being employed for BCS class II drugs, i.e. drugs with high permeability and low aqueous solubility. Drug delivery involves many important aspects such as delivery to a specific target size, fast release of low solubility drugs, and sustained release of drugs that are soluble in aqueous solutions. According to the fundamental principle of general oral drug formulation, an ideal drug delivery system should deliver the API to the required site in a controlled manner, which in turn, reduces the frequency of dosage.

#### **7.1.2.1 Importance of amorphous state in pharmaceutical systems**

The basic difference between crystalline and amorphous state is that the former is characterized by a higher degree of order of molecular arrangement.<sup>200</sup> Amorphous state is the highest energy form of a solid

substance.<sup>201</sup> When a crystalline material is heated, it melts at its melting temperature. If this molten material is cooled slowly, the molecules are packed in an orderly arrangement (crystalline state), since it gets enough time to move from their current position to thermodynamically stable position in the crystal lattice. Likewise, if the molten material is cooled rapidly, it doesn't have enough time to orderly arrange the molecules and it goes to an amorphous state, and sometimes a super-cooled state or glassy state, characterized by a glass transition temperature ( $T_g$ ).<sup>202,203</sup> Often, the glassy state is described as a solid with liquid-like order.

In the case of a crystalline drug, the lattice energy barrier is a major limitation in the dissolution, although it has several advantages such as high purity and physical, chemical stability. On the other hand, amorphous state is characterized by higher entropy, free energy and volume, and a higher molecular mobility, leading to a faster dissolution and oral availability of the drug.<sup>204</sup>

### **7.1.3 Different methods for the preparation of solid dispersions**

Melting and solvent evaporation methods are the most commonly used methods for the preparation of solid dispersions.

#### **7.1.3.1 Melting method<sup>205,206</sup>**

Melting method also known as fusion method was first proposed by Sekiguchi and Obi.<sup>197</sup> In this method, the physical mixture of drug and the excipient is directly heated until melting occurs. The mixture is then rapidly cooled in ice bath with vigorous stirring and solidified.



The final product obtained is then crushed, pulverized and finally sieved. Although this technique is easier and simple, still there exist serious concerns associated with this technique. Firstly, there are chances for the drug or the carrier to decompose or evaporate at the higher temperature employed. Secondly, the drug and the carrier may be immiscible, resulting in inhomogeneity or separation between the drug and the excipient. These limitations were overcome to a great extent by modified melt methods such as hot melt extrusion method, melt agglomeration method etc.

Hot Melt Extrusion (HME) method is having high similarity with the melting method except that the mixing of the components is carried out with the aid of an extruder. Herein, the drug-carrier powder blend is introduced into a heated barrel provided with a rotating screw via a hopper. Inside this barrel, the components are mixed in the liquid state and moved towards a die, which shapes the blend according to our requirement as pellets, tablets, films etc. In this case too, miscibility of drug and the carrier is a matter of serious concern. Also, the amount of heat and the high shear forces applied is an issue for heat sensitive substances. Unlike melting method, this method suggests the opportunity of continuous production. Again, this method is disadvantageous for thermally labile materials, which cannot withstand high temperature and works have been carried out in this line wherein a reduction in processing temperature was achieved with the use of CO<sub>2</sub>.

Meltrex<sup>TM</sup> is a patented method for the preparation of solid dispersion and is also considered as a modified melting method, just as HME.<sup>207</sup>

The major aids included in Meltrex<sup>TM</sup> manufacturing set up is the use of twin screw extruder and two independent hoppers to provide a broad temperature range. In this set up, the residence time of the components in the extruder are lowered, ensuring continuous mass flow, thereby reducing thermal stress experienced by drug and the carrier.

Melt agglomeration is yet another modified melting method, wherein the solid dispersions are prepared in conventional high shear mixers. In this method, the mixture containing the drug, carrier and the excipient is heated to a temperature within or above the melting point of the carrier. This method offers stable solid dispersions, when prepared in a rotary processor. The binder type, manufacturing method and particle size are the major parameters which decide the final nature of solid dispersions prepared via melt agglomeration method.

#### **7.1.3.2 Solvent method<sup>205,206</sup>**

This technique is the most commonly used one for the preparation of solid dispersions. In this method, the physical mixture of the drug and the carrier is dissolved in a common solvent and later evaporated. As already mentioned, one of the major limitation faced by the melting method is the degradation of the drug or the carrier. This can be prevented by adopting the solvent technique, since only low temperatures are required for the evaporation of organic solvents. One of the major drawbacks of this technique, however, is the difficulty associated with the complete removal of the solvent, negatively affecting the chemical stability of the drug. The use of organic solvents and higher cost of preparation are also known to be its demerits. Based

on the method adopted for evaporation of solvent, this technique can be classified into different classes such as vacuum drying, slow evaporation of the solvent at low temperatures, use of rotary evaporators, a stream of nitrogen, freeze-drying, spray-drying, heating of the mixture on a hot plate etc. Among those listed, spray-drying and freeze-drying are the most common ones and herein spray-drying, the physical mixture of drug and the carrier dissolved in the solvent is sprayed into a stream of heated air flow. In freeze-drying method, the physical mixture of the drug and carrier solubilized in the solvent is immersed in liquid nitrogen until completely frozen and later this solution is lyophilized.

#### **7.1.4 Supercritical fluid methods**

As mentioned in the introduction, SCFs exhibit both liquid-like and gas-like properties. This has enabled the SCF technology with notable applications in pharmaceutical industry such as micronization to enhance the bioavailability of poorly water soluble drugs.<sup>208</sup> In this process, the average particle size of API are reduced to micrometer or sub-micron range. Conventional methods that are being employed for this purpose are milling, bashing and grinding.<sup>209</sup> All these methods are working on the phenomenon of friction and thence are energy and time consuming ones. SCF technology has emerged as a promising one, which could overcome the curbs of conventional processing methodologies. Additionally, this technique ensures a clean or a 'solvent free' process. Among the various supercritical fluids available in industry, SCF technology is the most commonly applied with scCO<sub>2</sub> taking into consideration its environmentally benign features and

economically promising aspects. SCF methods are primarily classified into two broad categories based on the role played by scCO<sub>2</sub>.

(I) scCO<sub>2</sub> as solvent

(II) scCO<sub>2</sub> as antisolvent

#### **7.1.4.1 SCF used as solvent**

In this SCF method, SCF is utilized as a solvent for both API and excipient. A typical example is the Rapid Expansion of a Supercritical Solution (RESS), demonstrated first by Hannay and Hogarth.<sup>210</sup> This is a two-step process. First, the solid is dissolved in SCF under pressure. The SCF solution thus obtained is then expanded and finally suddenly depressurized. This rapid depressurization leads to supersaturation and super fluid nucleation and hence results in the generation of sub-micron or nano-sized sized particles. Although RESS is regarded as a simple and efficient technique, the major drawbacks that are limiting its application is the high cost of production, poor control on the particle size and also the poor solubility of many pharmaceutical products in SCF. Several modified RESS methods are industrially available in order to overcome its limitations and they are RESOLV (Rapid Expansion of a Supercritical Solution into a Liquid Solvent) and RESS-SC (Rapid Expansion of Supercritical Solution with Solid Co-solvent).<sup>211,212</sup>

#### **7.1.4.2 SCF used as antisolvent<sup>213</sup>**

Bleich and coworkers were the first to demonstrate the use of SCF as antisolvent and the related SCF techniques.<sup>214,101</sup> The low solubility of

most of the pharmaceutical ingredients in SCF, limited the production of micro or nanosized particles using RESS and modified RESS methods. Here, SCF is regarded as an antisolvent and this must be completely miscible with the liquid solvent used. Also, the solute must be insoluble in the antisolvent. If one considers the microscopic solvation structures, one can perceive this as a case of preferential solvation. In general, this technique is considered as an alternative to recrystallization in order to process insoluble solute in SCF. This technique exploits the ability of the gas to sufficiently expand the liquid, wherein a large number of solute-solvent interactions will be replaced by solvent – SCF (or gas) interactions thereby limiting the solvation of the solute molecules, leading to precipitation of solutes.

Based on the modes of mixing between SCF and the antisolvent, antisolvent processes are classified into different categories which are briefly described in the coming sessions.

### **1. Gas Anti Solvent (GAS)<sup>215</sup>**

Here, the solute is dissolved in the solvent and the gas is flowed through this in a closed chamber. Upon increasing the pressure, the concentration of gas increases, which in turn reduces the solvation power of the solvent for the solute particles, thus leading to the precipitation of the solute particles.

### **2. Precipitation with Compressed Antisolvent (PCA)<sup>215</sup>**

This method involves the spraying of the drug/polymer solution through a nozzle into a chamber containing SCF as the antisolvent.

SAS process shows higher drug loading capacity over GAS, since very smaller particles could be achieved in this method. This may be attributed to immediate contact between solute and SCF achieved via this method, which further leads to faster nucleation.

#### **(a) Supercritical Antisolvent (SAS) Recrystallization**<sup>216,217</sup>

SAS method is similar to PCA. The basic difference between PCA and SAS is that PCA utilizes liquid or supercritical antisolvent whereas SAS makes use of SCF as antisolvent. Recently, many advancements have been reported for SAS process such as Supercritical-Assisted Injection in a Liquid Anti-solvent (SAILA) and Expanded Liquid anti-Solvent (ELS) methods.

#### **(b) Aerosol Solvent Extraction System (ASES)**<sup>216,217</sup>

ASES method was patented by Müller and Fischer in 1989. The working principle is based on the extraction properties of supercritical gases. In this method, the drug/polymer mixture and the organic solvent (soluble in scCO<sub>2</sub>) is sprayed into a chamber containing SCF. Thereafter, the organic solvent is extracted, leading to the formation of particles of smaller size. The major limitation noticed for this particular method is its inability to load higher drug amount since it is having high affinity for organic solvent, which in turn reduces the loading amount in the polymer matrix.

### **3. Solution Enhanced Dispersion by SCFs (SEDS)**<sup>216,217</sup>

SEDS is considered as a modified SAS technique with the only difference observed in the design of the nozzle. In SEDS coaxial

nozzle is used and it aids the dispersion of the drug solution by SCF, thereby leading to enhanced mass transfer and formation of particles with small size and fast nucleation rate.

#### **4. Particles from Gas Saturated Solutions (PGSS)**

In PGSS method, SCF is playing the role of a co-solute. SCF is initially dissolved in a drug-solvent suspension and finally depressurized through a nozzle. This results in the formation of particles of smaller size. This method has found wide application for micronization of formulation for BCS class II drugs.

##### **7.1.5 Applications of SCF technologies**

SCF strategy provides a promising technology platform for the design, manufacture and modification of pharmaceutical substances. SCF-based methods have been widely explored for controlling the morphology, crystallinity etc. of the pharmaceutical ingredients, thereby controlling the drug-release kinetics of the preparations. Several works have been reported in this line of study and some selected works are summarized in the upcoming section.

Toropainen et al., studied the variation in morphology of a commonly used excipient  $\gamma$ -cyclodextrin ( $\gamma$ -CD) using SEDS process and observed that upon increasing the processing temperature, crystallinity of  $\gamma$ -CD was completely lost and got transformed into an amorphous state.<sup>218</sup> Nanosizing of Ibuprofen and Naproxen drugs via RESOLV method is already reported. Micronization of Cyclosporine carried out via RESS and PGSS techniques was carried out by Tandya et al.<sup>219</sup>

This processes resulted in the formation of micron sized cyclosporine. Generally this drug exists as a liquid crystal and this was evidenced from DSC results too. But upon scCO<sub>2</sub> processing, solid to liquid crystal transition peak vanished. Tsivintzelis et al. studied the effect of pressure, temperature and rate of depressurization on the structure of Polystyrene and Poly(D,L-lactic acid).<sup>220</sup>

Mishima et al. made use of a modified RESS method with a non-solvent for the encapsulation of proteins such as lipase, lysozyme with polymers (such as Poly(ethylene glycol), Poly(methyl methacrylate) etc.).<sup>221</sup> Works related to the preparation of inclusion complexes are also being carried out. One such notable work reported was the scCO<sub>2</sub> processing of Ibuprofen and cyclodextrins to create inclusion complexes of both.<sup>222</sup> Also, Lee et al. reported the preparation of inclusion complexes of Itraconazole with hydroxypropyl- $\beta$ -cyclodextrin.<sup>223</sup>

The primary objective of the work presented in this chapter is to investigate the viability of using scCO<sub>2</sub> as an alternative solvent and certain inexpensive and FDA approved CO<sub>2</sub>-philes namely, SOA, AGLU and PEG as excipients for the preparation of drug-excipient composites for the controlled release of Atenolol (AT). We specifically wanted to mix the drug and the excipient homogeneously in the CO<sub>2</sub>-solution and were motivated by some of the previous works from our group demonstrating that SOA forms a glass when treated with CO<sub>2</sub>.<sup>122</sup> For comparison, drug-excipient composites were also prepared using EA as solvent. AT is a relatively hydrophilic drug and hence its controlled release has always been an important problem in



pharmaceutical chemistry, which makes it possible to reduce the drug dosage. Specifically, we have prepared six systems to study in this chapter namely, AGLU-AT-CO<sub>2</sub>, AGLU-AT-EA, SOA-AT-CO<sub>2</sub>, SOA-AT-EA, PEG-AT-CO<sub>2</sub> and PEG-AT-EA, respectively. The abbreviations mentioned are in the order: excipient-drug-solvent and represents the encapsulation of drug in the excipient matrix using the particular solvent.

In general, we have used a weight ratio of 1:20 for the preparation of composites of drug and the excipient. Also, weight ratios of 1:10 and 1:50 were also investigated to examine the effect of concentration in the release kinetics of AT from the matrix. Detailed experimental procedure for the preparation of the drug-excipient composites using CO<sub>2</sub> and EA as media are provided in Chapter 2.

## **7.2 Results and Discussion**

First of all, we examine whether the drug is completely dispersed in the drug-excipient composites prepared using XRD. We also investigate the changes in morphology of the composites.

### **7.2.1 XRD studies**

The X-ray diffraction patterns of AT, AGLU, AGLU-AT-EA and AGLU-AT-CO<sub>2</sub> are provided in Figure 7.1. As observed from the XRD pattern, all the diffraction peaks of AT are absent in the composites processed in both EA and CO<sub>2</sub>, indicating that the drug is molecularly dispersed in AGLU matrices.

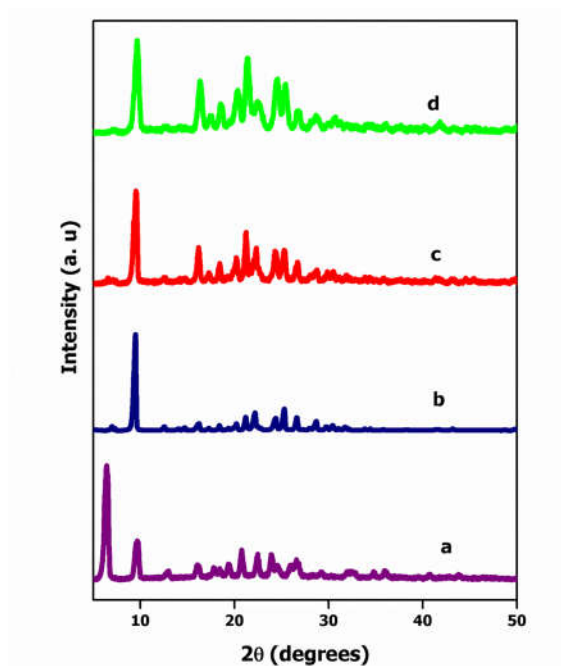


**Figure 7.1** XRD pattern for AT, AGLU, and the different composites prepared using EA and CO<sub>2</sub>: (a) AT (b) AGLU, (c) AGLU-AT-EA, and (d) AGLU-AT-CO<sub>2</sub>.

Upon examination of the XRD peaks of AGLU, in the composites prepared in EA and CO<sub>2</sub>, one could easily say that there is a slight broadening of the peaks indicating a small decrease in the degree the crystallite sizes.

Similar studies were also carried out for SOA composites prepared in both EA and CO<sub>2</sub>. The XRD patterns of AT, SOA, SOA-AT-EA, and SOA-AT-CO<sub>2</sub> are shown in Figure 7.2. The XRD data reveals that all the peaks corresponding to AT have disappeared in the SOA composites prepared in EA and CO<sub>2</sub>, confirming that the drug is molecularly dispersed in the SOA matrix.

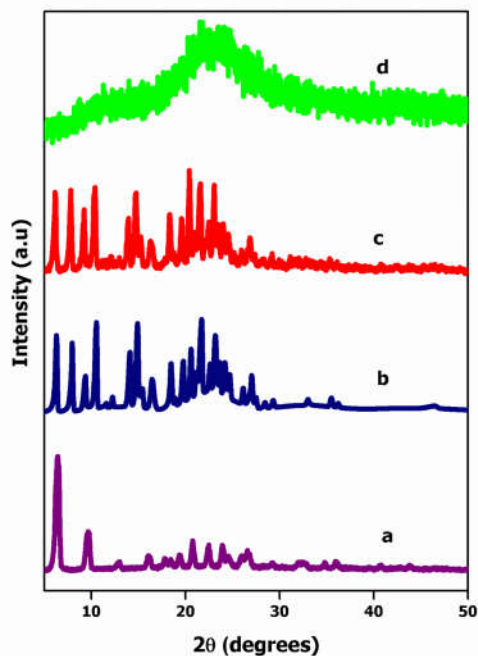


**Figure 7.2** XRD pattern for AT, SOA, and the different composites prepared using EA and CO<sub>2</sub>: (a) AT (b) SOA, (c) SOA-AT-EA, and (d) SOA-AT-CO<sub>2</sub>.

In this case, the XRD data shows an amorphous state for SOA-AT composites prepared in CO<sub>2</sub> medium. On the other hand, for the SOA-AT-EA composite, SOA remains in the crystalline state.

The XRD patterns of AT, PEG, PEG-AT-EA and PEG-AT-CO<sub>2</sub> are presented in Figure 7.3.

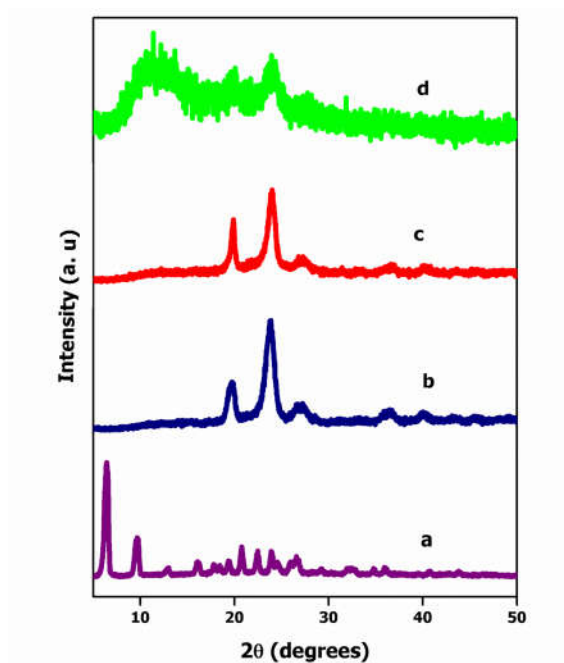


**Figure 7.3** XRD patterns for AT, PEG, and the different composites prepared using EA and CO<sub>2</sub>: (a) AT (b) PEG, (c) PEG-AT-EA, and (d) PEG-AT-CO<sub>2</sub>.

It is clear that there is significant difference in the degree of crystallinity of PEG between PEG-AT-EA and PEG-AT-CO<sub>2</sub>, with an increased degree of disorder in the latter. The broad peak centred around 12° may be either due to the presence of amorphous AT in the system, indicating that the drug is not fully dispersed in the system, plausibly due to the hydrophilic nature of both AT and PEG as against the solvent CO<sub>2</sub>.

## 7.2.2 Raman spectroscopic studies

The FT-Raman spectra of AGLU and AGLU-AT-CO<sub>2</sub> corresponding to the C=O stretch region and the C-H stretch region, respectively, are provided in Figure 7.4

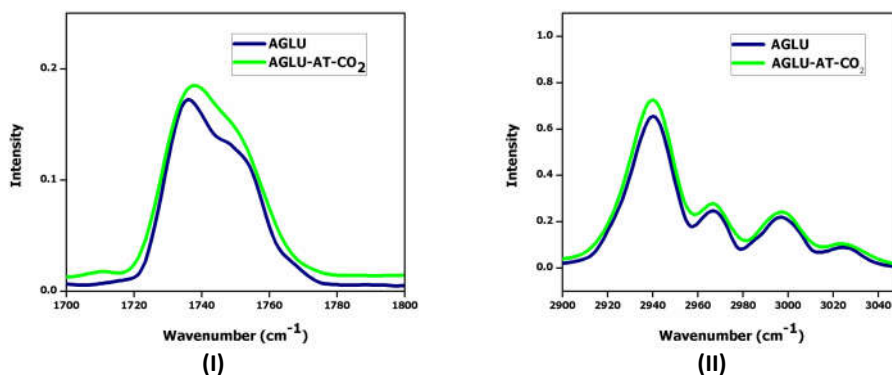


**Figure 7.4** FT-Raman spectra of AGLU and AGLU composites at two different regions: (I) 1700-1800 cm<sup>-1</sup> and (II) 2900-3050 cm<sup>-1</sup>.

No significant change in either the peak positions or the line-widths are observed for the carbonyl stretching band or in the C-H stretch region indicating that there are no significant changes in the physicochemical states of AGLU. In fact, the results reveal that the crystallinity of AGLU in the composite remains almost the same even after CO<sub>2</sub> processing. One also doesn't observe any change in the vibrational band positions corresponding to the drug after it is dispersed in CO<sub>2</sub>.

Along similar lines, the FT-Raman spectra of SOA and SOA composite at two different regions are provided in Figure 7.5, in the C=O stretch and C-H stretch regions. As observed in the previous

chapter, one observed both an increase in the line widths as well as a slight blue-shift in the bands corresponding to both these vibrational modes for SOA-AT-CO<sub>2</sub>.

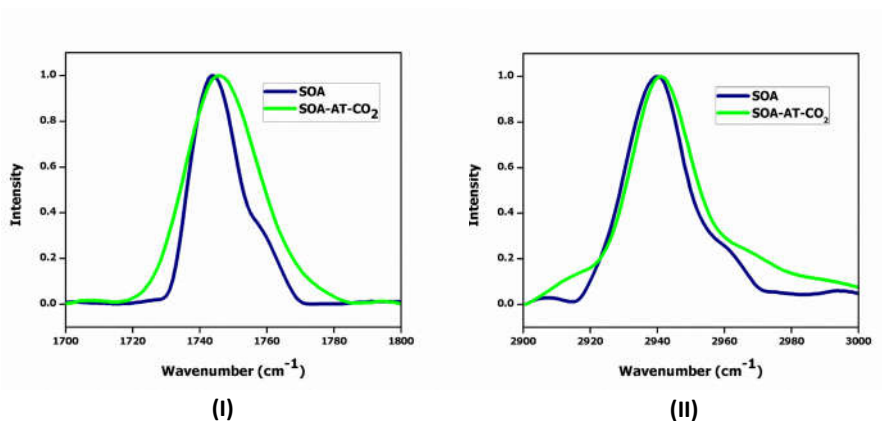


**Figure 7.5** FT-Raman spectra of SOA and SOA composites at two different regions: (I) 1700-1800 cm<sup>-1</sup> and (II) 2900-3000 cm<sup>-1</sup>.

In fact, the carbonyl stretching band is blue shifted by 2 cm<sup>-1</sup> from 1743 to 1745 cm<sup>-1</sup> and the C-H stretching band by 2 cm<sup>-1</sup> from 2939 to 2941 cm<sup>-1</sup>. Both these indicate an increased disorder in SOA-AT-CO<sub>2</sub> as compared to pure SOA. The FT-Raman spectra of pure AT and the SOA-AT-CO<sub>2</sub> composite in the 1550 -1650 cm<sup>-1</sup> region is provided in Figure 7.6 to investigate the binding between the drug and SOA.

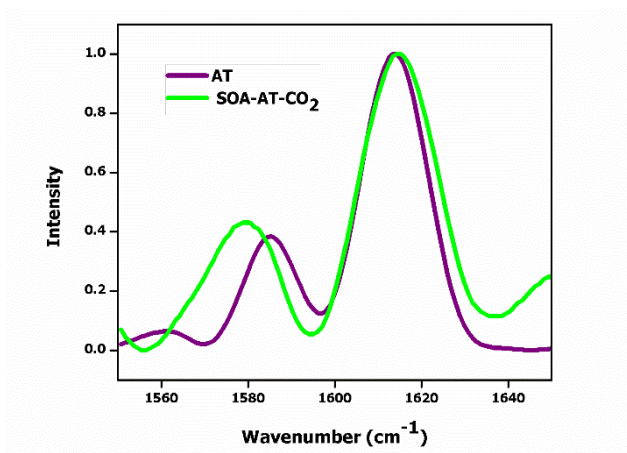


**Figure 7.6** FT-Raman spectra of AT and SOA-AT-CO<sub>2</sub>: 1550 to 1650 cm<sup>-1</sup> vibrational frequency region.

It is observed that the peak at 1584 cm<sup>-1</sup> (corresponding to the C-C ring vibration) is red shifted by 5 cm<sup>-1</sup> to 1579 cm<sup>-1</sup>, indicating a strong interaction between the drug and the excipient.

Finally, we also investigate the FT-Raman spectra of PEG and PEG-AT-CO<sub>2</sub> (Figure 7.7). All the bands represented in figure clearly shows a line broadening indicating a decrease in the lattice order upon composite formation using CO<sub>2</sub>.

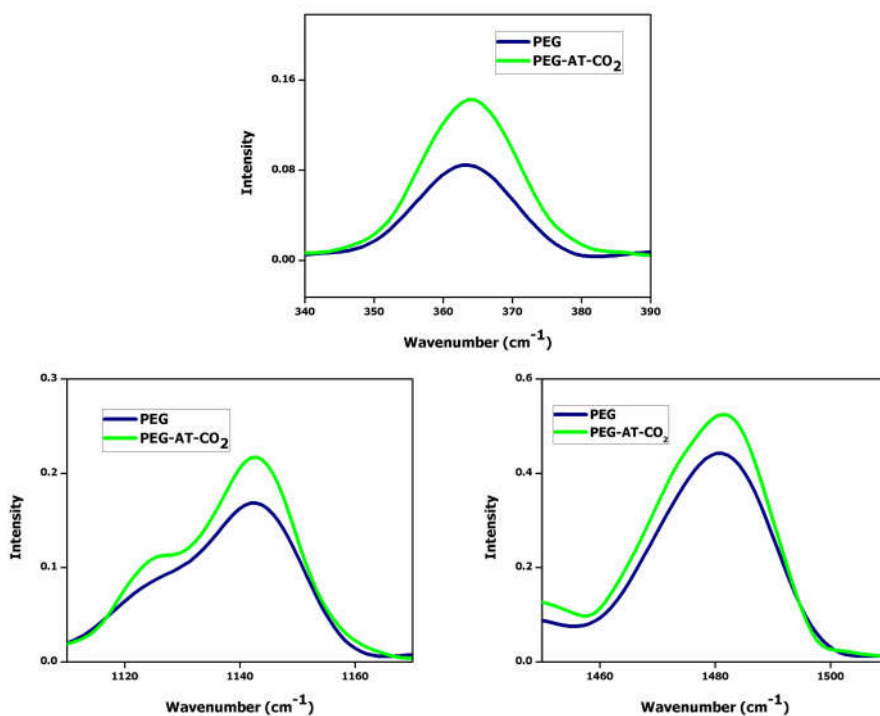


**Figure 7.7** FT-Raman spectra of PEG and PEG composites at three different regions.

In fact, the bands at  $363\text{ cm}^{-1}$ ,  $1142\text{ cm}^{-1}$  and  $1480\text{ cm}^{-1}$ , corresponding to C-C-O bending, C-C stretching and  $\text{CH}_2\text{-CH}_2$  symmetric bending, respectively, clearly show line broadening, demonstrating a decrease in the lattice order in the PEG composite.

For the PEG-AT- $\text{CO}_2$ , we also observe that the peak at  $1585\text{ cm}^{-1}$  corresponding to the C-C ring vibration of AT is blue-shifted to  $1587\text{ cm}^{-1}$  (Figure 7.8), which may be attributed to an increased degree of disorder in the PEG-AT- $\text{CO}_2$  composite.



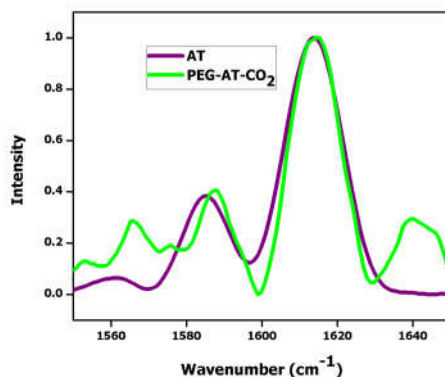


**Figure 7.8** FT-Raman spectra of AT and PEG-AT-CO<sub>2</sub> in the 1550-1650 cm<sup>-1</sup> region.

#### 7.2.4 SEM studies

Scanning electron microscopic studies provides structural and morphological information on different systems. As we had earlier seen in the case of the UR composites in the previous chapter, surface morphology and structure will have significant implications on the drug release kinetics. The rate of release of a guest molecule from a host matrix will depend on the environment in which the molecule is encapsulated inside the matrix as well as the access of the solvent molecules to the drug molecule. On similar lines with the UR composites (Chapter 6), we investigate the surface morphology of the various composites prepared using CO<sub>2</sub> and EA. The FESEM images of AT, AGLU, AGLU-AT-CO<sub>2</sub>, AGLU-AT-EA, SOA, SOA-AT-CO<sub>2</sub>, SOA-AT-EA, PEG, PEG-AT-CO<sub>2</sub>, and PEG-AT-EA are provided in Figure 7.9.

In general, the results are very similar to what we had observed in the case of the UR composites. A few general characteristics observed may be summarized as below:

SEM images show that the AGLU-AT-EA and AGLU-AT-CO<sub>2</sub> composites appear crystalline with slight morphological variations. On the contrary, the SOA-AT composites prepared using EA and CO<sub>2</sub> have completely different morphologies. The SOA-AT-EA presents closely networked aggregates, while the SOA-AT-CO<sub>2</sub> composite has a very smooth surface, as observed in the case of the SOA-UR-CO<sub>2</sub> composite.

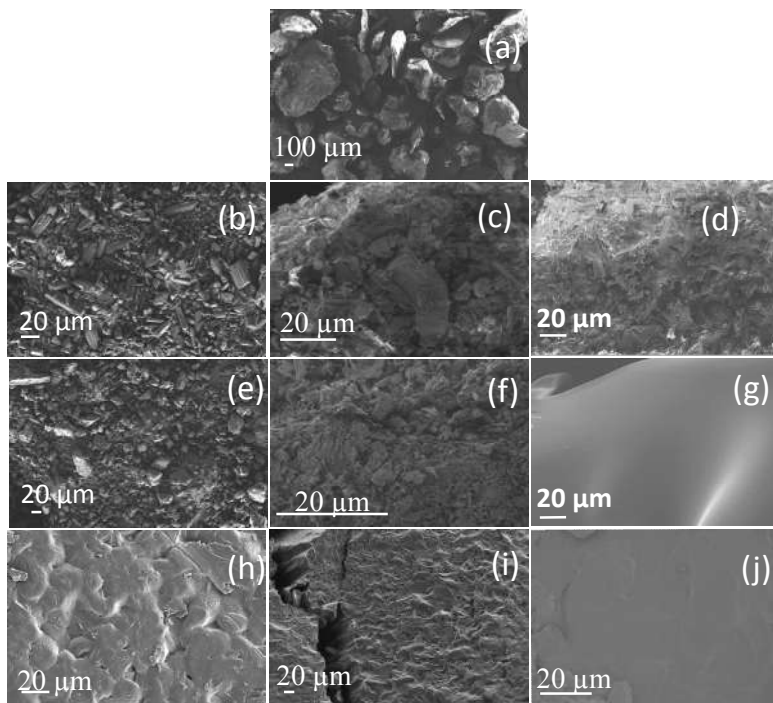


**Figure 7.9** FE-SEM images of a) AT, b) AGLU, c) AGLU-AT-EA, d) AGLU-AT-CO<sub>2</sub>, e) SOA, f) SOA-AT-EA, g) SOA-AT-CO<sub>2</sub>, h) PEG, i) PEG-AT-EA, and j) PEG-AT-CO<sub>2</sub>, respectively.

PEG has a waxy flake like morphology as evidenced from the SEM image. PEG-AT-EA also shows a similar surface texture. But, PEG-AT-CO<sub>2</sub> presents a smooth surface, much like that of SOA. However, it must be remembered that while SOA is hydrophobic, PEG is hydrophilic.

### **7.2.3 Drug release studies**

In the previous sections, we have discussed the various structural, morphological and drug-excipient micro environment changes in various composites under study. In this section, we investigate how and to what extent these changes affect the kinetics of drug release from these composites. From the results shown in the earlier Chapter on the Urea composites, one would expect significant changes in the drug release kinetics in these systems. Even though both AGLU and SOA are hydrophobic, it was shown that the CO<sub>2</sub>-induced SOA glass does immobilize the guest molecules inside, making the drug release much slower as compared to the AGLU composites. PEG is hydrophilic with a decreased order, after CO<sub>2</sub> treatment.

The drug release kinetics from AGLU composites processed using EA and CO<sub>2</sub> is shown in Figure 7.10. One observes a similar drug release pattern for both the composites. For both these, about 80% of the drug is released within 2 hours and complete release in about 40 hours, indicating that the drug molecules are located on the crystallite surfaces

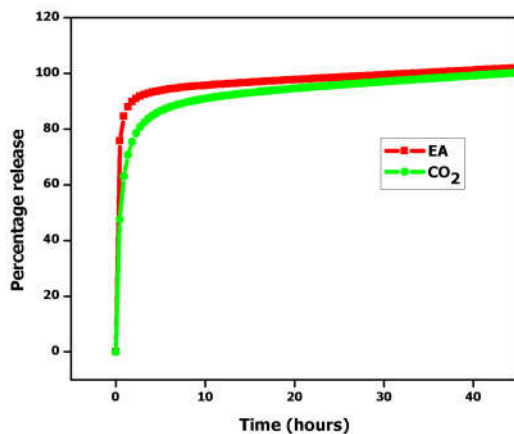


**Figure 7.10** Drug release profile of AT from AGLU-AT-EA and AGLU-AT-CO<sub>2</sub>.

The drug release kinetics from SOA-AT-EA and SOA-AT-CO<sub>2</sub> are shown in Figure 7.11. Similar to the observations in the case of release studies of the Urea composites, the drug release from SOA-AT-EA is observed to be much faster in comparison with that from the SOA-AT-CO<sub>2</sub>. While 80 percent of AT gets released within about 10 hours in the case of SOA-AT-EA, it takes nearly 70 hours for the drug to get completely released from SOA-AT-CO<sub>2</sub>.

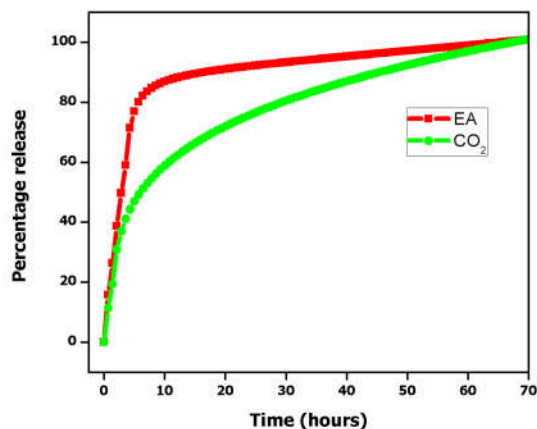


**Figure 7.11** Drug release profile of AT from SOA-AT-EA and SOA-AT-CO<sub>2</sub>.

This enormous difference in the release kinetics between SOA-AT-EA and SOA-AT-CO<sub>2</sub> may be correlated with XRD and FT-Raman studies. It is plausible that the drug molecules are thrown to the exterior of the small crystallites of SOA in the SOA-AT-EA composite, causing their faster release. On the other hand, in the case of SOA-AT-CO<sub>2</sub>, the drug molecules appear to be immobilized inside the glassy and hydrophobic SOA, making solvent access more difficult to the vicinity of these molecules; making their release much slower.

PEG is one among the most commonly used excipients in pharmaceutical industry due to its benign attributes such as non-toxicity, biocompatibility, low cost and low volatility. As discussed in the introductory chapter, PEG (M.W 1500) is a highly CO<sub>2</sub>-philic compound (also hydrophilic) and hence can be utilized as an excipient in supercritical drug processing. The drug release kinetics from PEG

composites processed using EA and CO<sub>2</sub> are shown in Figure 7.12. Interestingly, one observes similar drug release profile for the PEG composites processed in EA and CO<sub>2</sub>; taking about 18 hours for the entire drug release.

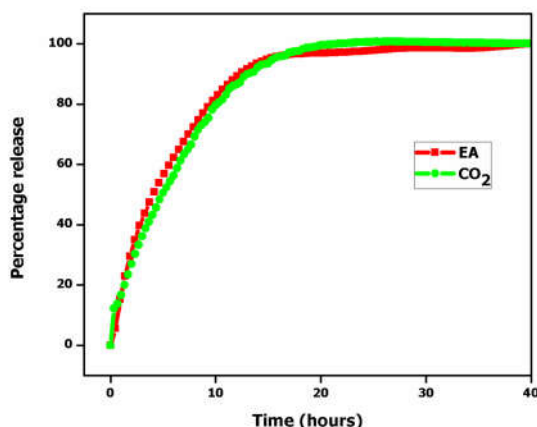


**Figure 7.12** Drug release profile of AT from PEG-AT-EA and PEG-AT-CO<sub>2</sub>.

It is interesting to note that the drug release profile for these two composites are quite similar in spite of the differences in their structure and morphology as evidenced by the XRD and SEM results. Since PEG is hydrophilic, one would expect that the solvent penetration into the excipient matrix happens spontaneously and one would also expect a fast release of the drug. However, it takes nearly 18 hours for the complete drug release in spite of the structural or morphological differences as evidenced by the XRD and SEM, even though the drug used is highly water-soluble. This suggests that the drug release kinetics in the case of the PEG-AT-EA and PEG-AT-CO<sub>2</sub> is governed

by a different criterion. It appears that the hydrophilic drug molecules are encapsulated well in the polymer chains and are bound to the PEG molecule.

### **7.2.5 Effect of concentration of drug**

Effect of concentration of drug on the drug-release is another important matter that needs consideration. Generally, the drug release kinetics is governed by a set of interactions, *viz.*, drug-drug interaction, excipient-excipient interaction and drug-excipient interaction. If the concentration of drug is very low, the drug-drug interaction may be ruled out and also there will be better encapsulation of the drug molecules; leading to slow drug release. Also, when the concentration of the drug in the system is higher, the drug-drug interactions will be significant. Accordingly, one would expect a faster drug release. In order to investigate the effect of concentration on the drug release, we employ drug-excipient composites (processed using CO<sub>2</sub>) of three different weight ratios *viz.*, 1:10, 1:20 and 1:50, respectively.

The kinetics of release of AT from AGLU matrix with three different weight ratios of AT: AGLU is provided in Figure 7.13. One could clearly observe a small variation in the drug release profile as the concentration changes. As the concentration of drug increases, release is noticed to be faster *i.e.* 1:10 > 1:20 > 1:50.

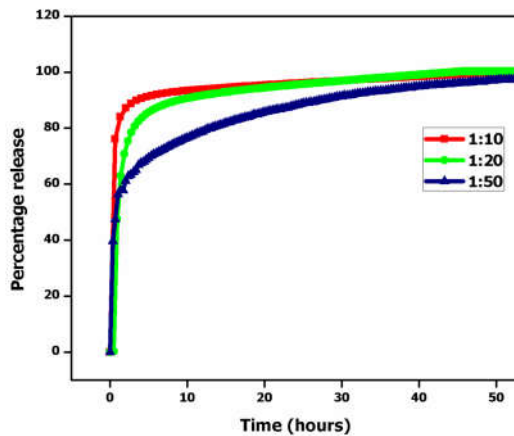


**Figure 7.13** Drug release kinetics of AT from AGLU matrix with different AT/AGLU ratios.

The results indicate that, the lower the drug concentration, the better it is encapsulated in the excipient matrix.

The drug release kinetics in the case of the SOA-AT-CO<sub>2</sub> composites with three different AT/SOA weight ratios is presented in Figure 7.14. Interestingly, in this case, one doesn't observe any difference for the compositions 1:20 and 1:50. However, a drastic difference is observed in the case of the 1:10 composite, where the drug release is fast, indicating that the drug is not encapsulated inside the SOA or the drug has disrupted the glassy structure of SOA, as was reported in the case of PEG/SOA composites.<sup>122</sup>



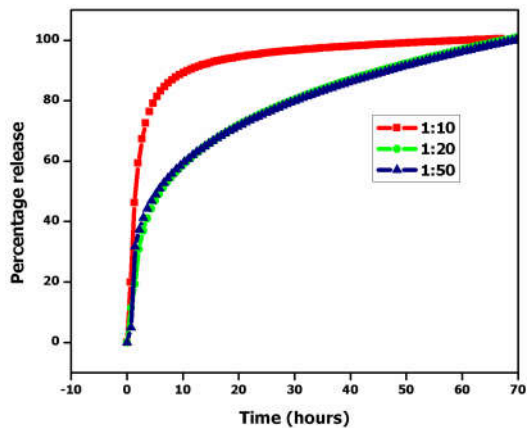


**Figure 7.14** Drug release kinetics of AT from SOA matrix with different AT/SOA ratios.

The kinetics of release of AT from PEG matrix with three different weight ratios of AT/PEG is shown in Figure 7.15. No regular trend is observed in the kinetics profile as a function of concentration.

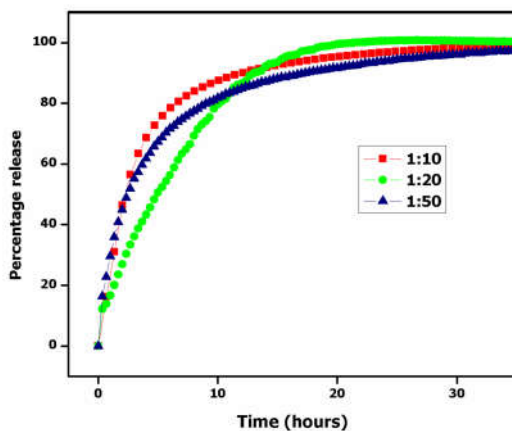


**Figure 7.15** Drug release kinetics of AT from PEG matrix with different AT/PEG ratios.

This may be due to the better encapsulation of the drug inside the hydrophilic matrix and also due to higher drug-excipient interactions observed. The hydrophilic nature of the excipient outweighs the effect of concentration. This is why, all the composite ratios are showing similar release kinetics.

### **7.3 Summary and Conclusions**

In this work, we have studied the variations in the kinetics of the drug (AT) release from CO<sub>2</sub>-philic matrices such as AGLU, SOA and PEG and its correlations to the structural and morphological variations of the excipient matrices brought about by the effects of solvent and composition. There are several factors which can influence the drug-release kinetics such as the solubility of the drug in water, hydrophobicity/hydrophilicity of the excipient, crystallinity of the excipient, and how well the drug is encapsulated inside the excipient matrix. Crystallinity of the excipient matrix ensures that drug is pushed out to the peripheral regions of the crystal, providing easy access to the water molecules. We observed significant differences for the drug-excipient composites prepared using CO<sub>2</sub> vs. conventional solvents (EA). While EA does not affect the crystallinity of the excipients, CO<sub>2</sub> does. As we had discussed in the earlier chapters, SOA is a unique matrix by virtue of the CO<sub>2</sub>-induced glass formation and the consequent immobilization of the drug inside the drug. Thus the CO<sub>2</sub>-processed SOA composites of the drug provided very slow release, while EA-processed samples provide fast release of the excipients. For the AGLU matrix, both EA and CO<sub>2</sub> yield crystalline composites and consequently provide fast release. In the case of PEG, both EA and

CO<sub>2</sub>-processed composites provide similar drug-release kinetics. The results are of significance not only from the perspective of the utilization of a safe and environmentally benign CO<sub>2</sub>-solvent platform in the pharmaceutical industry, but also in its unique capability in the design of drug-excipient composites for sustained drug release.



## CHAPTER 8

# CONCLUSIONS AND OUTLOOK

---

Chemical industry has been identified as the single largest industry that is responsible for the large scale degradation in the quality of our environment. About 30–40 million tons of VOCs are being used as solvents for various chemical industries around the world and a major part of this escapes into the atmosphere, causing a serious threat to our sphere of life. This has generated much interest in the search for more environmentally responsible alternative solvents and is one of the key issues in the emerging green chemistry research. Among the various alternative solvents proposed, liquid and supercritical CO<sub>2</sub> has been widely regarded as potential green solvent alternative for future. In the last three decades, this solvent system has made inroads into many industrial applications. The synthesis of fluoropolymers such as Teflon (where CO<sub>2</sub> replaces CFCs as solvent), CO<sub>2</sub>-based dry cleaning, synthetic organic chemistry, extraction of natural products, microelectronic cleaning, food and pharmaceutical chemistry, industrial coatings, etc. are some of the areas where the CO<sub>2</sub>-solvent system has already made a mark. In fact, the *DuPont* company has already set up an industrial facility for the synthesis and processing of fluoropolymers in the state of North Carolina, USA.

One of the major limitations for the expansion of this green solvent system was the lack of understanding on the solvent attributes of CO<sub>2</sub>. The rule of thumb regarding solvation is that “the like dissolves like”. CO<sub>2</sub> is a linear, triatomic molecule with zero dipole moment and liquid

and supercritical CO<sub>2</sub> possess dielectric constants even lesser than that of hexane, leading many to believe that CO<sub>2</sub> represents the solvent extreme of water. This view was discarded by Kazarian et al.<sup>39</sup> and later by Raveendran et al.<sup>33,42</sup> and it has now been accepted that one needs to consider CO<sub>2</sub> as a charge-separated molecule capable of participating in both Lewis acid- Lewis base interactions with solute functionalities and that this needs to be borne in mind while investigating the microscopic solvation of compounds in CO<sub>2</sub>. This view, supported by rigorous quantum chemical calculations suggested that acetylation of polyhydroxy systems such as carbohydrates can indeed be an important method for the synthesis of renewable and inexpensive CO<sub>2</sub>-philes<sup>53</sup> with newer possibilities for implementation of newer techniques in chemistry. It may be remembered that, much earlier, it was identified that fluorocarbons have high miscibility with CO<sub>2</sub> (mainly supported by dispersive interactions), but the utilization of these systems as CO<sub>2</sub>-philes was limited by the high cost and the associated environmental issues. Theories on the solvation of these molecules in CO<sub>2</sub> are still inconclusive and are still active areas of engagement in theoretical and experimental chemistry.

The work presented in this thesis is an attempt to bring together the CO<sub>2</sub>-solvent platform and the inexpensive CO<sub>2</sub>-philes together for industrial applications by virtue of the high solubility of these compounds. In fact, sugar acetates are the most CO<sub>2</sub>-philic compounds identified so far. Compounds such as SOA and AGLU undergo deliquescence in gas phase CO<sub>2</sub> at room temperature and are miscible with liquid and supercritical CO<sub>2</sub> for any concentration. PEG

(M.W.1500) is another compound we have investigated in this work. This system also exhibits similar solvation behaviour in CO<sub>2</sub>, plausibly aided by the Lewis acid-Lewis base interaction between the carbon atom of CO<sub>2</sub> and the ether oxygen of PEG. The flexibility of the polymer chain may support the solvation of molecules entropically. PEG also has an important feature that it is hydrophilic.

Three CO<sub>2</sub>-philes, viz., SOA, AGLU, and PEG are used in this study. The applications in which we have employed these are sizing and desizing of yarn in the textiles industry, sizing of paper, wood processing, preparation of composites for the sustained release of drugs (AT) and sustained release of fertilizers (UR). Earlier work from our own research group has shown that among the CO<sub>2</sub>-philes used, SOA forms a glass, AGLU remains crystalline, and PEG transforms into an amorphous phase after CO<sub>2</sub>-treatment.<sup>122</sup> Interestingly, SOA, when treated with conventional solvents such as Ethyl Acetate and Acetone does not transform into a glass and retains its crystalline behaviour. Thus, SOA is a classic example for a system where the lattice energy and solvation energy has struck a subtle balance.

The thesis is divided into eight chapters. The first Chapter gives a historical introduction into the development of green chemistry and alternative solvents, with a particular focus on the solvent attributes of CO<sub>2</sub>. The second chapter deals with the materials and experimental methods applied in this study. The third Chapter discuss the results on the investigations carried on the sizing of textile yarn with these CO<sub>2</sub>-philes and its desizing, using scCO<sub>2</sub> vs. conventional solvents. The fourth Chapter describes the results of our studies on sizing of paper

using liquid/scCO<sub>2</sub> as the medium with the different CO<sub>2</sub>-philes as size materials. Wood processing is another industrially important area. Conventional wood processing involves the peracetylation of cellulose by heating the wood in boiling acetic anhydride, an environmentally harmful irritant. In Chapter 5, we present a strategy of impregnating and coating wood with sensorially active compounds like SOA using scCO<sub>2</sub> as the medium. It is worthy of mention that SOA is one of the bittermost compounds identified so far. Chapter 6 and Chapter 7 deals with two different applications, viz., preparations of composites of these CO<sub>2</sub>-philes with Urea and a hydrophilic drug (AT), respectively, to investigate the possibility of sustained release composites for Urea (relevant for agriculture) and AT (pharmaceutical industry), respectively.

Some important features need to be emphasized with respect to these applications. The most important one is the CO<sub>2</sub>-induced glassification of SOA which has significant consequences on the binding of SOA with yarn, paper and wood, as well as the immobilization of guest molecular systems in the glassy SOA. SOA coatings are also characterized by a smooth surface. One must note that among the systems studied, SOA and AGLU are hydrophobic, but the former is glassy, and the latter crystalline, after CO<sub>2</sub>-treatment. PEG forms a waxy and smooth coating upon CO<sub>2</sub>-treatment and it is hydrophilic.

It can be seen that both for the sizing of yarn (both cotton and polyester) and paper, SOA provides much superior sizing in terms of its strength, binding, and surface smoothness as compared to the other systems.



The UR composites prepared too are unique as compared to the others. The glassy composite of SOA and UR prepared using CO<sub>2</sub> results in a very slow release of UR, taking about 93 hours for the complete release of UR when dispersed in water. In all other cases, the release of UR is much faster. In fact, the similar composite with AGLU, releases most of UR in about 20 hours. We also prepared composites of UR with different SOA/AGLU compositions and we observe that one can in fact tune the UR release by tailoring the composite structure and morphology. These are observations with important bearing on enabling these applications.

Kinetics of release of the hydrophilic drug AT (Chapter 7) from different excipients such as SOA, AGLU, and PEG also provide significant insights into how structural and morphological variations as well as the hydrophobicity/hydrophilicity of the excipient systems can affect the drug release. As expected, we observe that the SOA composite provide the slowest release (70 hours). This may be attributed to its smooth, hydrophobic surface (that reduces the solvent access) and the glassy state of the CO<sub>2</sub>-processed SOA (that immobilizes the drug molecule inside).

In summary, the results presented in this work with regard to the various applications presented in this thesis have important consequences with regard to enabling these strategies as greener technological innovations for a sustainable future.



## REFERENCES

---

- (1) Rachel Carson, *Silent Spring*, Penguin Books, Houghton, USA, 1962.
- (2) Poliakoff, M.; Licence, P. Green chemistry. *Nature* 2007, 450, 810-812.
- (3) Anastas, P. T.; Warner, J. C. *Green Chemistry: Theory and Practice*. Oxford University Press, 1998.
- (4) Anastas, P.; Kirchoff, M. M. Origin, Current Status and Future Challenges of Green Chemistry. *Acc. Chem. Res.* 2002, 35, 686-694.
- (5) Anastas, P.; Eghbali, N. *Green Chemistry: Principles and Practice*. *Chem. Soc. Rev.* 2010, 39, 301–312.
- (6) Poliakoff, M.; Fitzpatrick, J. M.; Farren, T. R.; Anastas, P. *Green Chemistry: Science and Politics of Change*. *Science* 2002, 297, 807-810.
- (7) DeSimone, J. M. *Practical Approaches to Green Solvents*. *Science*, 2002, 297, 799-803.
- (8) Capello, C.; Fischer, U.; Hungerbuhler, K. What is a green solvent? A comprehensive framework for the environmental assessment of solvents. *Green Chem.* 2007, 9, 927–934.

- (9) Clark, J. H.; Tavener, S. J. *Alternative Solvents: Shades of Green. Org. Process Res. Dev.* 2007, 11, 149-155.
- (10) Andrade, C. K. Z.; Alves, L. M. *Environmentally Benign Solvents in Organic Synthesis: Current Topics. Curr. Org. Chem.* 2005, 9, 195-218.
- (11) Keskin, S.; Kayrak-Talay, D.; Akman, U.; Hortacsu, O. *Review of ionic liquids towards supercritical fluid applications. J. Supercrit. Fluids.* 2007, 43, 150-180.
- (12) Dzyuba, S. V.; Bartsch, R. A. *Recent Advances in Applications of Room-Temperature Ionic Liquid/Supercritical CO<sub>2</sub> Systems. Angew. Chem. Int. Ed.* 2003, 42, 148-150.
- (13) Sihvonen, M.; Jarvenpaa, E.; Hietaniemi, V.; Huopalahti, R. *Advances in supercritical carbon dioxide technologies. Trends Food Sci. Technol.* 1999, 10, 217-222.
- (14) Knez, Z.; Markocic, E.; Leitgeb, M.; Primožic, M.; Hrncic, M. K.; Skerget, M. *Industrial applications of supercritical fluids: A review. Energy* 2014, 77, 235-243
- (15) Palmer, M. V.; Ting, S. S. T. *Applications for supercritical fluid technology in food processing. Food Chemistry,* 1995, 52, 345-352.
- (16) [https://en.wikipedia.org/wiki/Supercritical\\_fluid](https://en.wikipedia.org/wiki/Supercritical_fluid)
- (17) Maçaira, J.; Santana, A.; Recasens, F.; Larrayoz, M. A. *Biodiesel production using supercritical methanol/carbon*

- dioxide mixtures in a continuous reactor. *Fuel* 2011, 90, 2280–2288.
- (18) An, G.; Ma, W.; Sun, Z.; Liu, Z.; Han, B.; Miao, S.; Miao, Z.; Ding, K. Preparation of titania/carbon nanotube composites using supercritical ethanol and their photocatalytic activity for phenol degradation under visible light irradiation. *Carbon* 2007, 45, 1795–1801.
- (19) Cason, J. P.; Roberts, C. B. Metallic Copper Nanoparticle Synthesis in AOT Reverse Micelles in Compressed Propane and Supercritical Ethane Solutions. *J. Phys. Chem. B* 2000, 104, 1217-1221.
- (20) Ikushima, Y.; Hatakeda, K.; Sato, O.; Yokoyama, T.; Arai, M. Acceleration of Synthetic Organic Reactions Using Supercritical Water: Noncatalytic Beckmann and Pinacol Rearrangements. *J. Am. Chem. Soc.* 2000, 122, 1908-1918.
- (21) Savage, P. E. Organic Chemical Reactions in Supercritical Water. *Chem. Rev.* 1999, 99, 603-621.
- (22) Boero, M.; Ikeshoji, T.; Liew, C. C.; Terakura, K.; Parrinello, M. Hydrogen Bond Driven Chemical Reactions: Beckmann Rearrangement of Cyclohexanone Oxime into E-Caprolactam in Supercritical Water. *J. Am. Chem. Soc.* 2004, 126, 6280-6286.
- (23) Farran, A.; Cai, C.; Sandoval, M.; Xu, y.; Liu, J.; Hernaiz, M. J.; Linhardt, R. J. Green Solvents in Carbohydrate Chemistry:

From Raw Materials to Fine Chemicals. *Chem. Rev.* 2015, 115, 6811–6853.

- (24) Bröll, D.; Kaul, C.; Krämer, A.; Krammer, P.; Richter, T.; Jung, M.; Vogel, H.; Zehner, P. *Chemistry in Supercritical Water. Angew. Chem. Int. Ed.* 1999, 38, 2998 -3014.
- (25) Weingartner, H.; Franck, E. L. *Supercritical Water as a Solvent. Angew. Chem. Int. Ed.* 2005, 44, 2672–2692.
- (26) Peach, J.; Eastoe, J. *Supercritical carbon dioxide: a solvent like no other. Beilstein J. Org. Chem.* 2014, 10, 1878-1895.
- (27) Mohamed, A.; Eastoe, J. *How can we use carbon dioxide as a solvent? SSR*, 2011, 93(343), 73-80.
- (28) Zhang, X.; Heinonen, S.; Levanen, E. *Applications of supercritical carbon dioxide in materials processing and synthesis. RSC Adv.* 2014, 4, 61137-61152.
- (29) Beckman, E. J. *Supercritical and near-critical CO<sub>2</sub> in green chemical synthesis and processing. J. Supercrit. Fluids.* 2004, 28, 121-191.
- (30) Consani, K. A.; Smith, R. D. *Observations on the Solubility of Surfactants and Related Molecules in Carbon Dioxide at 50 °C. J. Supercrit. Fluids* 1990, 3, 51-65.

- (31) Kauffman, J. F. Quadrupolar Solvent Effects on Solvation and Reactivity of Solutes Dissolved in Supercritical CO<sub>2</sub>. *J. Phys. Chem. A.* 2001, 105, 3433-3442.
- (32) Reynolds, L.; Gardecki, J. A.; Frankland, S. J. V.; Horng, M. L.; Maroncelli, M. Dipole Solvation in Nondipolar Solvents: Experimental Studies of Reorganization Energies and Solvation Dynamics. *J. Phys. Chem.* 1996, 100, 10337-10354.
- (33) Raveendran, P.; Ikushima, Y.; Wallen, S. L. Polar Attributes of Supercritical Carbon Dioxide. *Acc. Chem. Res.* 2005, 38, 478-485.
- (34) Sato, H.; Matubayasi, N.; Nakahara, M.; Hirata, F. Which Carbon Oxide is More Soluble? Ab Initio Study on Carbon Monoxide and Dioxide in Aqueous Solution. *Chem. Phys. Lett.* 2000, 323, 257-262.
- (35) Beckman, E. J. A challenge for green chemistry: designing molecules that readily dissolve in carbon dioxide. *Chem. Commun.* 2004, 1885-1888.
- (36) DeSimone, J. M.; Guan, Z.; Elsebernd, C. S. Synthesis of Fluoropolymers in Supercritical Carbon Dioxide. *Science.* 1992, 257, 945-947.
- (37) Yee, G. G.; Fulton, J. L.; Smith, R. D. Fourier transform infrared spectroscopy of molecular interactions of heptafluoro-1-butanol or 1-butanol in supercritical carbon dioxide and supercritical ethane. *J. Phys. Chem.* 1992, 96, 6172-6181.

- (38) Dardin, A.; DeSimone, J. M.; Samulski, E. T. Fluorocarbons Dissolved in Supercritical Carbon Dioxide. NMR Evidence for Specific Solute- Solvent Interactions. *J. Phys. Chem. B* 1998, 102, 1775-1780.
- (39) Kazarian, S. G.; Vincent, M. F.; Bright, F. V.; Liotta, C. L.; Eckert, C. A. Specific Intermolecular Interaction of Carbon Dioxide with Polymers. *J. Am. Chem. Soc.* 1996, 118, 1729-1736.
- (40) Taylor, D. K; Keiper, J. S.; DeSimone, J. M. Polymer Self-Assembly in Carbon Dioxide. *Ind. Eng. Chem. Res.* 2002, 41, 4451-4459.
- (41) Raveendran, P; Wallen, S. L. Exploring CO<sub>2</sub>-Philicity: Effects of Stepwise Fluorination. *J. Phys. Chem. B.* 2003, 107, 1473-1477.
- (42) Raveendran, P.; Wallen, S. L. Cooperative C-H···O Hydrogen Bonding in CO<sub>2</sub> -Lewis Base Complexes: Implications for Solvation in Supercritical CO<sub>2</sub>. *J. Am. Chem. Soc.* 2002, 124, 12590- 12599.
- (43) Danten, Y.; Tassaing, T.; Besnard, M. Vibrational Spectra of CO<sub>2</sub>-Electron Donor-Acceptor Complexes from ab Initio. *J. Phys.Chem. A* 2002, 106, 11831-11840.
- (44) Van Ginderen, P.; Herrebout, W. A.; van der Veken, B. J. van der Waals Complex of Dimethyl Ether with CO<sub>2</sub>. *J. Phys. Chem. A* 2003, 107, 5391-5396.



- (45) Kilic, S.; Michalik, S.; Wang, Y.; Johnson, J. K.; Enick, R. M.; Beckman, E. J. Effect of Grafted Lewis Base Groups on the Phase Behavior of Model Poly(dimethyl siloxanes) in CO<sub>2</sub>. *Ind. Eng. Chem. Res.* 2003, 42, 6415-6424.
- (46) Heldebrant, D. J.; Jessop, P. G. Liquid Poly(ethylene glycol) and Supercritical Carbon Dioxide: A Benign Biphasic Solvent System for Use and Recycling of Homogeneous Catalysts. *J. Am. Chem. Soc.* 2003, 125, 5600-5601.
- (47) Sarbu, T.; Styranec, T.; Beckman, E. J. Non-fluorous polymers with very high solubility in supercritical CO<sub>2</sub> down to low pressures. *Nature* 2000, 405, 165-168.
- (48) Blatchford, M. A.; Raveendran, P.; Wallen, S. L. Raman Spectroscopic Evidence for Cooperative C-H···O interactions in then Acetaldehyde-CO<sub>2</sub> Complex. *J. Am. Chem. Soc.* 2002, 124, 14818-14819.
- (49) Fujii, A.; Ebata, T.; Mikami, N. Direct Observation of Weak Hydrogen Bonds in Microsolvated Phenol: Infrared Spectroscopy of O-H Stretching Vibrations of Phenol-CO and -CO<sub>2</sub> in S<sub>0</sub> and D<sub>0</sub>. *J. Phys. Chem. A* 2002, 106, 10124-10129.
- (50) Melikova, S. M.; Rutkowski, K. S.; Rodziewicz, P.; Koll, A. Unusual Spectroscopic Properties of CF<sub>3</sub>H Dissolved in Liquefied Ar, N<sub>2</sub>, CO, and CO<sub>2</sub>. *Chem. Phys. Lett.* 2002, 352, 301-310.

- (51) Sarbu, T.; Styranec, T.; Beckman, E. J. Non-fluorous Polymers with Very High Solubility in Supercritical CO<sub>2</sub> Down to Low Pressures. *Nature* 2000, 405, 165-168.
- (52) Kilic, S.; Michalik, S.; Wang, Y.; Johnson, J. K.; Enick, R. M.; Beckman, E. J. Phase Behavior of Oxygen-Containing Polymers in CO<sub>2</sub>. *Macromolecules* 2007, 40, 1332-1341.
- (53) Raveendran, P; Wallen, S. L. Sugar Acetates as Novel, Renewable CO<sub>2</sub>-philes. *J. Am. Chem. Soc.* 2002, 124, 7274-7275.
- (54) Potluri, V. K.; Xu, J.; Enick, R.; Beckman, E.; Hamilton, A. D. Peracetylated Sugar Derivatives Show High Solubility in Liquid and Supercritical Carbon Dioxide. *Org. Lett.* 2002, 4, 2333-2335.
- (55) Potluri, V. K.; Hamilton, A. D.; Karanikas, C. F.; Ban, S. E.; Xu, J.; Beckman, E. J.; Enick, R. M. The high CO<sub>2</sub>-solubility of per-acetylated  $\alpha$ -,  $\beta$ -, and  $\gamma$ -cyclodextrin. *Fluid Phase Equilib.* 2003, 211, 211–217.
- (56) Dilek, C.; Manke, C. W.; Gulari, E. Phase behavior of  $\beta$ -D galactose pentaacetate–carbon dioxide binary system. *Fluid Phase Equilib.* 2006, 239, 172–177.
- (57) Haines, A. H.; Steytler, D. C.; Rivett, C. Solubility dependence of peracylated d-glucopyranoses in supercritical carbon dioxide on the structure of their acyl moieties. *J. Supercrit. Fluids* 2008, 44, 21–24.

- (58) Raveendran, P.; Blatchford, M. A.; Hurrey, M. L.; White, P.S.; Wallen, S. L. Crystallization and processing of carbohydrates using carbon dioxide. *Green Chem.* 2005, 7, 129–131.
- (59) Ma, S.-L.; Wu, Y.-T.; Hurrey, M. L.; Wallen, S. L.; Grant, C. S. Sugar Acetates as CO<sub>2</sub>-philes: Molecular Interactions and Structure Aspects from Absorption Measurement Using Quartz Crystal Microbalance. *J. Phys. Chem. B* 2010, 114, 3809–3817.
- (60) Hurrey, M. L.; Wallen, S. L. Examination of Glass Transitions in CO<sub>2</sub>-Processed, Peracetylated Sugars Using Sum Frequency Generation Spectroscopy. *Langmuir* 2006, 22, 7324-7330.
- (61) Hong, L.; Thies, M. C.; Enick, R. M. Global phase behavior for CO<sub>2</sub>-philic solids: the CO<sub>2</sub> +  $\beta$ -D-Maltose octaacetate system. *J. Supercrit. Fluids* 2005, 34, 11-16.
- (62) Liu, J.; Shervani, Z.; Raveendran, P.; Ikushima, Y. Micellization of sodium bis(2-ethylhexyl)sulfosuccinate in supercritical CO<sub>2</sub> with fluorinated co-surfactant and its solubilization of hydrophilic species. *J. Supercrit. Fluids* 2005, 33, 121-130.
- (63) Harrison, K.; Goveas, J.; Johnston, K. P. Water-in-Carbon Dioxide Microemulsions with a Fluorocarbon-Hydrocarbon Hybrid Surfactant. *Langmuir* 1994, 10, 3536-3541.

- (64) Hoefling, T. A.; Enick, R. M.; Beckman, E. J. Microemulsions in Near-Critical and Supercritical CO<sub>2</sub>. *J Phys Chem* 1991, 95, 7127-7129.
- (65) Hoefling, T. A.; Stofesky, D.; Reid, M.; Beckman, E. J.; Enick, R. M. The incorporation of a fluorinated ether functionality into a polymer of surfactant to enhance CO<sub>2</sub>-solubility, *J. Supercrit. Fluids* 1992, 5, 237-241.
- (66) Eastoe, J.; Dupont, A.; Steytler, D. C. Fluorinated surfactants in supercritical CO<sub>2</sub>, *Curr. Opin. Coll. Interf. Sci.* 2003, 8, 267-273.
- (67) Fink, R.; Beckman, E. J. Phase behavior of siloxane-based amphiphiles in supercritical carbon dioxide, *J. Supercrit. Fluids* 2000, 18, 101-110.
- (68) Psatthas, P. A.; da Rocha, S. R. P.; Lee, C. T.; Johnston, K. P.; Lim, K. T.; Weber, S. Water-in-carbon dioxide emulsions with poly(dimethylsiloxane)-based block copolymer ionomers, *Ind. End. Chem. Res.* 2000, 39, 2655-2664.
- (69) Shi, Q.; Qiao, W. Synthesis of Siloxane Polyether Surfactants and Their Solubility in Supercritical CO<sub>2</sub>. *J Surfact Deterg* 2017, 20, 453–458.
- (70) Liu, Z. T.; Erkey, C. Water in carbon dioxide microemulsions with fluorinated analogues of AOT, *Langmuir* 2001, 17, 274-277.

- (71) Johnston, K. P.; Harrison, K. L.; Clarke, M. J.; Howdle, S. M.; Bright, F. V.; Carlier, C.; Randolph, T. W. An environment for hydrophiles including proteins, *Science* 1996, 271, 624-626.
- (72) Eastoe, J.; Gold, S.; Rogers, S.; Wyatt, P.; Steytler, D. C.; Gurgel, A.; Heenan, R. K.; Fan, X.; Beckman, E. J.; Enick, R. M. Designed CO<sub>2</sub>-Philes Stabilize Water-in-Carbon Dioxide Microemulsion. *Angew. Chem.* 2006, 118, 3757–3759.
- (73) Shieh, Y.-T.; Su, J.-H.; Manivannan, G.; Lee, P. H. C.; Sawan, S. P.; Spall, W. D. Interaction of supercritical carbon dioxide with polymers. *J. Appl. Polym. Sci.* 1996, 59, 695–705.
- (74) Jin, J.; Chang, C.; Zhu, J.; Wu, H.; Zhang, Z. Solubility of Poly(vinylpyrrolidone) with Different Molecular Weights in Supercritical Carbon Dioxide. *J. Chem. Eng. Data* 2015, 60, 3397–3403.
- (75) Sarbu, T.; Styrane, T. J.; Beckman, E. J. Design and Synthesis of Low Cost, Sustainable CO<sub>2</sub>-philes. *Ind. Eng. Chem. Res.* 2000, 39, 4678-4683.
- (76) Li, J.; Yinmei, Y.; Chen, L.; Qi, Z. Solubilities of CO<sub>2</sub> in Poly(ethylene glycols) from (303.15 to 333.15)K. *J. Chem. Eng. Data.* 2012, 57, 610-616.
- (77) Rindfleisch, F.; DiNoia, T. P.; McHugh, M. A. Solubility of Polymers and Copolymers in Supercritical CO<sub>2</sub>. *J. Phys. Chem.* 1996, 100, 15581-15587.

- (78) Palmer, M. V.; Ting, S. S. T. Applications for supercritical fluid technology in food processing. *Food Chemistry* 1995, 52, 345-352.
- (79) Raventos, M.; Duarte, S.; Alarcon, R. Application and Possibilities of Supercritical CO<sub>2</sub> Extraction in Food Processing Industry: An Overview. *Food Sci Tech Int* 2002, 8(5), 269–284.
- (80) Sahena, F.; Zaidul, I, S, M.; Jinap, S.; Karim, A. A.; Abbas, K. A.; Norulaini, N. A. N.; Omar, A. K. M. Application of supercritical CO<sub>2</sub> in lipid extraction- A review. *J. Food Eng.* 2009, 95, 240–253.
- (81) McHugh, M.; Krukonis, V. J. Supercritical fluid extractions: Principles and practice, 2nd ed., Butterworth- Heinerman: Boston, MA, 1994.
- (82) Ayre, A.; Ghude, K.; Mane, P.; Nemade, M.; Gosavi, S.; Pathare, A.; Lad, A. Supercritical fluid extraction- A green paradigm in the area of separation science. *Asian j. biomed. Pharm. Sci.* 2013, 23, 1-7.
- (83) Wells, S. L.; DeSimone, J. CO<sub>2</sub> technology platform: An important tool for environmental problem solving. *Angew. Chem. Int. Ed.* 2001, 40, 518-527.
- (84) Kendall, J. L.; Canelas, D. A.; Young, J. L.; DeSimone, J. M. Polymerizations in Supercritical Carbon Dioxide. *Chem. Rev.* 1999, 99, 543-563.

- (85) Kazarian, S. G. Polymer Processing with Supercritical Fluids. *Polymer Science* 2000, 42, 78–101.
- (86) Cooper, A. I. Polymer synthesis and processing using supercritical carbon dioxide. *J. Mater. Chem.*, 2000, 10, 207-234.
- (87) Cooper, A. I.; DeSimone, J. M. Polymer synthesis and characterization in liquid / supercritical carbon dioxide. *Current Opinion In Solid State & Materials Science* 1996, 1, 761-766.
- (88) Tomasko, D. L.; Li, H.; Liu, D.; Han, X.; Wingert, M. J.; Lee, L. J.; Koelling, K. W. A Review of CO<sub>2</sub> Applications in the Processing of Polymers. *Ind. Eng. Chem. Res.* 2003, 42, 6431-6456.
- (89) Cooper, A. I. Recent Developments in Materials Synthesis and Processing Using Supercritical CO<sub>2</sub>. *Adv. Mater.* 2001, 13, 1111- 1114.
- (90) Watkins, J. J.; McCarthy, T. J. Polymer/Metal Nanocomposite Synthesis in Supercritical CO<sub>2</sub>. *Chem. Mater.*, Vol. 7, No. 11, 1995.
- (91) Howdle, S. M.; Watson, M. S.; Whitaker, M. J.; Popov, V. K.; Davies, M. C.; Mandel, F. S.; Wang, J. D.; Shakesheff, K. M. Supercritical fluid mixing: preparation of thermally sensitive polymer composites containing bioactive materials. *Chem. Commun.* 2001, 109–110.

- (92) Davies, O. R.; Lewis, A. L.; Whitaker, M. J.; Tai, H.; Shakesheff, K. M.; Howdle, S. M. Applications of supercritical CO<sub>2</sub> in the fabrication of polymer systems for drug delivery and tissue engineering. *Adv. Drug Delivery Rev.* 2008, 60, 373–387.
- (93) Hoggan, E. N.; Flowers, D.; Wang, K.; DeSimone, J. M.; Carbonell, R. G.; Spin Coating of Photoresists Using Liquid Carbon Dioxide. *Ind. Eng. Chem. Res.* 2004, 43, 2113–2122.
- (94) Ji, M.; Chen, X.; Wai, C. M.; Fulton, J. L. Synthesizing and Dispersing Silver Nanoparticles in a Water-in-Supercritical Carbon Dioxide Microemulsion. *J. Am. Chem. Soc.* 1999, 121, 2631-2632.
- (95) Shah, P. S.; Holmes, J. D.; Doty, R. C.; Johnston, K. P.; Korgel, B. A. Steric Stabilization of Nanocrystals in Supercritical CO<sub>2</sub> Using Fluorinated Ligands. *J. Am. Chem. Soc.* 2000, 122, 4245-4246.
- (96) Shah, P. S.; Husain, S.; Johnston, K. P.; Korgel, B. A. Role of Steric Stabilization on the Arrested Growth of Silver Nanocrystals in Supercritical Carbon Dioxide. *J. Phys. Chem. B* 2002, 106, 12178-12185.
- (97) Sihvonen, M.; Jarvenpaa, E.; Hietaniemi, V.; Huopalahti, R. Advances in supercritical carbon dioxide technologies. *Trends Food Sci. & Technol.* 1999, 10, 217-222.



- (98) Marr, R.; Gamse, T. Use of supercritical fluids for different processes including new developments-A review. *Chem. Process Eng.* 2000, 39, 19–28.
- (99) Esfandiari, N. Production of micro and nano particles of pharmaceutical by supercritical carbondioxide. *J. Supercrit. Fluids* 2015, 100, 129–141.
- (100) Moribe, K.; Tozuka, Y.; Yamamoto, K. Supercritical carbon dioxide processing of active pharmaceutical ingredients for polymorphic control and for complex formation. *Adv. Drug Delivery Rev.* 2008, 60, 328–338.
- (101) Subramaniam, B.; Rajewski, R. A.; Snavely, K. Pharmaceutical Processing with Supercritical Carbon Dioxide. *J. Pharm. Sci.* 1997, 86, 885-890.
- (102) Maeda, S.; Kunitou, K. One-Bath Dyeing of Polyester/Cotton Blends with Reactive Disperse Dyes in Supercritical Carbon Dioxide. *Textile Res. J.* 2004, 74, 989-994.
- (103) Liao, S-K.; Chang, P.-S. Literatures on Dyeing Technique of Supercritical Fluid Carbon Dioxide. *Am. J. Anal. Chem.* 2012, 3, 923-930.
- (104) Iliff, R. J. et al. Liquid/supercritical carbon dioxide/dry cleaning system. U.S. Patent 5412958, May 9, 1995.

- (105) Knez, Z.; Markocic, E.; Leitgeb, M.; Primožic, M.; Hrncic, M. K.; Skerget, M. Industrial applications of supercritical fluids: A review. *Energy* 2014, 77, 235-243.
- (106) Brady, B. O.; Kao, C-P. C.; Dooley, K. M.; Knopf, F. C. Supercritical Extraction of Toxic Organics from Soils. *Ind. Eng. Chem. Res.* 1987, 26, 261-268.
- (107) Weibel, G. L.; Ober, C. K. An overview of supercritical CO<sub>2</sub> applications in microelectronics processing. *Microelectron. Eng.* 2003, 65, 145–152.
- (108) Eckert, C. A.; Knutson, B. L.; Debenedetti, P. G. Supercritical fluids as solvent for chemical and materials processing. *Nature* 1996, 383, 313-318.
- (109) Dillow, A. K.; Yun, S. L. J.; Suleiman, D.; Boatright, D. L.; Liotta, C. L.; Eckert, C. A. Kinetics of a Phase-Transfer Catalysis Reaction in Supercritical Fluid Carbon Dioxide. *Ind. Eng. Chem. Res.* 1996, 35, 1801-1806.
- (110) Chandler, K.; Culp, C. W.; Lamb, D. R.; Liotta, C. L.; Eckert, C. A. Phase-Transfer Catalysis in Supercritical Carbon Dioxide: Kinetic and Mechanistic Investigations of Cyanide Displacement on Benzyl Chloride. *Ind. Eng. Chem. Res.* 1998, 37, 3252-3259.
- (111) Oakes, R. S.; Clifford, A. A.; Rayner, C. M. The use of supercritical fluids in synthetic organic chemistry. *J. Chem. Soc., Perkin Trans.* 2001, 1, 917–941.

- (112) Brown, R. A.; Pollet, P.; McKoon, E.; Eckert, C. A.; Liotta, C. L. Jessop, P. G. Asymmetric Hydrogenation and Catalyst Recycling Using Ionic Liquid and Supercritical Carbon Dioxide. *J. Am. Chem. Soc.* 2001, 123, 1254-1255
- (113) Burk, M. J.; Feng, S.; Gross, M. F.; Turnas, W. Asymmetric Catalytic Hydrogenation Reactions in Supercritical Carbon Dioxide. *J. Am. Chem. Soc.* 1995, 117, 8277-8278.
- (114) Koch, D.; Leitner, W. Rhodium-Catalyzed Hydroformylation in Supercritical Carbon Dioxide. *J. Am. Chem. Soc.* 1998, 120, 13398-13404.
- (115) Tanko, J. M.; Blackert, J. F. Free-Radical Side-Chain Bromination of Alkylaromatics in Supercritical Carbon Dioxide. *Science* 1994, 263, 203-205.
- (116) Bhanage, B. M.; Fujita, S-i.; Arai, M. Heck reactions with various types of palladium complex catalysts: application of multiphase catalysis and supercritical carbon dioxide. *J. Organomet. Chem.* 2003, 687, 211-218.
- (117) Kayaki, Y.; Yamamoto, M.; Ikariya, T. Stereoselective Formation of  $\alpha$ -Alkylidene Cyclic Carbonates via Carboxylative Cyclization of Propargyl Alcohols in Supercritical Carbon Dioxide. *J. Org. Chem.* 2007, 72, 647-649.
- (118) Birnbaum, E. R.; Le Lacheur, R. M.; Horton, A. C.; Tumas, W. Metalloporphyrin-catalyzed homogeneous oxidation in

- supercritical carbon dioxide. *J. Mol. Catal. A: Chem.* 1999, 139, 11–24.
- (119) Smith, C. J.; Tsang, M. W. S.; Holmes, A. B.; Danheiser, R. L.; Tester, J. W. Palladium catalysed aryl amination reactions in supercritical carbon dioxide. *Org. Biomol. Chem.* 2005, 3, 3767 – 37819.
- (120) Hay, J. N.; Khan, A. Review Environmentally friendly coatings using carbon dioxide as the carrier medium. *J. Mater. Sci.* 2002, 37, 4743 – 4752.
- (121) DeSimone, J. M.; Tumas, W. *Green Chemistry Using Liquid and Supercritical Carbon Dioxide*, Oxford University Press; 1<sup>st</sup> ed.; New York, 2003.
- (122) Ramachandran, J. P. (2019). Utilization of supercritical CO<sub>2</sub> as a green solvent in the preparation of drug-excipient composites for controlled drug release. Ph.D Thesis. University of Calicut, Kerala, India.
- (123) Griffiths, P. R.; De Hasseth, J. A.; Winefordner, J. D. *Fourier Transform Infrared Spectrometry* (2nd ed.). Wiley-Blackwell., 2007.
- (124) Skoog, D. A.; Holler, F. J.; Crouch, S. R. *Principles of instrumental analysis* (6th ed.), Cengage Learning, Brooks Cole, 2006.

- (125) Wang, J.; Dang, M.; Duan, C.; Qian, L. Further understanding on the mechanism of alkyl ketene dimer sizing on the causticized calcium carbonate filled paper and its improvements, *Environ Sci Pollut Res* 2017, 24, 4822–4827.
- (126) Vashi, K. N.; Patel, M. C.; Patel, M. C. Analysis of Number of Yarn Breaks during Warping Process. *Int. J. Sci. Res.* 2016, 6, 45-52.
- (127) Kovacevic, S.; Penava, Z. Impact of Sizing on Physico-Mechanical Properties of Yarn. *Fibres Text. East. Eur.* 2004, 12, 32–36.
- (128) Kuemmerer, H. R.; Walhalla, S. C. Sizing Textile Yarns. U.S. Patent US3061470, October 30, 1962.
- (129) Fulton, J. L.; Yonker, C. R.; Hallen, R. R.; Baker, E. G.; Bowman, L. E.; Silva, L. Method for sizing and desizing yarns with liquid and supercritical carbon dioxide solvent. U.S. Patent US5863298, January 26, 1999.
- (130) Bowman, L. E.; Caley, C. G.; Hallen, R. T.; Fulton, J. L. Sizing and Desizing of Polyester/ Cotton Blend Yarns Using Liquid Carbon Dioxide. *Text. Res. J.* 1996, 66, 795–802.
- (131) Barhoum, A.; Rahier, H.; Abou- Zaied, R. E.; Rehan, M.; Dufour, T.; Hill, G.; Dufresne, A. Effect of cationic and anionic surfactants on the application of calcium carbonate nanoparticles in paper coating. *ACS Appl. Mater. Interfaces* 2014, 6, 2734-2744.

- (132) Bourbonnais, R.; Marchessault, R. H. Application of polyhydroxyalkanoate granules for sizing of paper. *Biomacromolecules* 2010, 11, 989-993.
- (133) Wang, X.; Hao, X.; Ren, L.; Qiang, T.; Zhang, S. Study of the preparation, characterization, and sizing performance of modified collagen surface sizing agent. *BioResources* 2014, 9, 1255–1266.
- (134) Kumar, S.; Chauhan, V. S.; Chakrabarti, S. K. Separation and analysis techniques for bound and unbound alkyl ketene dimer (AKD) in paper: A review. *Arabian J. Chem.* 2016, 9, 1636–1642.
- (135) Quan, C.; Werner, O.; Wagberg, L. Turner, C. Generation of superhydrophobic paper surfaces by a rapidly expanding supercritical carbon dioxide–alkyl ketene dimer solution. *J. Supercritic. Fluids* 2009, 49, 117–124.
- (136) Werner, O.; Quan, C.; Turner, C.; Pettersson, B.; Wagberg, L. Properties of superhydrophobic paper treated with rapid expansion of supercritical CO<sub>2</sub> containing a crystallizing wax. *Cellulose* 2010, 17, 187–198.
- (137) Ferreira, P. J.; Gamelas, J. A.; Moutinho, I. M.; Ferreira, A. G.; Gomez, N.; Molleda, C.; Figueiredo, M. M. Application of FT-IR-ATR Spectroscopy to evaluate the penetration of surface sizing agents into the paper structure. *Ind. Eng. Chem. Res.* 2009, 48, 3867–3872.

- (138) Causin, V.; Marega, C.; Marigo, A.; Casamassima, R.; Peluso, G.; Ripani, L. Forensic differentiation of paper by X-ray diffraction and infrared spectroscopy. *Forensic Sci. Int.* 2010, 197, 70–74.
- (139) Ghule, K.; Ghule, A. V.; Chen, B.-J.; Ling, Y.-C. Preparation and characterization of ZnO nanoparticles coated paper and its antibacterial activity study. *Green Chem.* 2006, 8, 1034–1041.
- (140) Saraiva, M. S.; Gamelas, J. A. F.; Mendes de Sousa, A. P.; Reis, B. M.; Amaral, J. L.; Ferreira, P. J. A new approach for the modification of paper surface properties using polyoxometalates. *Materials* 2010, 3, 201–215.
- (141) George, J.; Sajeevkumar, V. A.; Kumar, R.; Ramana, K. V.; Sabapathy, S. N.; Bawa, A. S. Enhancement of thermal stability associated with the chemical treatment of bacterial (*Gluconacetobacter xylinus*). *J. Appl. Polym. Sci.* 2008, 108, 1845–1851.
- (142) Kang, Y.-R.; Li, Y.-L.; Hou, F.; Wen, Y.-Y.; Su, D. Fabrication of electric papers of graphene nanosheet shelled cellulose fibres by dispersion and infiltration as flexible electrodes for energy storage. *Nanoscale* 2012, 4, 3248–3253.
- (143) Zhang, K.; Feldner, A.; Fischer, S. FT Raman spectroscopic investigation of cellulose acetate. *Cellulose* 2011, 18, 995–1003.

- (144) Moutinho, I.; Ihalainen, P.; Figueiredo, M.; Peltonen, J.; Ferreira, P.; Evaluation of the topography of surface sized eucalyptus based papers. *Ind. Eng. Chem. Res.* 2010, 49, 1–5.
- (145) Irvine, J. A.; Aston, D. E.; Berg, J. C. The use of atomic force microscopy to measure the adhesive properties of sized and unsized papers. *Tappi J.* 1999, 82, 172–174.
- (146) Chinga-carrasco, G. Complementary microscopy techniques for surface characterisation of uncoated and mineral pigment coated paper. *Curr. Microsc. Contrib. Adv. Sci. Technol.* 2012, 1448–1455.
- (147) Gallyamov, M. O.; Nikitin, L. N.; Nikolaev, A. Yu.; Obratsov, A. N.; Bouznic, V. M.; Khokhlov, A. R. Formation of superhydrophobic surfaces by the deposition of coatings from supercritical carbon dioxide. *Colloid J.* 2007, 69, 411–424.
- (148) Kannagara, D.; Shen, W.; Roughness effects of cellulose and paper substrates on water drop impact and recoil. *Colloids Surf. A: Physicochem. Eng. Aspects* 2008, 330, 151–160.
- (149) Shen, W.; Filonanko, Y.; Truong, Y.; Parker, I. H.; Brack, N.; Pigram, P.; Liesegang, J. Contact angle measurement and surface energetics of sized and unsized paper. *Colloids Surf. A: Physico. Eng. Asp.* 2000, 173, 117–126.
- (150) Yang, H.; Deng, Y. Preparation and physical properties of superhydrophobic papers. *J. Colloid Interface Sci.* 325, 2008, 588–593.



- (151) Rowell, R. M. Chemical modification of wood: A short review. *Wood Mater. Sci. Eng.*, 2006, 1, 29-33
- (152) Ozmen, N. Dimensional Stabilization of Fast Growing Forest Species by Acetylation. *J. Appl. Sci.* 2007, 7(5), 710-714.
- (153) Hingston, J. A.; Collins, C. D.; Murphy, R. J.; Lester, J. N. Leaching of chromated copper arsenate wood preservatives: a review. *Environ. Pollut.* 2001, 111, 53-66.
- (154) Hay, J. N.; Johns, K. Supercritical fluids-A potential revolution in wood treatment and coating. *Surf. Coat. Int.* 2000, 3, 106-110.
- (155) Sunol, A. K.; Richey, P. Supercritical Fluid-Aided Treatment of Porous Materials. U. S. Patent 4,992,308, February 12, 1991.
- (156) Kjellow, A. W.; Henriksen, O. Supercritical wood impregnation. *J. of Supercrit. Fluids* 2009, 50, 297–304.
- (157) Matsunaga, M.; Kataoka, Y.; Matsunaga, H.; Matsui, H. A novel method of acetylation of wood using supercritical carbon dioxide. *J Wood Sci* 2010, 56, 293–298.
- (158) Matsunaga, M.; Hewage, D. C.; Kataoka, Y.; Ishikawa, A.; Kobayashi, M.; Kiguchi, M. Acetylation of wood using supercritical carbondioxide. *J. Trop. For Sci.* 2016, 28, 132-138.
- (159) Gabitov, R. F.; Khairutdinov, V. F.; Gumerov, F. M.; Gabitov, F. R.; Zaripov, Z. I.; Gaifullina, R.; Farakhov, M. I. Drying and

- Impregnation of Wood with Propiconazole Using Supercritical Carbon Dioxide. *Russ. J. Phys. Chem. B* 2017, 11, 1223–1230.
- (160) Acda, M. N.; Morrell, J. J.; Levein, K. L. Supercritical fluid impregnation of selected wood species with tebuconazole. *Wood Sci. Technol.* 2001, 35, 127-136.
- (161) Ichino, T. Sensorially Active Substance Embedded in Plastic. U. S. Patent US 6468554 B1, October 22, 2002.
- (162) Petkova, N.; Vassilev, D.; Grudeva, R.; Tumbarski, Y.; Vasileva, I.; Koleva, M.; Denev, P. “Green” Synthesis of Sucrose Octaacetate and Characterization of Its Physicochemical Properties and Antimicrobial Activity. *Chem. Biochem. Eng. Q.* 2017, 31, 395–402.
- (163) Rahman, M. R. *Wood Polymer Nanocomposites: Chemical Modifications, Properties and Sustainable Applications*, Springer 2018.
- (164) Devi, R. R.; Maji, T. K.; Banerjee, A. N. Studies on Dimensional Stability and Thermal Properties of Rubber Wood Chemically Modified with Styrene and Glycidyl Methacrylate. *J. Appl. Polym. Sci.* 2004, 93, 1938–1945.
- (165) Dong, Y.; Yan, Y.; Zhang, S.; Li, J. Wood/Polymer nanocomposites Prepared by Impregnation with Furfuryl Alcohol and Nano-SiO<sub>2</sub>. *BioResources* 2014, 9, 6028-6040.

- (166) Agarwal, U. P.; Ralph, S. A. FT-Raman Spectroscopy of Wood: Identifying Contributions of Lignin and Carbohydrate Polymers in the Spectrum of Black Spruce (*Piceamariana*). *Appl. Spectrosc.* 1997, 51, 1648-1655.
- (167) Azeem, B.; KuShaari, K.; Man, Z. B.; Basit, A.; Thanh, T. H. Review on materials & methods to produce controlled release coated Urea fertilizer. *J. Controlled Release* 181, 2014, 11-21.
- (168) Trenkel, M. E. Controlled-Release and Stabilized Fertilizers in Agriculture. International Fertilizer Industry Association, Paris, December 1997.
- (169) Lubkowski, K.; Grzmil, B. Controlled release fertilizers. *Pol. J. Chem. Technol.* 9, 4, 81-84.
- (170) Shaviv, A.; Mikkelsen, R, L. Controlled-release fertilizers to increase efficiency of nutrient use and minimize environmental degradation- A review. *Fert. Res.* 1993, 35, 1-12.
- (171) Chen, L.; Xie, Z.; Zhuang, X.; Chen, X.; Jing, X. Controlled release of urea encapsulated by starch-g-poly(L-lactide). *Carbohydr. Polym.* 2008, 72 342-348.
- (172) Kottegoda, N. et al., Urea-Hydroxyapatite Nanohybrids for Slow Release of Nitrogen. *ACS Nano* 2017, 11, 1214-1221.
- (173) X. Yang, et al., Cumulative release characteristics of controlled-release nitrogen and potassium fertilizers and their

effects on soil fertility, and cotton growth. *Sci. Rep.* 6, 2016, 39030.

- (174) Blouin, G.M. Method of making sulfur-coated fertilizer pallet having a controlled dissolution rate, U. S. Patent 3295950, January 3, 1967.
- (175) Tsai, B. S. (1986). Continuous spouted bed process for sulphur-coating. Ph.D Thesis, The University of British Columbia.
- (176) Detrick, J. H., Process for producing improved sulfur-coated urea slow release fertilizers, U. S. Patent 5599374, February 4, 1997.
- (177) Detrick, J. H.; and Hargrove, G, L. Polymer-sulfur-polymer coated fertilizers, U. S. Patent US 6338746 B1, January 15, 2002.
- (178) Qingshan, L.; Shu, W.; Tiejun, R.; Limin, W.; Guangzhong, X.; Jinming, W. Synthesis and performance of polyurethane coated urea as slow/controlled release fertilizer, *J. Wuhan Univ. Technol. Mater. Sci. Ed.* 2012, 27, 126–129.
- (179) Han, W.-Y.; Ma, L.-F.; Shi, Y.-Z.; Ruan, J.-Y.; Kemmitt, S. J. Nitrogen release dynamics and transformation of slow release fertiliser products and their effects on tea yield and quality, *J. Sci. Food Agric.* 2008, 88, 839–846.

- (180) Jintakanon, N.; Opaprakasit, P.; Petchsuk, A.; Opaprakasit, M. Controlled-release materials for fertilizer based on lactic acid polymers, *Adv. Mater. Res.* 2008, 55, 905–908.
- (181) Costa, M. M. E.; Cabral-Albuquerque, E. C. M.; Alves, T. L. M.; Pinto, J. C.; Fialho, R. L. Use of polyhydroxybutyrate and ethyl cellulose for coating of urea granules, *J. Agric. Food Chem.* 2013, 61, 9984–9991.
- (182) Guo, M.; Liu, M.; Zhan, F.; Lan Wu, L. Preparation and properties of a slow-release membrane-encapsulated urea fertilizer with superabsorbent and moisture preservation, *Ind. Eng. Chem. Res.* 2005, 44, 4206–4211.
- (183) Liang, R.; Liu, M. Preparation and properties of a double-coated slow-release and water-retention urea fertilizer, *J. Agric. Food Chem.* 2006, 54, 1392–1398.
- (184) Tao, S.; Liu, J.; Jin, K.; Qiu, X.; Zhang, Y.; Ren, X.; Hu, S. Preparation and characterization of triple polymer-coated controlled release urea with water-retention property and enhanced durability, *J. Appl. Polym. Sci.* 2011, 120, 2103–2111.
- (185) Ko, B.-S.; Cho, Y.-S.; Rhee, H.-K. Controlled Release of Urea from Rosin-Coated Fertilizer Particles. *Ind. Eng. Chem.* 1996, 35, 250-257.

- (186) Giroto, A. S.; Fidelis, S. C.; Ribeiro, C. Controlled release from hydroxyapatite nanoparticles incorporated into biodegradable, soluble host matrixes. *RSC Adv.* 2015, 5, 104179-104186.
- (187) Lu, P.; Zhang, Y.; Jia, C.; Li, Y.; Mao, Z. Use of polyurea from urea for coating of urea granules. *SpringerPlus* 2016, 5, 457-462.
- (188) Campos, O. R.; Mattiello, E. M.; Cantarutti, R. B.; Vergutz, L. Nitrogen release from urea with different coatings. *J Sci Food Agric* 2018, 98, 775–780.
- (189) Chen, C.; Gao, Z.; Qiu, X.; Hu, S. Enhancement of the Controlled-Release Properties of Chitosan Membranes by Crosslinking with Suberoyl Chloride. *Molecules* 2013, 18, 7239-7252.
- (190) Ito, R.; Golman, B.; Shinohara, K. Design of multi-layer coated particles with sigmoidal release pattern, *Chem. Eng. Sci.* 2005, 60, 5415–5424.
- (191) Suherman; Anggoro, D. D. Producing slow release urea by coating with starch/acrylic acid in fluid bed spraying, *Int. J. Eng. Technol. IJET-IJENS* 2011, 11, 62-66.
- (192) Fernandez-Perez, M.; Garrido-Herrera, F. J.; Gonza´lez-Pradas, E.; Villafranca-Sanchez, M.; Flores-Cespedes, F. Lignin and ethylcellulose as polymers in controlled release formulations of urea, *J. Appl. Polym. Sci.* 2008, 108, 3796–3803.

- (193) [https://www.who.int/medicines/areas/quality\\_safety/quality\\_assurance/DefinitionAPI-QAS11-426Rev1-08082011.pdf](https://www.who.int/medicines/areas/quality_safety/quality_assurance/DefinitionAPI-QAS11-426Rev1-08082011.pdf)
- (194) Blecher, L. Excipients-the important components. *Pharm process*. 1995, 12(1), 6-7.
- (195) Fathima, N.; Mamatha, T.; Qureshi, H. K.; Anitha, N.; Rao, J. V. Drug-excipient interaction and its importance in dosage form development. *J. Appl. Pharm. Sci. Res.* 2011, 1, 66-71.
- (196) Edward, M.; Rudnic, Schwartz, J. B. *Oral solid dosage forms*, 21<sup>st</sup> ed.; Remington Science and Practice of Pharmacy, (Ed 21) Williams and Wilkins Baltimore, USA, 2005.
- (197) Sekiguchi, K.; Obi, N. Studies on Absorption of Eutectic Mixture. I. A Comparison of the Behavior of Eutectic Mixture of Sulfathiazole and that of Ordinary Sulfathiazole in Man. *Chem. Pharm. Bull.* 1961, 9, 866–872.
- (198) Allawadi, D.; Singh, N.; Singh, S.; Arora, S. Solid Dispersions: A Review on Drug Delivery System and Solubility Enhancement. *Int. J. Appl. Pharm. Sci. Res.* 2013, 4, 2094-2105.
- (199) Shahi, S. R.; Arshiya, K.; Bhalerao, P.; Pavan, A. A Review on Formulation Aspects of Solid Dispersions. *Eur J Pharm Med Res* 2017, 4, 148-160.

- (200) Teja, S.B.; Patila, S.P.; Shetea, G.; Patel S.; Bansala, A.K. Drug-excipient behaviour in polymeric amorphous solid dispersions. *J. Excip. food chem.* 2013, 4 , 70-94.
- (201) Laitinen, R.; Lobmann, K.; Strachan, C.J.; Grohganz, H.; Rades, T. Emerging trends in the stabilization of amorphous drugs. *Int. J. Pharm.* 2013, 453, 65–79.
- (202) Hancock, B.C.; Zografi, G. Characteristics and Significance of the Amorphous State in Pharmaceutical Systems. *J. Pharm. Sci.* 1997, 86, 1-11.
- (203) Baghel, S.; Cathcart, H.; O'Reilly, N. J. Polymeric Amorphous Solid Dispersions: A Review of Amorphization, Crystallization, Stabilization, Solid-State Characterization, and Aqueous Solubilization of Biopharmaceutical Classification System Class II Drugs. *J. Pharm. Sci.* 2016, 105, 2527-2544.
- (204) Yu, L. Amorphous pharmaceutical solids: preparation, characterization and stabilization. *Adv. Drug Deliv. Rev.* 2001, 48, 27–42.
- (205) Dhirendra, K.; Lewis, S.; Udupa, N.; Atin, K. Solid Dispersions: A Review. *Pak. J. Pharm. Sci.* 2009, 22, 234-246.
- (206) Chiou, W. L.; Riegelman, S. Pharmaceutical Applications of Solid Dispersion Systems. *J. Pharm. Sci.* 1971, 60, 1281-1302.



- (207) Vasconcelos, T.; Sarmiento, B.; Costa, P. Solid dispersions as strategy to improve oral bioavailability of poor water soluble drugs. *Drug Discov. Today*. 2007, 12, 1068-1075.
- (208) Sekhon, B. S. Supercritical Fluid Technology: An Overview of Pharmaceutical Applications. *Int. J. PharmTech Res.* 2010, 2, 810-826.
- (209) Girotra, P.; Singh, S. K.; Nagpal, K. Supercritical fluid technology: a promising approach in pharmaceutical research. *Pharm. Dev. Technol.* 2013, 18, 22–38.
- (210) Hannay, J. B.; Hogarth, J. On the Solubility of Solids in Gases. *Proc. R. Soc. Lond* 1879, 29, 324-326.
- (211) Taranjit, K.; Prachi, S.; Sandeep, K. Supercritical Fluid Technology: An Innovative Approach Used to Enhance Solubility Of Water Insoluble Drugs. *J. Drug Delivery Ther.* 2017, 7, 22-26.
- (212) Yoshida, V. M. H.; Balcão, V. M. C. F.; Vila, M. M. D. C.; Júnior, J. M. O.; Aranha, N.; Gremião, M. P. D.; Chaud, M. V. Supercritical fluid and pharmaceutical applications. Part I: Process classification. *Afr. J. Pharm. Pharmacol.* 2016, 10, 132-144.
- (213) Kalani, M.; Yunus, R. Application of supercritical antisolvent method in drug encapsulation: a review. *Int. J. Nanomed.* 2011, 6, 1429–1442

- (214) Bleich, J.; Kleinebudde, P.; Muller, B. W. Influence of gas-density and pressure on microparticles produced with the ASES process, *Int. J. Pharm.* 1994, 106, 77–84.
- (215) Bhardwaj, L.; Sharma, P. K.; Visht, S.; Garg, V. K.; Kumar, N. A review on methodology and application of supercritical fluid technology in pharmaceutical industry. *Der Pharmacia Sinica* 2010, 1, 83-194.
- (216) Deshpande, P. B.; Kumar, G. A.; Kumar, A. R.; Shavi, G, V.; Karthik, A.; Reddy, M. S.; Udupa, N. Supercritical Fluid Technology: Concepts and Pharmaceutical Applications. *PDA J. Pharm. Sci. Technol.* 2011, 65, 333-344.
- (217) Kankala, R. K.; Zhang, Y. S.; Wang, S.-B.; Lee, C.-H.; Chen, A.-Z. Supercritical Fluid Technology: An Emphasis on Drug Delivery and Related Biomedical Applications. *Adv. Healthcare Mater.* 2017, 6, 1700433.
- (218) Toropainen, T.; Heikkila, T.; Leppanen, J.; Matilainen, L.; Velaga, S.P.; Jarbo, P.; Carlfors, J.; Lehto, V.-P.; Jarvinen, T.; Jarvinen, K. Crystal structure changes of  $\gamma$ -cyclodextrine after the SEDS process in supercritical carbon dioxide affect the dissolution rate of complexed budesonide. *Pharm. Res.* 2007, 24, 1058–1066.
- (219) Tandy, A.; Dehghani, F.; Foster, N. R. Micronization of cyclosporine using dense gas techniques, *J. Supercrit. Fluids* 2006, 37, 272–278.

- (220) Tsivintzelis, I.; Angelopoulou, A.G.; Panayiotou, C. Foaming of polymers with supercritical CO<sub>2</sub>: an experimental and theoretical study. *Polymer* 2007, 48, 5928–5939.
- (221) Mishima, K.; Matsuyama, K.; Tanabe, D.; Yamauchi, S.; Young, T.J.; Johnston, K.P. Microencapsulation of proteins by rapid expansion of supercritical solution with a nonsolvent. *AIChE* 2000, 46, 857–865.
- (222) Tozuka, Y.; Fujito, T.; Moribe, K.; Yamamoto, K. Ibuprofen–cyclodextrin inclusion complex formation using supercritical carbon dioxide, *J. Incl. Phenom. Macrocycl. Chem.* 2006, 56, 33–37.
- (223) Lee, J.A.; Jung, I.-I.; Kim, J.S.; Lim, G.-B.; Ryu, J.-H. Preparation of itraconazole/HP- $\beta$ -CD inclusion complexes using supercritical aerosol solvent extraction system and their dissolution characteristics. *J. Supercrit. Fluids* 2008, 44, 400–408.



## **PUBLICATIONS**

1. Antony, A. ; Raj, A.; Ramachandran, J. P.; Ramakrishnan, R.M.; Wallen, S. L.; Raveendran, P. Sizing and Desizing of Cotton and Polyester Yarns Using Liquid and Supercritical Carbon Dioxide with Nonfluorous CO<sub>2</sub>-Philes as Size Compounds. ACS Sustainable Chem. Eng. 2018, 6, 12275–12280.
2. Antony, A.; Ramachandran, J. P. ; Ramakrishnan, R. M.; Raveendran, P. Sizing of paper with Sucrose octaacetate using liquid and supercritical carbondioxide as a green alternative medium. J. CO<sub>2</sub> Utilization. 2018, 28, 306-312.
3. Safna, H. K. P.; Thayyil, M. S.; Rajan, V. K.; Antony, A. The Interplay between Charge Transport and CO<sub>2</sub> Capturing Mechanism in [EMIM][SCN] Ionic Liquid: A Broadband Dielectric Study. J. Phys. Chem. B 2019, 123, 6618–6626.



## **PRESENTATIONS**

1. Oral presentation in UGC sponsored National Seminar on Green Chemistry for Environmental Sustainability (2017) at Bharathmatha College, Thrikakara.
2. Poster presentation in KSCSTE sponsored International conference on Tropical Plants and Molecular Design (2017) at T.K.M College, Kollam.
3. Oral presentation in UGC sponsored National seminar on Emerging trends in chemical research (2017), Christ College, Irinjalakuda. [ISBN: 978-81-930507-3-6]
4. Oral presentation at National Conference on Innovations in Green Chemistry (2017), PSG College of Arts and Science, Avinashi road, Coimbatore.
5. Oral presentation at International Conference on Advanced Materials for Technological Applications (2018), PSGR Krishnammal College for Women, Peelamedu, Coimbatore. [ISBN-9788193469163]
6. Poster presentation at the First International Conference on Emerging Frontiers in Chemical Sciences, EFCS (2017) at Farook College. [ISBN No.978-93-5279-617-5].
7. Poster presentation at National seminar on Frontiers in chemical science, FCS (2019) at University of Calicut, Malappuram.